NOVEL FUNCTIONAL HYDROGELS AND POLYMER COATED MAGNETIC NANOPARTICLES WITH DEGRADABLE LINKERS FOR BIOMEDICAL APPLICATIONS

by

Duygu Aydın

M.S., Chemistry, Selçuk University

B.S., Chemistry, Selçuk University

Submitted to the Institute for Graduate Studies in
Science and Engineering in partial fulfillment of
the requirements for the degree of
Doctor of Philosophy

Graduate Program in Chemistry

Boğaziçi University

2017

ACKNOWLEDGEMENTS

I would like to express my most sincere gratitudes to my PhD advisors, Prof. Amitav SANYAL and Prof. Rana SANYAL for their encouraging attitude, endless support and scientific guidance throughout the study. I deeply appreciate their useful comments and helpful discussions regarding all my research. It was a great pleasure for me to work in their laboratory.

I would like to extend my thanks to my thesis advisors and members of my thesis committee Prof. İlknur Doğan, Prof. Sinan Şen, Assoc. Prof. Bülent Akgün and Assist. Prof. Özgül Gök, for their careful and constructive review of the final manuscript and for their care and help during my PhD program.

I would like to express all of my labmates for their help and support. I thank my family for their encouragement and support.

Finally I would also want to thank the gradute scholarship program by The Scientific and Technological Research Council of Turkey (TUBITAK) (2211-C) for supporting me during my Phd program.

ABSTRACT

NOVEL FUNCTIONAL HYDROGELS AND POLYMER COATED MAGNETIC NANOPARTICLES WITH DEGRADABLE LINKERS FOR BIOMEDICAL APPLICATIONS

In this thesis, the design and fabrication of novel reactive interfaces such as hydrogels and polymer coated nanoparticles were investigated for applications related to the delivery of therapeutic agents. Randomly crosslinked hydrogels incorporating amine and thiol reactive groups that allow conjugation of various bioactive molecules in a releasable fashion were synthesized. Apart from using novel modes of conjugation and release from non-degradable hydrogel scaffolds, synthesis of a new class of degradable hydrogels with well-defined network structure was also established. Effective thiol-disulfide exchange reaction based strategies were used to synthesize hydrogels where the crosslinked density could be changed and protein release profiles could be modulated. Importantly, very fast and complete degradation of these hydrogels to release the encapsulated protein was achieved. The first project involves preparation and functionalization of the amin reactive poly(ethylene glycol) (PEG) based bulk hydrogels and cryogels. Obtained activated carbonate containing 3D networks were evaluated as slow releasing drug reservoirs. In the second project, preparation of stimuli responsive well-defined polymeric networks with disulfide linkers was proposed. Hydrogels fabricated by different moleculer weight polymer were investigated in terms of their encapsulation and degradation behavior. In the third study, synthesize of cyclodextrin containing well-defined hydrogels and release behavior through thiol-disulfide exchange reaction were reported for controlled drug release application. In the fourth study, fabrication of functional hydrogels with dual functional monomers was demonstrated and functionalization and release studies were performed. In the final study, novel functionalizable polymer coated hydrophilic magnetic nanoparticles that contain thiol-reactive polymeric coatings were prepared via a ‘graft-from’ approach to design pyridyl disulfide containing polymer coated magnetic nanoparticles.

ÖZET

BİYOMEDİKAL UYGULAMALAR İÇİN KULLANILABİLECEK FONKSİYONLAŞTIRILABİLEN VE BOZULABİLEN YENİ HİDROJELLER VE POLİMER KAPLI MANYETİK NANOPARTİKÜLLER

Bu tezde, fonksiyonlaştırılabilen yeni tipteki hidrojel ve polimer kaplı nanoparçacıklar terapötik ajanların salımı ile ilgili uygulamalar için araştırılmıştır. Çeşitli biyoaktif moleküllerin serbest bırakılmasına izin veren amin ve tiyol reaktif grupları içeren rastgele çapraz bağlanmış hidrojeller sentezlenmiştir. Konjügasyonun yeni modlarını kullanmak ve parçalanmayan hidrojel iskeletlerini parçalamanın dışında, iyi tanımlanmış ağ yapısına sahip parçalanabilir hidrojel sentezi de gösterilmiştir. Etkili tiyol-disülfit değişim reaksiyonuna dayalı stratejiler hidrojel sentezinde kullanılmış ayrıca çapraz bağ yoğunluğu değiştirilerek sentezlenen hidrojellerden protein salınım profillerini gösterilmiştir. Ayrıca, kapsüllenmiş proteini serbest bırakmak için bu hidrojellerin çok hızlı ve tam bir şekilde parçalanması sağlanmıştır. Birinci proje, amin reaktif poli(etilen glikol) (PEG) bazlı hidrojellerin ve kroyojellerin sentezi ve fonksiyonelleştirilmesini içerir. Elde edilen aktifleştirilmiş karbonat içeren üç boyutlu ağlar, yavaş ilaç salım sistemi olarak değerlendirilmiştir. İkinci projede, uyarıya yanıt veren iyi tanımlanmış polimerik ağların disülfür bağlayıcılarla hazırlanması anlatılmıştır. Farklı polimer zincir uzunlukları ile sentezlenen hidrojeller, kapsüllenme ve bozunma davranışları açısından incelenmiştir. Üçüncü çalışmada, iyi tanımlanmış siklodekstrin içeren hidrojeller üretimi tiyol-disülfit değişim reaksiyonu yoluyla sentezlenmiş ve ilaç kapsülleme davranışları incelenmiş sonrasında kontrollü ilaç salınım uygulaması için araştırılmıştır. Dördüncü çalışmada, iki fonksiyonel monomeri içeren reaktif hidrojellerin hazırlanması gösterilmiş ayrıca fonksiyonelleştirme ve salınım çalışmaları incellenmiştir. Son çalışmada, tiyol içeren moleküllere karşı reaktif olan polimerik kaplamaları içeren yeni fonksiyonelleştirilebilen polimer kaplı manyetik nanopartiküller 'graft-from' yaklaşımı ile sentezlen ve tiyol içeren molaküller ile fonksiyonelleştirme çalışmaları ve ayrıca salım incelenmiştir.

TABLE OF CONTENTS

LIST OF FIGURES

LIST OF TABLES

LIST OF ACRONYMS/ABBREVIATIONS

AIBN	2,2′-Azobis(2-methylpropionitrile)
β-CD	β-Cyclodextrin
BODIPY	4,4-Difluoro-4-bora-3a,4a-diaza-s-indacene
BSA	Bovine Serum Albumin
CCK-8	Cell Counting Kit-8
$CDCl_3$	Deuterated chloroform
CTA	Chain Transfer Agent
CUR	Curcumin
DA	Diels-Alder
DAPI	4’,6-Damino-2-Phenylindole
DCM	Dichloromethane
DLS	Dynamic Light Scattering
DMAP	4-Dimethylaminopyridine
DMF	Dimethyl formamide
DMPA	2,2-Dimethoxy-2-phenylacetophenone
DMSO	Dimethyl Sulfoxide
DOX	Doxorubicin
DSC	N,N’-disuccinimidyl carbonate
DTNB	5,5′-Dithiobis(2-nitrobenzoic acid)
DTT	L-Dithiothreitol
EDCI	1-Ethyl-3-(3-dimethylaminopropyl) carbodiimide
EDTA	Ethylene Diamine Tetra Acidic Acid
EtOAc	Ethyl Acetate
FITC	Fluorescein Isotiyocyanate
FT-IR	Fourier Transform Infrared
FuMaMa	Furan protected maleimide monomer
GSH	Glutathione
HEMA	2-hydroxyethyl methacrylate
IONP	Iron Oxide Nano Particles
MeOH	Methanol

MHz	Mega hertz
NHS	N-hydroxysuccinimide
NMR	Nuclear Magnetic Resonance
NPs	Nanoparticles
PBS	Phosphate buffer saline
PDS	Pyridyl-disulfide
PDSMA	Pyridyl-disulfide methacrylate
PEG	Poly(ethylene glycol)
PEGDMA	Poly(ethylene glycol) dimethyl ether acrylate
PEGMEMA	Poly(ethylene glycol) methyl ether methacrylate
RAFT	Reversible-Addition Fragmentation Chain Transfer Polymerization
rDA	Retro Diels-Alder
RPMI	Roswell Park Memorial Institute Medium
SCEMA	2-(N-succinimidylcarboxy)ethyl methacrylate
SEM	Scanning Elektron Microscopy
TCEP	Tris(2-carboxyethyl)phosphine
TEA	Triethylamine
TGA	Thermo Gravimetric Analysis
THF	Tetrahydrofuran
TLC	Thin Layer Chromatography
UV	Ultraviolet

1. INTRODUCTION

1.1. Functionalizable Chemically Cross-linked Hydrogels as Biomedical Aids

1.1.1. Hydrogels

Hydrogels are three dimensional cross-linked networks with high water content that have been widely evaluated as hydrophilic matrices for various biomedical applications [1-3]. Hydrogel networks are generally composed of hydrophilic monomers and polymers and hence they become hydrated in aqueous environment and mimic the biological environments. The network remains insoluble in the aqueous media due to the chemical and physical crosslinks. Properties of hydrogels, such as their rate and degree of swelling depends upon factors such as the chemical composition, crosslinking density, nature of the solvent and response to external stimuli.

Hydrogels can be categorized in two groups based on the nature of the crosslinking: physically and chemically cross-linked hydrogels. Polymer chains in physically cross-linked hydrogels are held together by host–guest complexation, metal coordination, molecular entanglements and/or interactions such as H-bonding, hydrophobic and ionic interactions. In physical cross-linking, gelation takes place due to entanglements between polymer chains in aqueous environment without the need of cross-linkers. Because of the non-covalent nature of crosslinking, physically cross-linked hydrogels are weak and often reversible in nature under external stimuli. In contrast, chemically cross-linked hydrogels are formed by covalent bonds between polymer chains and hence are more stable than their physically cross-linked counterparts (Figure 1.1) [4, 5].

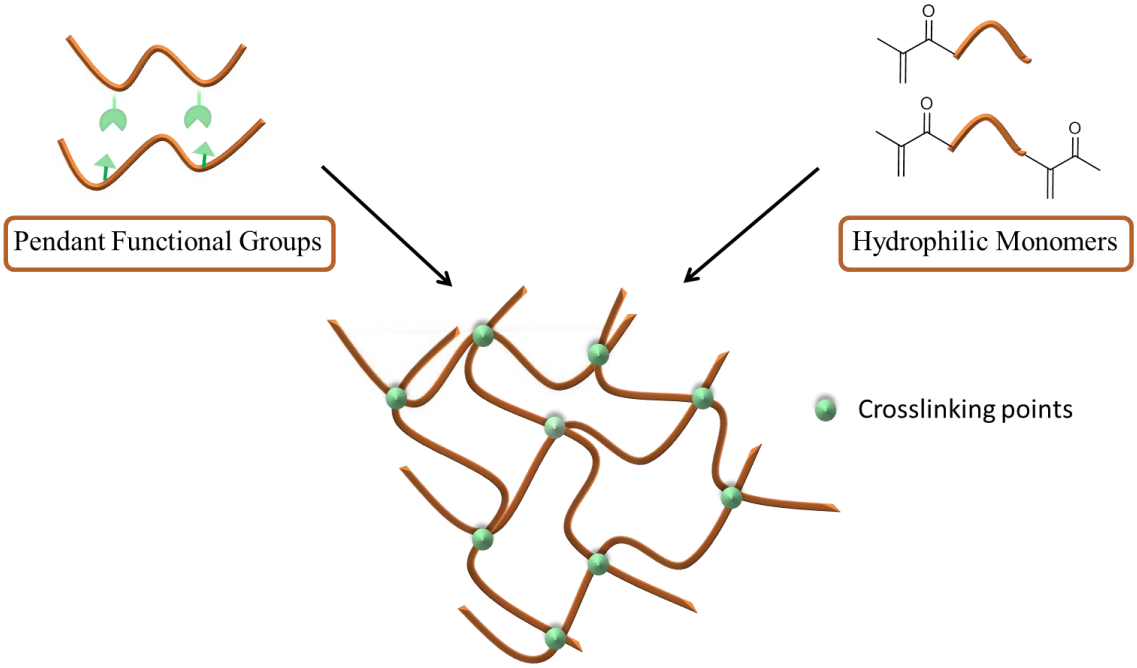

Figure 1.1. Representation of hydrogel formation via crosslinking of hydrophilic polymer or monomers or pendant functional groups.

1.1.2. Chemical Crosslinking of Hydrogels

Chemical crosslinking are commonly used for hydrogel preparation because of its high stability and good mechanical strength. By changing and controlling the degree of crosslinking, the network properties of hydrogels are tuned and so hydrogel's mechanical properties are optimized for different applications. In general, covalent cross-linked hydrogel networks are commonly prepared by either condensation polymerization or free radical polymerization (thermal, radiation, photo polymerization or plasma polymerization). In addition to these polymerization reactions, covalently crosslinking can be generated by the help of enzyme mediated polymerizations [6], click-chemistry based chemical transformations [7-8], including thioldisulfide exchange reaction [9], Diels-Alder [10, 11] and Michael type addition reactions [12, 13].

Among the many covalent crosslinking reactions, photo-induced reactions are also of particular interest due to the advantages such as operational simplicity, low energy requirements, temporal and spatial control of hydrogel features. Photo-polymerization is widely used for hydrogel formation due to the abovementioned advantages [14-16].

While photo-polymerization is an attractive method, generally, the obtained hydrogels are not degradable. Also the network structure of the hydrogels are random. Hence reactions that are reversible in nature have attracted attention in recent years, since they allow fabrication of hydrogels that can be degraded under specific stimuli such as pH, temperature or presence of a particular chemical. Among these reactions, the thiol-disulfide exchange reaction provides an attractive method for generating degradable hydrogels, and as outlined below, they have been used in biomedical application such delivery of drugs, proteins and cells.

1.1.2.1. Thiol-Disulfide Exchange Reaction. Thiol-disulfide exchange reaction is a highly efficient reaction that occurrs between the deprotonated thiolate anion (-S -) resulting from the deprotonation of a free thiol and a sulfur atom of the disulfide bond (R'SSR). This is an SN2-type nucleophilic substitution reaction and these chemical transformations create new degradable disulfide bonds. The main advantage of this reaction is that the S-S bonds are susceptible to reducing agents such as glutathione (GSH), a thiolcontaining materials that is benign and is present in our body. The thiol/disulfide exchange reaction already occurs within our body and plays an important role in field of fundamental biological processes such as enzymatic reaction or the regeneration of proteins [17].

A highly efficient thiol-disulfide exchange reaction takes place between pyridylthiolcontaining disulfide and thiol molecules (Figure 1.2). Pyridyl-2-sulfide is a functional group with one of the highest reactivity toward thiol-disulfide substitution reaction.

This group contains a leaving group that is pyridin-2-thione which can easily be removed without chromatography and does not lead to any side reactions. In addition, the release of a pyridine-2-thione group byproduct 4 formed during the new disulfide bond formation, gives rise to an absorbance at 343 nm, which can be easily followed using UV-vis spectroscopy, thus providing a simple method for determining the progress of reaction [18].

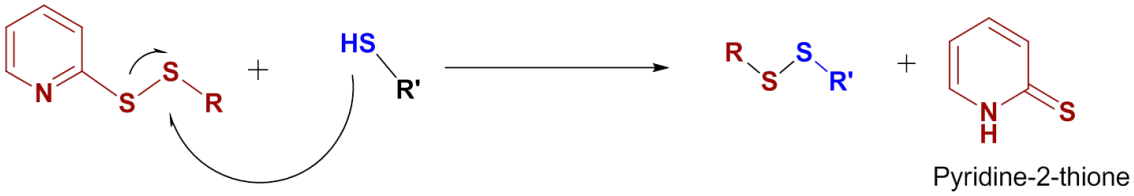

Figure 1.2. Mechanism of pyridyldisulfide-thiol exchange reaction.

As a seminal application of this reaction, Ryu and coworkers demonstrated fabrication of hydrophilic oligo(ethylene glycol) based nanogels (Figure 1.3). The nanogel formation resulted from disulfide based crosslinking upon treatment of the copolymer with dithiothreitol (DTT). In presence of DTT some of the pyridyldisulfide groups gets hydrolyzed to thiols and react with the residual disulfide groups on polymer chains to result in interchain crosslinking to yield nanogels [19]. When the crosslinking is carried out in the presence of hydrophobic drug molecules, they get encapsulated within these hydrogels.

1.1.2.2. Utilization of Thiol-Pyridyldisulfide Exchange Reaction in Hydrogel Fabrication.

Apart from formation of nanogels, the thiol-disulfide exchange reaction has also been utilized to synthesize bulk hydrogels. As mentioned before, among various disulfide groups, pyridyl-disulfide (PDS) groups are preferred for the construction of disulfide linkages due to the high efficiency. The thiol-pyridyldisulfide exchange reaction can be carried out under mild reaction conditions to provide products with very high yields. Due to these reasons, there has been growing interest in the use of thiol-pyridyldisulfide for fabrication and functionalization of hydrogels [15].

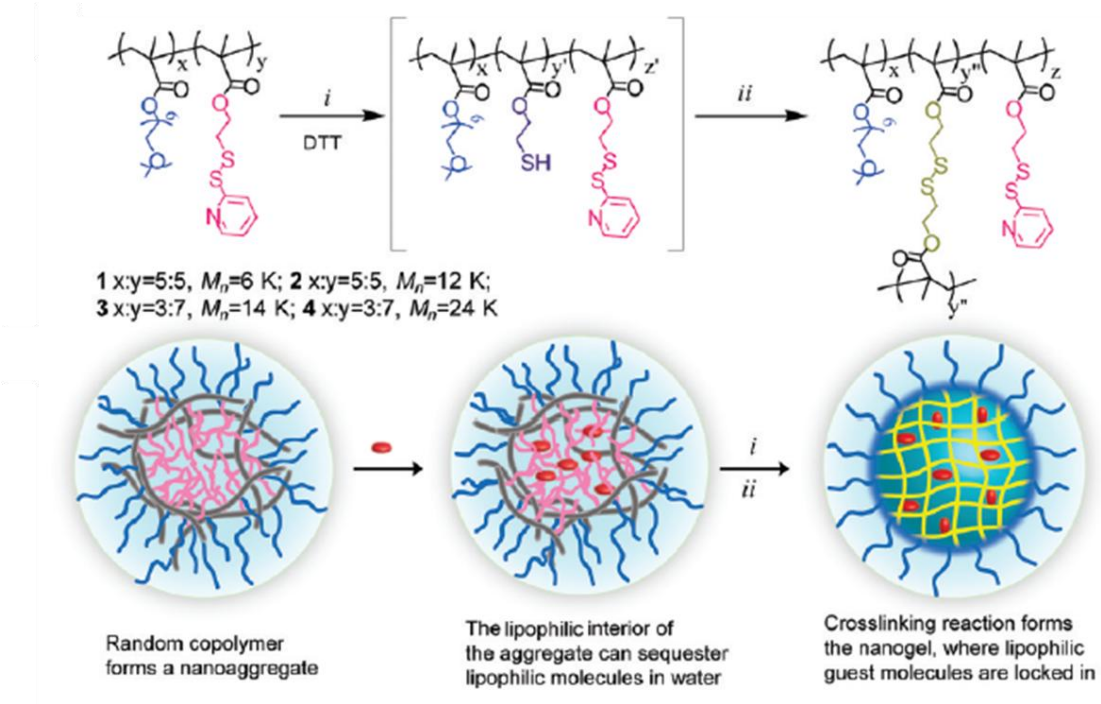

Figure 1.3. Nanogel formation using interchain crosslinking of PDS groups of polymer by DTT (From [19] with permission).

For example, PEG-dithiol and 2-pyridyldisulfide exchange reaction is used by Choh and co-workers to fabricate injectable hyaluronic acid hydrogels [9]. In this study, the concentration of pyridine- 2-thione by product during hydrogel formation was quantified by following the byproduct peak at 343 nm using UV-vis spectroscopy, to determine the speed of reaction. Since the synthesized hydrogels were crosslinked with disulfide bonds, it was found that they could degrade in the presence of thiol-containing biomolecules such as glutathione. They also demonstrated that protein encapsulation and delivery could be carried out by using the HA-SS-PEG hydrogel (Figure 1.4).

In another related example, Chien and co-workers designed a poly(carboxy betaine) based hydrogel by employing the pyridyldisulfide-thiol exchange reaction. Hydrogels with easily cleavable disulfide bonds were degraded in presence of reducing agents like glutathione and cysteine. To promote the interaction with cells, RGD containing peptides were incorporated into thus obtained hydrogels and they were employed for cell encapsulation studies (Figure 1.5) [21].

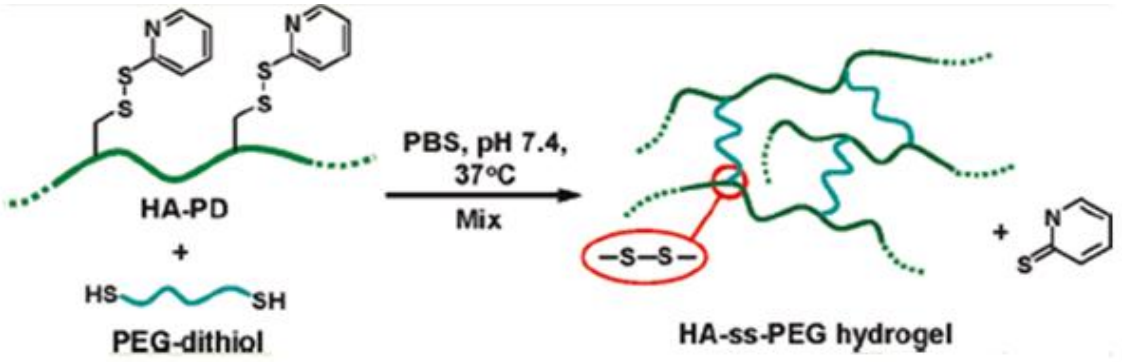

Figure 1.4. Preparation of hyaluronic acid- SS-PEG based hydrogels via pyridyldisulfide-thiol exchange reaction (From [9] with permission).

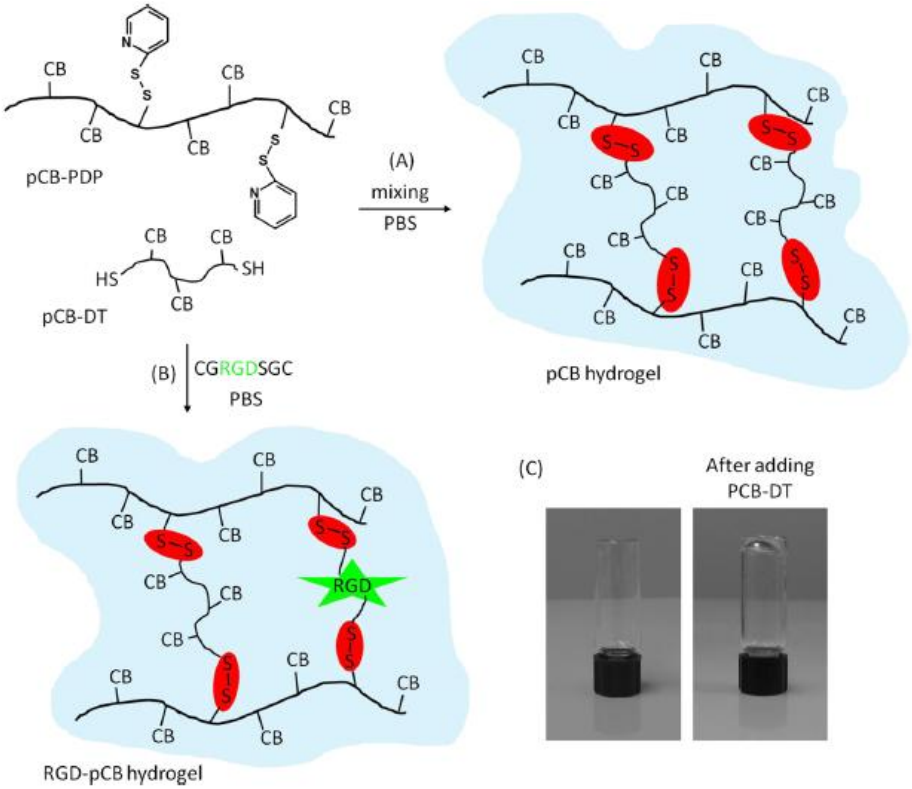

Figure 1.5. The fabrication and modification of hydrogels via pyridyldisulfide-thiol reaction (From [21] with permssion).

1.1.3. Macroporous gels

One of the challenges faced in using hydrogels as matrices for cell encapsulation and proliferation is due to the small pore size of hydrogels. Hydrogels with large pore sizes can be obtained by decreasing crosslinking density but it also reduces the mechanical robustness of the hydrogels. Hence, it is important to develop strategies that would lead to robust macroporous hydrogels that could house and nurture cells. Hence macroporous structures are a requirement in a wide range of applications, including tissue engineering, controlled drug delivery and cell encapsulation. Furthermore, these gels exhibit a fast response to external stimuli due to their high 7 porosity. Generally, macroporous gel structures are produced by phase separation, gas foaming, fiber bonding, and cryogelation techniques. Among these, a technique quite suitable for obtaining macroporous structures for biological applications is cryogelation due its environmentally friendly nature, hence often termed as a green process [22, 23].

Cryogels are commonly formed by polymerization of monomers with or without UV irradiation or crosslinking of polymers in the presence of crosslinker. In this technique, choice of suitable solvent is a very important issue because cryogels are synthesized at subzero temperature. Commonly used high freezing point solvents for cryogelation are water, dioxane, hexane and dimethyl sulfoxide (DMSO) [24, 25].

A porous structure can be formed due to polymerization or crosslinking around solvent crystals that are formed below their freezing points. These solvent crystals act as templates around which the monomer gets concentrated and eventually polymerize. Stable porous structure can be obtained upon melting of the solvent crystals after completion of gelation, where the areas occupied by the solvent forms the voids. Recently, macroporous gels have been designed using cryogelation method by the Mikhalovsky group. Poly(2-hydroxyethyl methacrylate) cryogels were obtained by free radical polymerization at -12 ^{o}C. Mechanically stable, soft and elastic gels were obtained with high yields (Figure 1.6) [26].

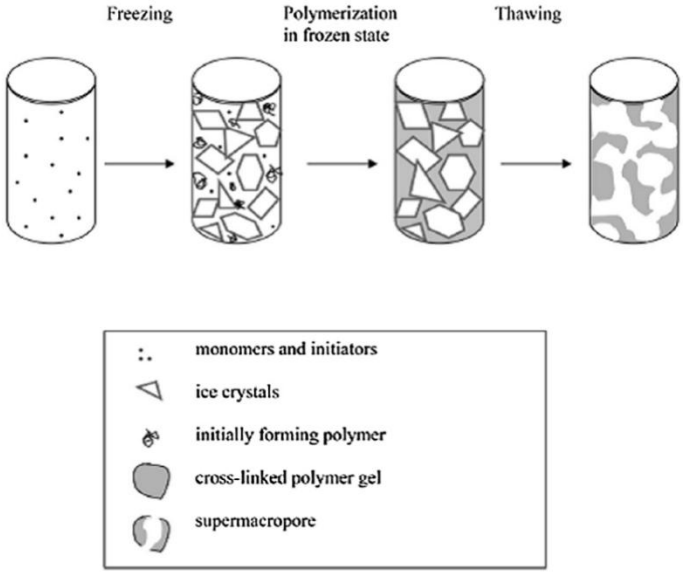

Figure 1.6. General scheme of producing of cryogel (From [27] with permission).

Not only the microscale morphology but also the physical appearance of cryogels can be quite different from hydrogels. Figure 1.7 shows dry and swollen gels formed by conventional and cryogelation techniques. It can be deduced that cryogels retain their original shape and porous structure, whereas conventional gels are partially destroyed upon squeezing because of brittle network structure and there lack of a homogenous pore structure [28].

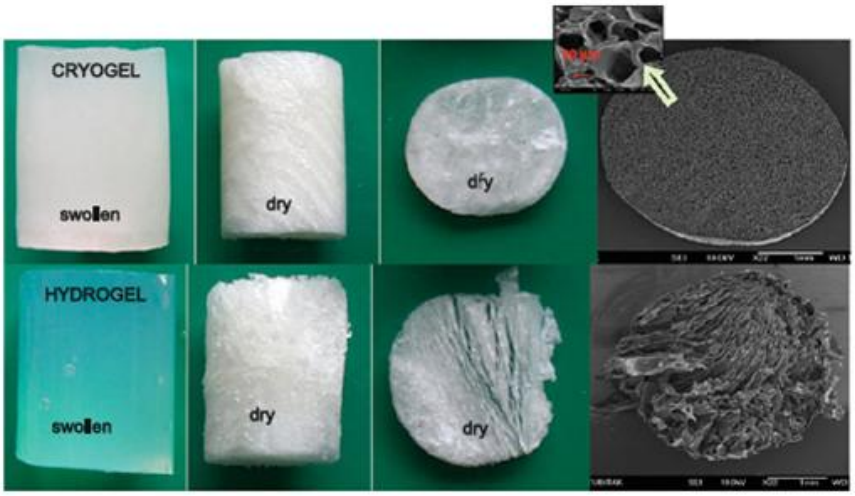

Figure 1.7. Dry and wet conventional and cryo-gels producing differences gelation techniques (From [28] with permission).

In 2010, Kahveci and coworkers reported an approach for synthesis of polyacrylamide cryogels using cryogelation techniques. Unlike conventional polyacrylamide cryogels obtained by redox process, the photo-polymerization based procedure initiates the gelation only after irradiation and thus prevents the formation of hydrogels during freezing, which leads to control over homogeneity of pore sizes [29]. In 2010, Dispinar and coworkers reported the preparation of PEG based degradable cryogels (Figure 1.8). Cryogels were fabricated by the Michael addition reaction between a trifunctional PEG-amine and maleimide based crosslinker. Cryogels with homogenous porous structures were obtained with high yields. Afterwards, the disulfide containing cryogels were degraded with a 9 thiol-based reducing agent to show that thiol-disulfide exchange reaction can be used for obtaining efficient degradation [30]. No information on the efficiency of network formation i.e. the welldefined nature of crosslinking was reported in this work.

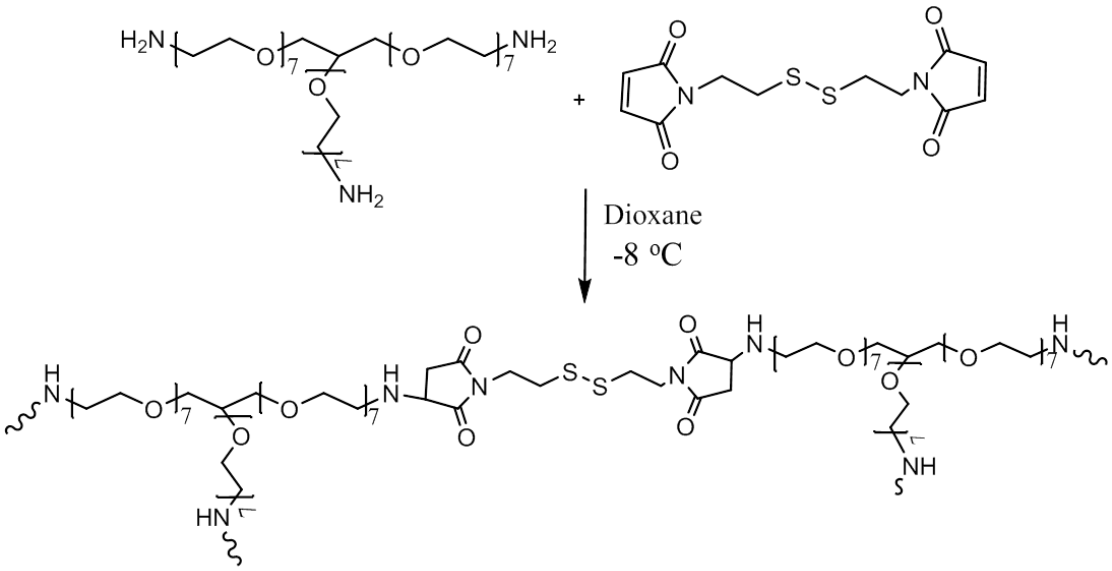

Figure 1.8. Fabrication of PEG based cryogels.

1.1.4. Functionalizable Hydrogels

While hydrogels have been widely evaluated as hydrophilic matrices for controlled drug release, tissue engineering applications, wound healing dressing, and contact lenses [2], for many of these applications, it is often beneficial to have functionalizable hydrogels. Hydrogels amenable to chemical conjugations are usually synthesized using reactive

monomers or macromers with reactive functional groups such as activated esters, click chemistry components, epoxides, activated carbonates, amines, aldehydes and ketones so that they can be functionalized with covalent linkages to molecules of interest.

Biologically relevant molecules can be chemically conjugated to hydrogels and these could be preferred method for attaching drugs, peptides or proteins to hydrogels. Thiol containing molecules are generally used for the functionalization since thiol groups present in several biomolecules. Thiols are either naturally present on many biomolecules or they can be 10 incorporated as cysteine residues at desired positions. Thiols of cysteine groups in biomolecules have been shown to undergo efficient reactions with maleimide [31, 32], disulfide containing molecules [33, 34] and vinyl sulfones [35].

These functional groups can be incorporated into hydrogels to offer a handle for obtaining polymer based bioconjugates. In 2014, Sanyal and coworkers published a paper containing thiol reactive PEG based bulk and micro-patterned hydrogels using photo-polymerization. As monomers, allyl methacrylate and PEG methacrylate were used. Functionalization of allyl groups in the gel with thiol containing molecules could be easily undertaken via the photochemical thiol-ene click chemistry under mild conditions (Figure 1.9) [36].

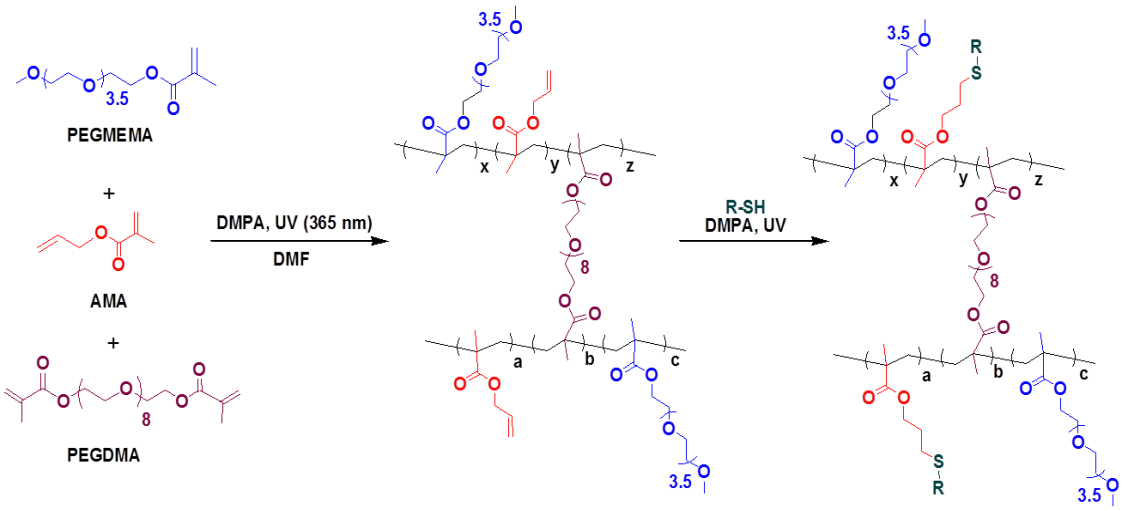

Figure 1.9. Functionalization of reactive hydrogels.

In 2010, Kosif and coworkers synthesized novel thiol-reactive hydrogels containing maleimide functional groups. As monomers, a furan-protected maleimide-containing monomer and PEGMA were used. By retro Dies-Alder reaction, some of the furan protecting groups were removed and so an in situ crosslinking during polymerization was achieved. Using the efficiency of functionalization of remaining maleimide groups, gels were treated with various thiol containing molecules via the Michael addition reaction (Figure 1.10). Using this approach, control over extent of protein immobilization was demonstrated [37].

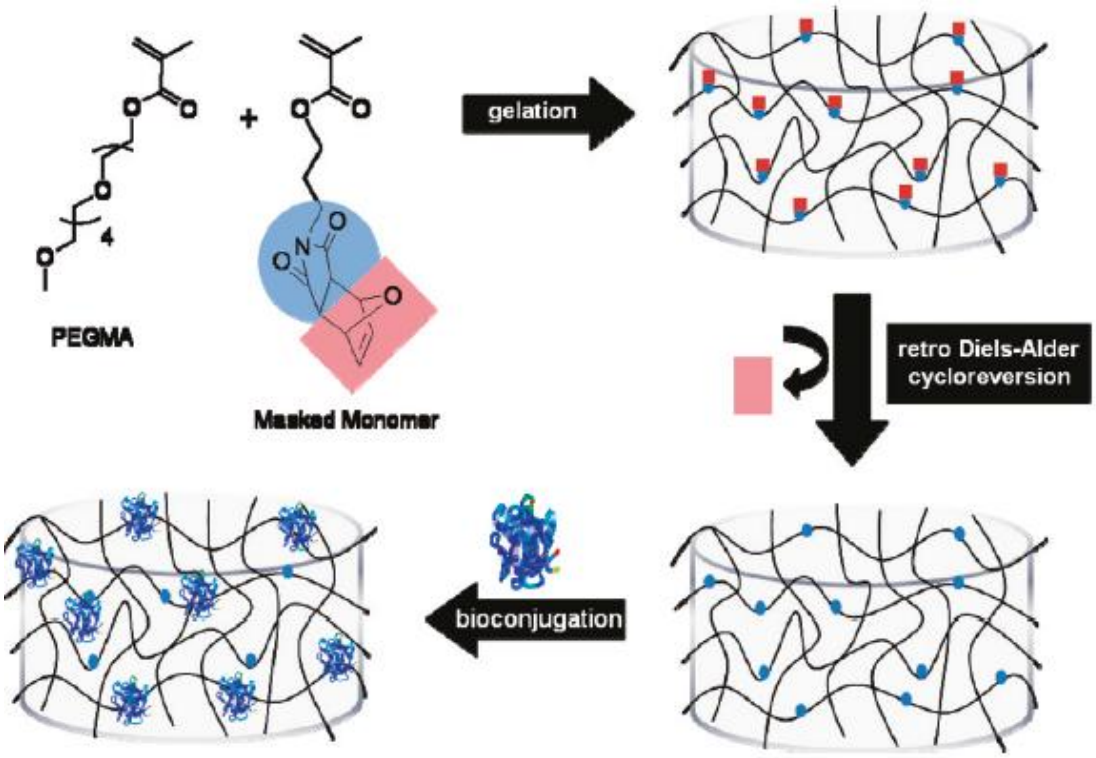

Figure 1.10. Schematic representation of production of reactive maleimide containing hydrogels and functionalization of these hydrogels with biomolecules (From [37] with permission).

As an extension of above work, Park and coworkers used a photo-polymerization based method to obtain reactive poly(ethylene glycol)-based bulk and micropatterned hydrogels. As photo-polymerization is an easily applicable method for obtaining microstructures, micropatterned hydrogels containing masked maleimide groups were successfully synthesized. Then, by the help of the retro Diels Alder reaction, masked

maleimide groups were converted to the thiol reactive groups. As an example for biomolecular immobilization, thiol-reactive maleimide containing hydrogel patterns were reacted with a thiol-containing biotin ligand. Afterwards, FITC labeled streptavidin was efficiently immobilized onto these hydrogel patterns and effective control over functionalization was achieved (Figure 1.11) [15].

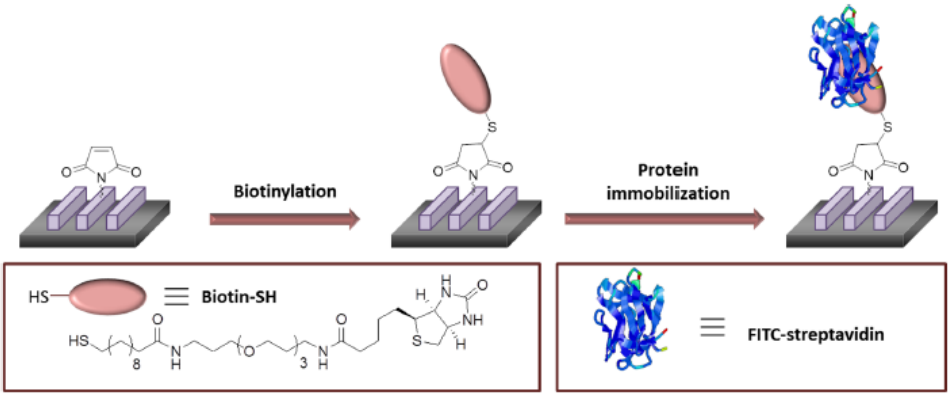

Figure 1.11. General scheme of functionalization of patterned hydrogel with biomolecules (from [15] with permission).

1.1.5. Hydrogels in Drug Delivery Applications and Protein Release

Hydrogels resemble the natural extracellular matrix (ECM) since they absorb high amount of water without decomposing its internal network structures. Also, their porous structures make them excellent candidates for controlled delivery of drugs and proteins. Functionalization of hydrogels with drug molecules can be achieved by either covalently or non-covalently bonding.

Recently, strategies have focused on degradable linkers as they can be used to attach targeting groups and drugs. Therefore, these linkers enable chemical attachment of the biomolecules to gels and depending on the nature of the linker offer stimuli responsive release of drugs. These types of linkers play crucial roles in obtaining effective drug loading and tuning the rate of drug release. In recent years, various degradable linkers have been developed to modify hydrogels with different molecules. Degradable linkers such as carbamate, ester, or disulfide linkages have been widely employed. Carbamate and disulfide linkages allow slow release of covalently attached molecules and they provide

more controlled release profiles than corresponding ester and carbonate linkers, and hence are preferred in the drug delivery applications. In this regard, in recent years, carbonate and disulfide linkages have been used in synthesis of hydrogels.

Goepferich and co-workers synthesized hydrogels using functional aromatic PEG succinimidyl carbonate and branched PEG amines (Figure 1.12). They showed that free succinimidyl carbonate groups in hydrogel reacted with amino groups of proteins, which were released by hydrogel degradation [38].

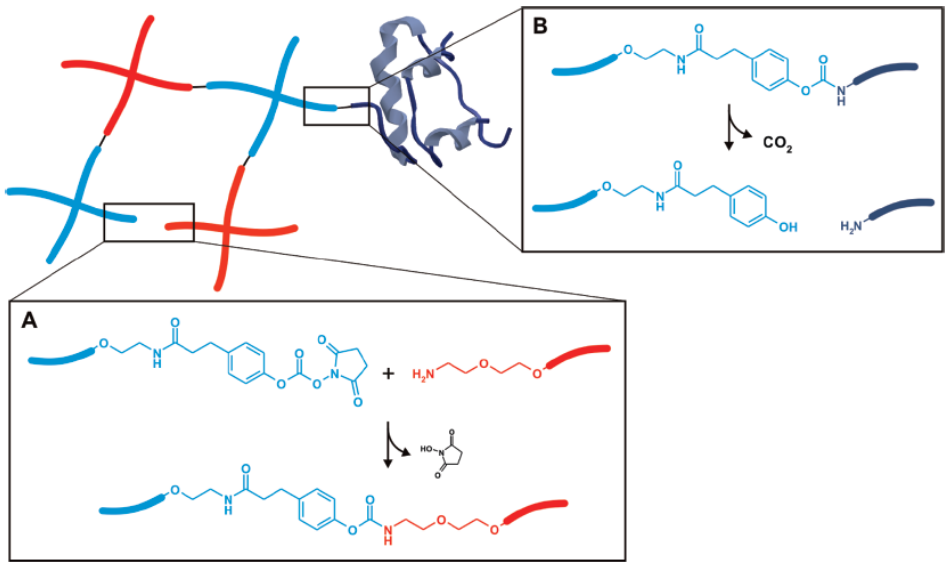

Figure 1.12. Schematic illustration of the protein release from PEG based hydrogel via carbamate cleavage (from [38] with permission).

Also, non-covalent attachment of biomolecules within hydrogel networks can be used in drug or protein delivery applications because of operational simplicity. Biomolecules can also be physically immobilized within hydrogels network with hydrophobic interactions, H-bonding and electrostatic interactions. The release profile of biomolecules can be controlled by diffusion, degradation and swelling properties. The release of biomolecules via diffusion thorough the porous network of hydrogels can be controlled by varying the molecular weight of polymer, nature of polymeric matrix, crosslinking density of hydrogel and the size of the protein in question.

Schmidt and co-workers reported the preparation of PEG based hydrogels obtained with the reaction between 4-armed PEG based polymer and modified hyaluronic acid. They investigated the diffusion properties and the release profile of encapsulated bovine serum albumin (BSA). The authors also succeeded in extending duration of protein release from hydrogel network by increasing crosslinking density of hydrogel [39]. In another example, Leach and co-workers designed a hydrolytically degradable hydrogel network via a Michael-type addition reaction between 4-arm PEG-vinyl sulfone (PEG-VS) and PEG-diester-dithiol. They demonstrated that the obtained hydrogel system was suitable for protein stability and drug delivery applications [40].

Stimuli responsive hydrogels were also synthesized by Sanyal and co-workers by using a novel approach that involved utilization of both Diels-Alder and thiol-disulfide exchange reaction. Hydrogels were obtained by the Diels-Alder reaction between furan-containing copolymer and a bismaleimide containing crosslinker in aqueous media (Figure 1.13). A novel crosslinker with a disulfide bridge was synthesized and varying amount of crosslinker was used to obtain hydrogels. Protein release studies were achieved by the help of the degradation of crosslinker under reducing agent and it was demonstrated that release was depended on the amount of crosslinker [41].

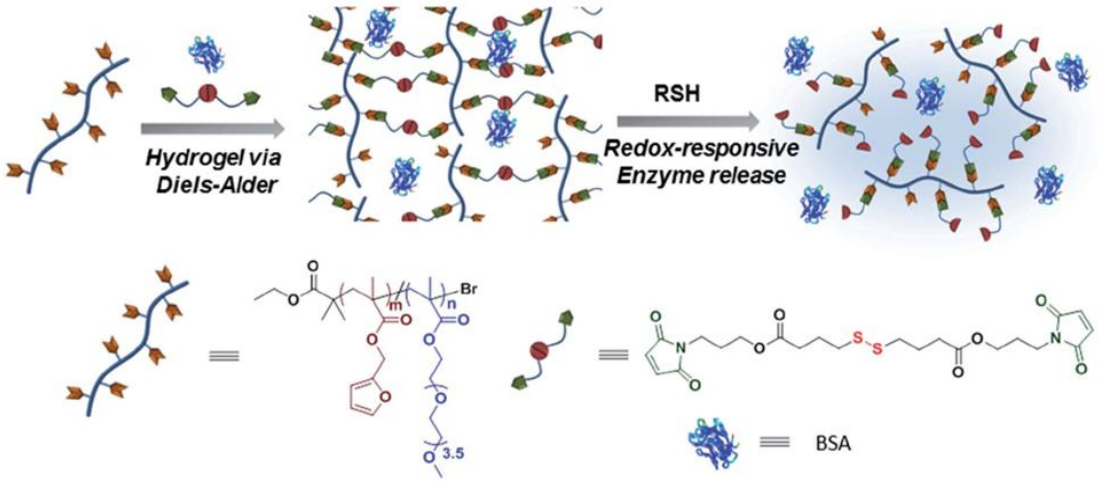

Figure 1.13. Formation and degradation of redox responsive hydrogels (from [41] with permission).

1.1.6. Cyclodextrin Containing Hydrogels

The main reasons for utilization of polymeric matrices for drug delivery is to improve properties such as drug solubility and the duration and location of release. Among the drug carriers, hydrogels with their hydrophilic structures are attractive materials for many hydrophilic drugs. However, majority of the drugs are either quite hydrophobic or poorly water soluble. As interaction between hydrophilic hydrogel and hydrophobic drug is very weak, both high loading and proper release is problematic. As one of the strategies to promote interactions between hydrophobic drug and hydrogel matrix, cyclodextrin (CD) containing hydrogels have been shown to possess high levels of complexation with hydrophobic drugs and they seem to eliminate some of these limitations [42, 43].

CDs are a class of macrocyclic oligosaccharides compose of 1,4-linked D-glucopyranose units. While CDs have hydrophilic outer shell due to hydroxyl groups, their interior cavities are hydrophobic. The hydrophobic cavities form inclusion complexes with hydrophobic drugs in aqueous environments, thus enhancing solubility of hydrophobic drugs in water. CDs have been utilized in pharmaceutical sciences because of these multifunctional characteristics [44-46]. Cyclodextrins can be classified in terms of their cavity sizes (Figure 1.14). The cavity size of α-CD is insufficient for many hydrophobic drugs and γ-CD is expensive. Thus β-CD has been widely used in pharmaceutical applications because of its availability and cavity size suitable for the widest range of drugs [47].

A study achieved by Arslan and coworkers reported CD-containing hydrogels that enabled sustained release of the hydrophobic drug puerarin, commonly employed in the treatment of glaucoma. Hydrogels were obtained by click chemistry reaction between PEGs containing bisallyl end groups and heptavalent thiol modified β-cyclodextrin (Figure 1.15). Drug content of resulting hydrogels were obtained by utilizing solution absorption method and puerarin release was investigated using UV-vis spectroscopy [48].

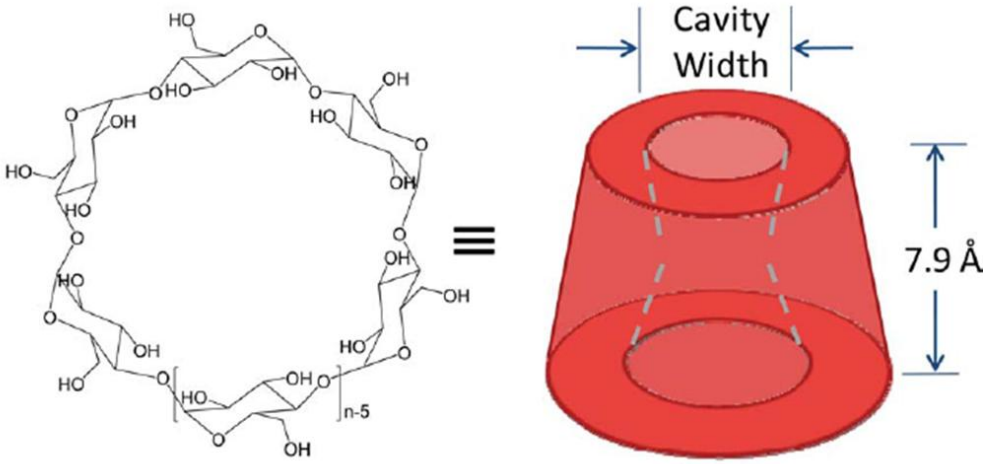

	Number of glucose units, n	Cavity Width (Å)
α-CD	6	4.7 – 5.3
β-CD	7	6.0 – 6.5
γ-CD	8	7.5 – 8.3

Figure 1.14. Chemical structure of CDs and their dimensions (From [47] with permission).

A study by Velaz and coworkers studied a hydrogel based drug delivery system. This system was generated by crosslinking of β-cyclodextrins with epichlorohydrin. For this purpose, four different model drugs were selected. While two of them have anti-inflammatory property (naproxen and nabumetone), the others are antifungal drugs (naftifine and terbinafine). The release of drugs from hydrogel were investigated and they observed that CD based hydrogels were suitable assustained release systems.

Another strategy for CD based hydrogel for drug delivery was reported by Kros and coworkers [49]. In this study, hydrogels was generated via Michael addition reaction between thiol functionalized β-CD and dextran appended with maleimide functional groups. β-CD was utilized both as a crosslinker and drug carrier, since it is multivalent and makes inclusion complex with hydrophobic drugs (Figure 1.16). Obtained drug loaded hydrogels proved to be highly potential candidates for controlled drug delivery applications.

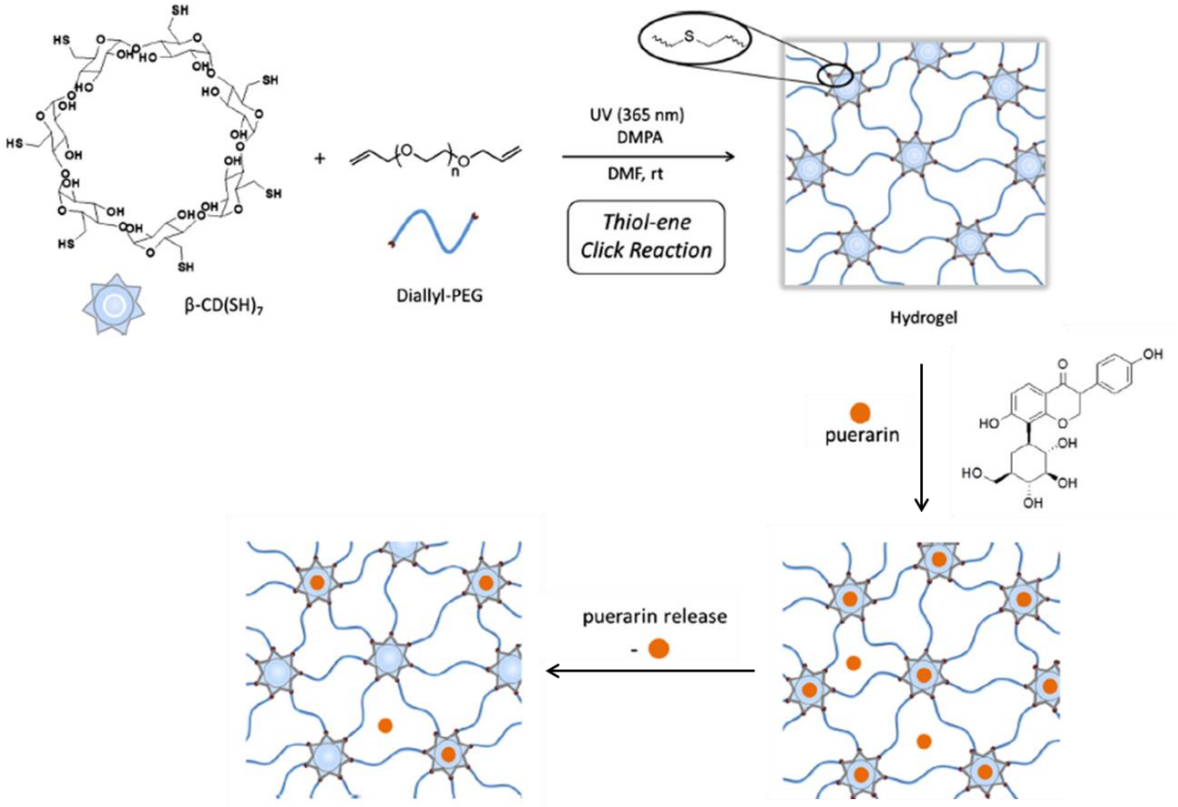

Figure 1.15. General scheme of hydrogel formation and puerarin release from hydrogel (from [48] with permission).

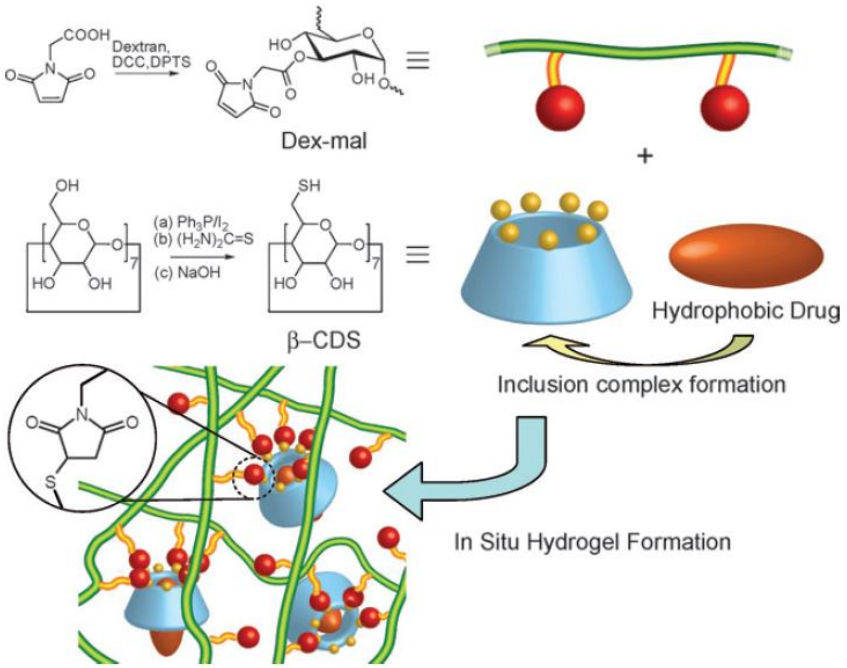

Figure 1.16. Schematic representation of in situ forming β-cyclodextrin based hydrogels for using drug delivery applications (from [49] with permission).

1.2. Iron Oxide Nanoparticles

Since part of the thesis utilizes modification of magnetic iron oxide nanoparticles, a brief summary of their properties are given in the following paragraphs. Employment of iron oxide nanoparticles in biological applications is an increasing trend for recent years. Especially their use in a wide spectrum of applications such as magnetic resonance imaging (MRI) contrast agent, magnetic cell labeling, drug delivery, and hyperthermia have attracted growing interest. The particular size of iron NPs plays a vital role determining in determining their physical and chemical properties because a narrow distribution of properties are required in obtaining consistent results in biomedical applications. Most efforts have focussed on their synthesis with uniform sizes in tens of nm and good dispersibility [50]. Surface modifications of NPs play a vital role since it inhibits their agglomeration and reduces their high surface energy. Solvent evaporation, salting-out, dialysis, supercritical fluid technology, micro-emulsion, mini-emulsion, surfactant-free emulsion, and interfacial polymerization are some of the methods for modification of iron nanoparticles.

The choice of preparation methods can vary depending on the desired application area and size requirement. Generally, biocompatible and reactive polymers are preferred in the surface modification of iron NPs since there is a need to allow conjugation of biological molecules to allow targeted delivery of desired molecules such as drug, peptide, antibody and enzymes.

1.2.1. Functional Polymers

Recently, functionalizable polymers have attracted interest due to the need of facile functionalization of a variety of polymers based nanomaterials such as nanoparticles, nanogels, polymer brushes and thin polymeric coatings in biomedical application. Reactive polymers are contain various reactive groups in the side chains on polymer. These reactive groups on the polymers may be due to various types of functional groups in the monomer. These groups on the polymer allow the attachment of new molecules or installment of desired molecules onto the polymer and so they contribute toward fabrication of biologically significant materials. The fabrication of functional materials such as

nanoparticles for delivery, biomolecular immobilization platforms and theranostic agents such as dye appended polymers for imaging and polymer coated nanoparticles. Nowadays, functional polymers are widely used as surface coatings on iron oxide nanoparticles to increase their biocompatibility and make them suitable for various applications by conjugation of desired molecules and ligands.

1.2.2. Functionalizable Polymers for Coating of Iron Oxide Nanoparticles

Generally, synthetic and naturally occurring polymers are used in surface modification of nanoparticles. Although natural polymers such as dextran, gelatin and chitosan are utilized in increasing numbers, modification with synthetic polymers like polystyrene, poly(Nisopropylacrylamide), poly(ethylene glycol) methylether methacrylate (PEGMEMA), poly(caprolactone) are also preferred since they can be synthesized with control and tailored for specific purpose.

Modifications of the surfaces of nanoparticles with synthetic reactive polymers are a highly desirable since polymers are multifunctional materials. For example, surface functionalization with hydrophilic groups by the help of the reactive groups simplifies solubility of NPs in aqueous 20 medium, and contributes to their biocompability and allows immobilization and release of guest molecules. Thus modifying their surface functional groups makes them promising materials for various biologically relevant applications.

Methods for obtaining polymer-coated NPs can be broadly divided in two categories: the ‘grafting to’ and ‘grafting from’ methods [51].

1.2.2.1. Grafting to Approach**.** In this method, the polymeric coating is formed by the reaction of preformed polymer containing reactive end groups and a suitable anchoring groups on the substrate surface (Figure 1.17). Reactions take place either via hydrophobic and electrostatic interactions or chemical attachment. The advantages of this method is that the exact composition of the preformed reactive polymers can be characterized by various analytical methods, and also due to ease of synthesis of free polymers in solution, this system emerges as a convenient method for controlling polymer architecture [52].

However, low grafting density of NPs is observed since steric hindrance of polymers in binding with the anchoring groups on nanoparticle surfaces.

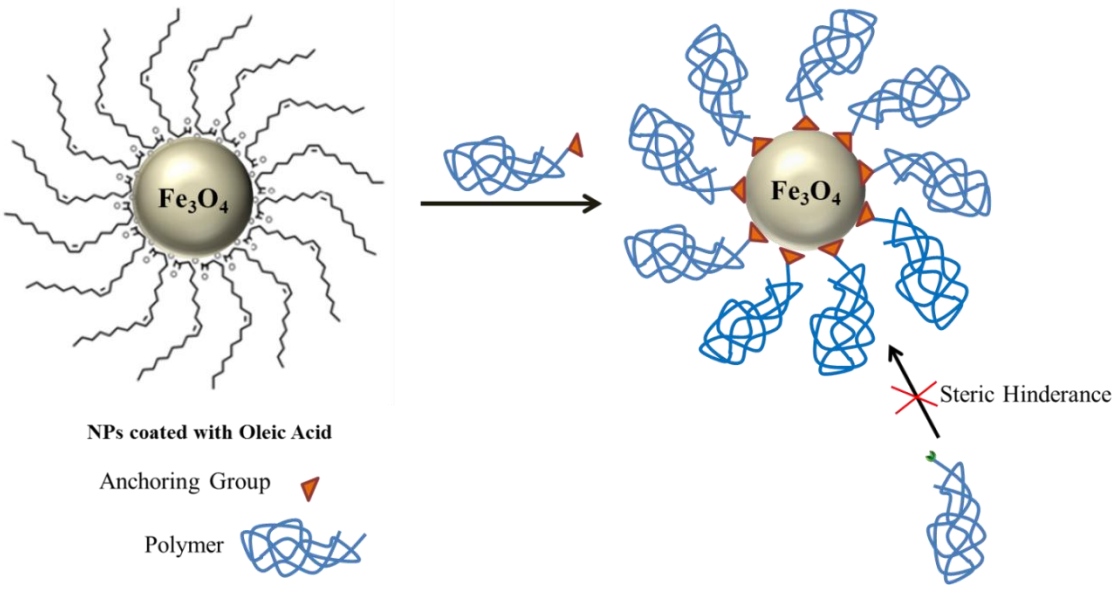

Figure 1.17. General scheme of surface-anchored polymer chains via Grafting to method.

Abundant examples are present in the literature that utilizes this strategy for modification of nanoparticles. Mattoussi and coworkers used this method for demonstrating surface modification of iron oxide nanoparticles. Oleic acid coated NPs are endowed functionalization ability with target molecules by coating them with a copolymer containing several catechol anchoring groups and terminally functionalizable PEG moieties (Figure 1.18) [53]. A functionalized polymer with azide groups was attached onto iron oxide surface and then modified surface was reacted with rhodamine B containing alkyne groups to demonstrate alkyne-azide cycloaddition as a tool of functionalization.

1.2.2.2 Grafting from Approach. Polymerization from the nanoparticle surface can be initiated via different polymerization techniques (Figure 1.19). Atom transfer radical polymerization (ATRP) [54], nitroxide-mediated polymerization (NMP) [55], reversible addition-fragmentation chain transfer polymerization (RAFT) [56] and ring opening polymerization (ROP) [57] are methods to prepare such end functional polymer that are tethered onto particle surface. Higher grafting density and better stability of NP-polymer composites can be acquired using this approach.

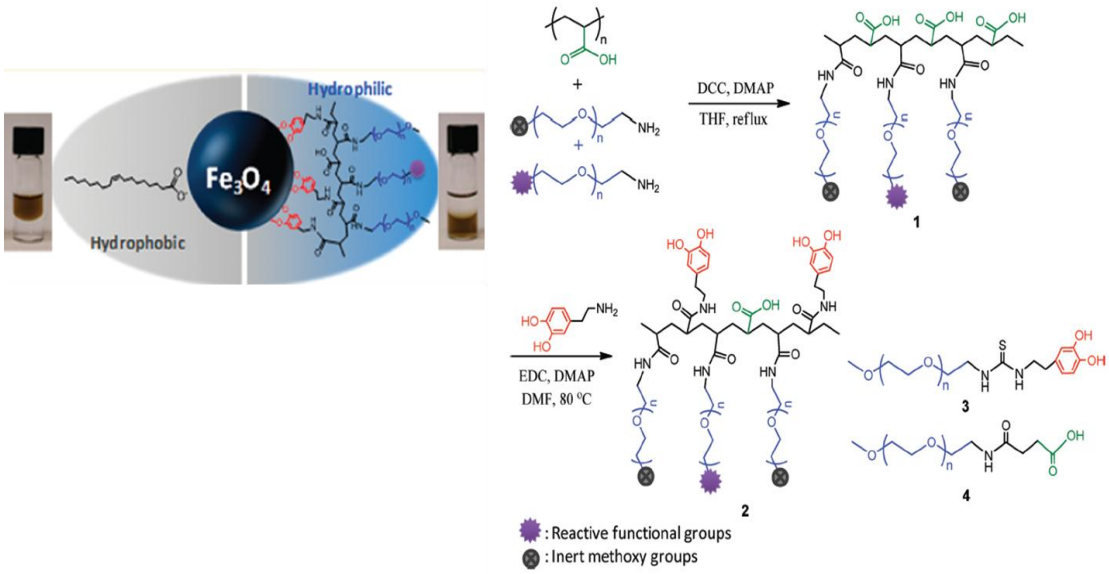

Figure 1.18. Reaction scheme of NPs employing grafting to method (from [53] with permission).

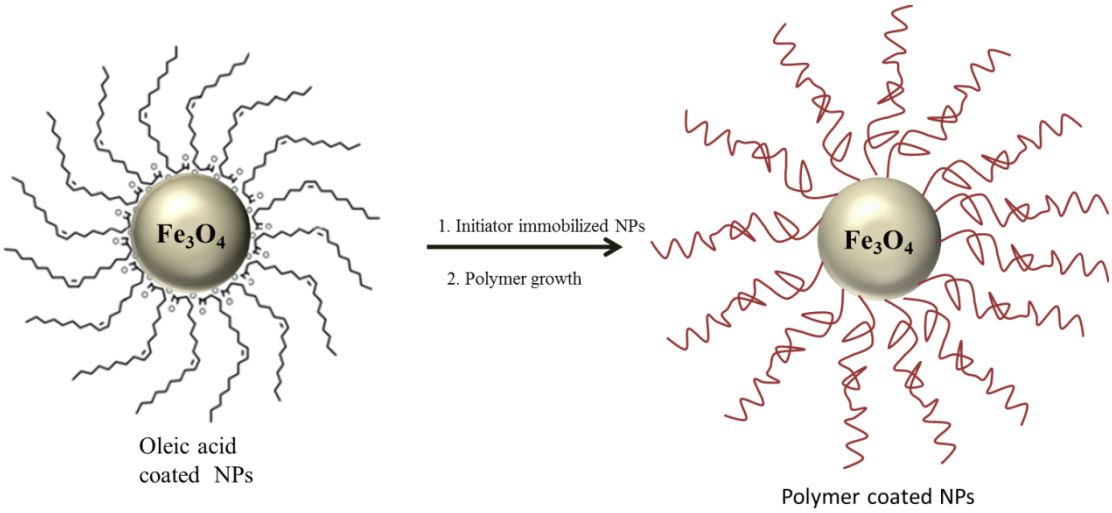

Figure 1.19. Polymer coated NPs via 'grafting from' method.

A recent study by Oz and coworkers disclosed a methodology to obtain polymer coated magnetic iron NPs utilizing the 'graft from' method. RAFT polymerization was utilized to synthesize polymer brushes and then brushes end-groups of these polymer chains were modified with azides and maleimide groups i.e. alkyne and thiol reactive units (Figure 1.20). Functionalization with reactive molecules on the chain ends of the polymer brushes resulted in a modular pathway for modification of magnetic NPs for use in various

biomedical applications, in particular targeted cancer cell imaging as demonstrated in this study [58].

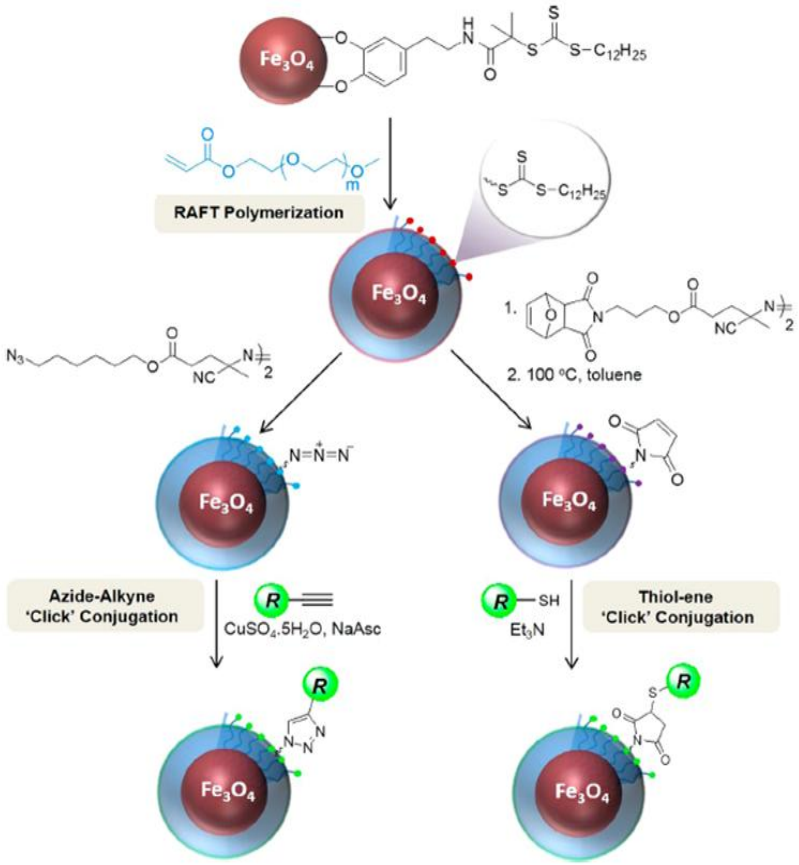

Figure 1.20. General scheme of reactive magnetic surface (from [58] with permission).

1.2.3. Reversible Addition Fragmentation Chain Transfer (RAFT) Polymerization

Reversible addition-fragmentation chain transfer (RAFT) polymerization, invented by Rizzardo and co-workers in 1998, is a method with growing application among the various controlled living radical polymerization techniques. RAFT polymerization is used in the synthesis of biologically compatible materials, owing to the fact that it does not require any toxic metal catalysts for the polymerization and also it's compatibility for different functional groups and monomers. The mechanism of RAFT polymerization is showed in Figure 1.21 [59-61]. As can be seen, chain transfer agents in the RAFT process are needed to facilitate the polymerization and to check molecular weight distribution since they allow the necessary polymer chain equilibrations. Dithioesters, dithiocarbamates, and

dithiocarbonates or xanthates are used to provide a reversible chain transfer process in RAFT polymerization.

Commonly, due to their facile preparation and versatility thiocarbonylthioesters are used as a reversible chain transfer agent in RAFT 24 polymerization [60]. Notably, the functional group present on the chain transfer agent (CTA) enables the addition of new monomers between the S-R bonds to yield block copolymers. Also, the RAFT group (the group of thiocarbonylthio and Z) which is activating group, can be altered in a variety of ways to introduce the desired functional group at the ω-end. The Z group on the RAFT group enables the radical groups to easily bind to the thiocarbonyl (C = S) bond, thus plays an important role in the efficiency of polymerization.

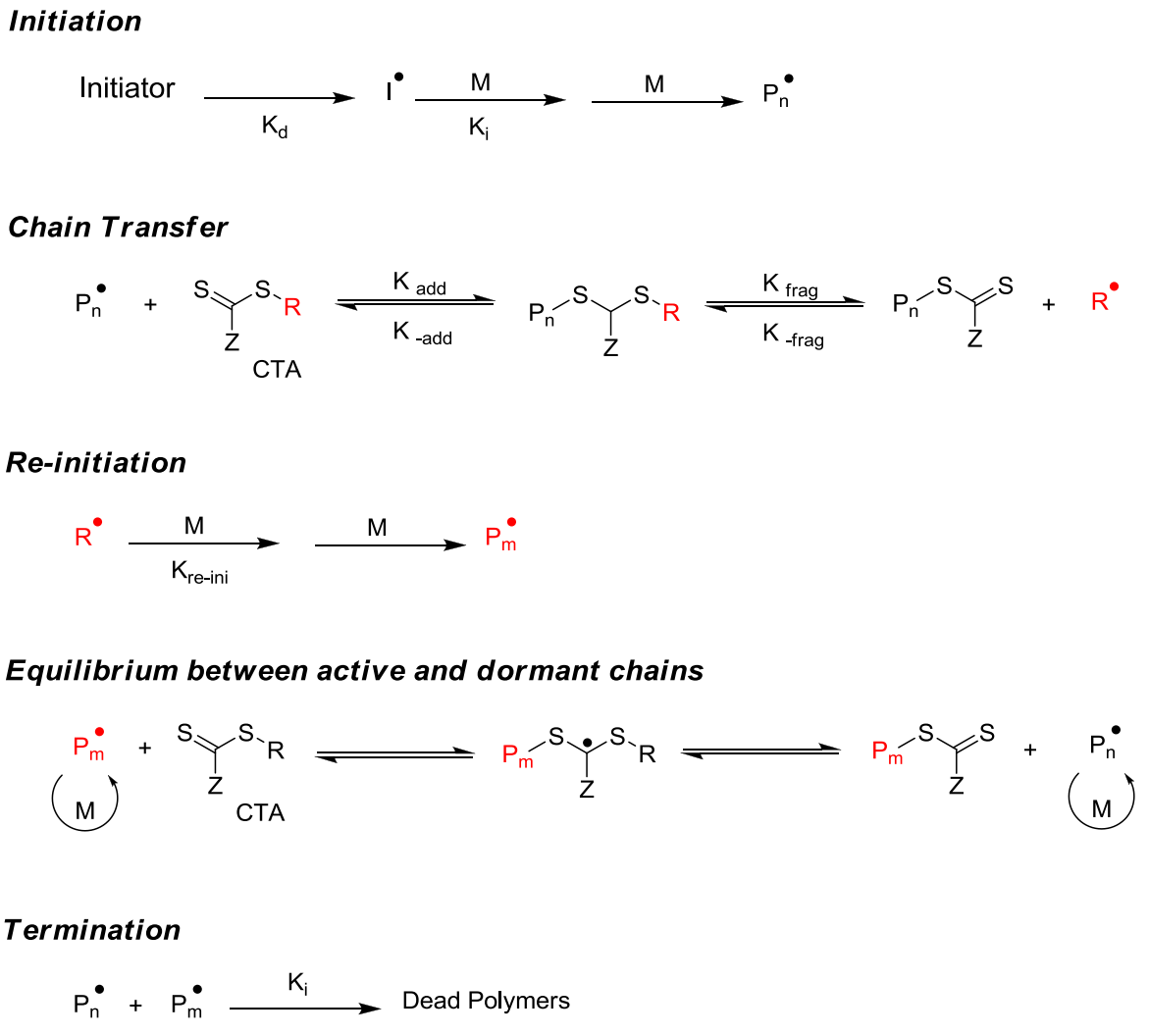

Figure 1.21. General mechanism of RAFT polymerization.

Selectivity of suitable RAFT agents is a very important issue since sustainability of polymers depends on the RAFT agent. Due to its living nature, RAFT is quite versatile. Homopolymers, block copolymers and brush type polymers can be prepared by RAFT polymerization.

1.2.4. End Group Modification of RAFT Polymers

RAFT polymerization, among various controlled radical polymerization techniques is quite effective since the process has good tolerance for a wide range of reactive groups, solvents, monomers and initiators. Thiocarbonylthio groups at the ω-ends of the polymers can serve to modify polymers as they easily react with nucleophiles or undergo thermal elimination. A lot of methods including thermolysis, hydrolysis, aminolysis, oxidation-reduction and radical induced cross couplings have been employed to combine diverse reactive groups onto ω-ends of RAFT polymers (Figure 1.22) [62]. The sixth chapter of this thesis focuses on utilization of RAFT polymerization technique to fabricate novel reactive polymer coated functionalizable magnetic NPs surface. Although, due to time constraints, we focused on installing reactive groups as side chains, one can also install reactive groups on chain ends using the chain end modification reactions listed in this section. These will be pursued in future studies.

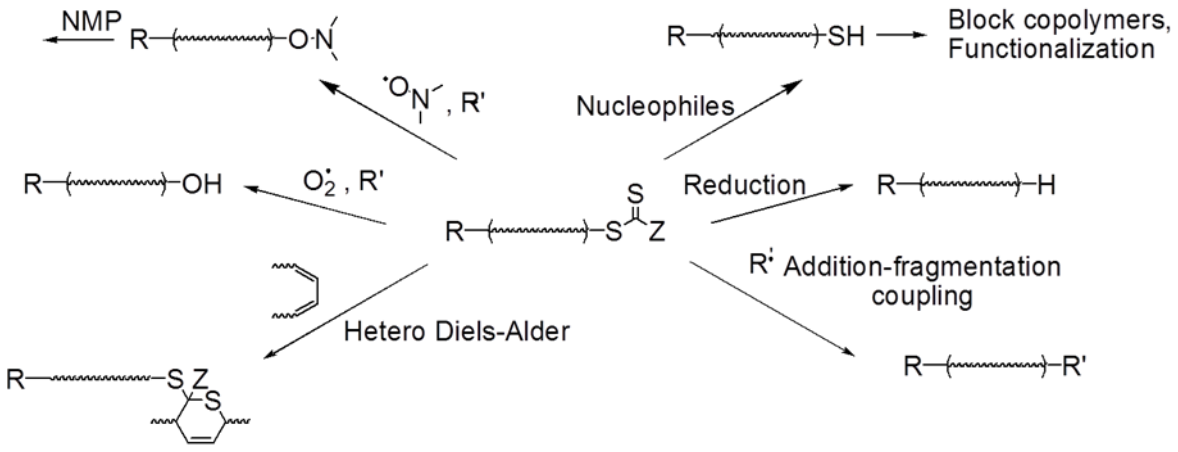

Figure 1.22. End group modification of RAFT polymers.

2. RESEARCH OVERVIEW

The research reported in this thesis explores five different projects with a common theme of developing polymeric materials as hydrogels or nanoparticle coatings suitable for delivery of therapeutic agents such as drugs or proteins. To obtain these novel materials, the power of various organic transformations is utilized either toward their synthesis, or conjugation and release of bioactive molecules.

Four projects in this thesis are connected to the synthesis, characterization, functionalization and release behavior of hydrogels. Hydrogels are materials that are commonly used for biomedical applications such as contact lenses, drug delivery or protein delivery systems. Functionalization of reactive hydrogels with drug molecules via covalent bonds plays an important role for controlled release systems because covalent linkages provide higher stability than physical encapsulation. The conjugated bioactive ingredients are intended for release over time in particular environments such as with low pH values or reducing agent. Thus novel hydrogels where molecules of interest can be conjugated through acid labile carbamate linkage or thiol-cleavable disulfide bonds were synthesized. Although chemical conjugation onto hydrogels is the method of choice for small bioactive molecules, physical entrapment plays an important role when larger macromolecules such as proteins are used as therapeutic agents. In these cases, the precise pore structure, as well as programmed degradation of hydrogels plays a vital role in release. One of the project investigates using thiol-disulfide exchange chemistry for formation of stimuli-responsive hydrogels. The next project combines the stimuli-responsive degradability of hydrogels with supramolecular complexation of hydrophobic drug molecules to increase effectiveness of delivery. In summary, these projects aim to create a novel and effective hydrogel system that can serve as a modular platform for predictable release system.

Additionally, the thiol-disulfide exchange chemistry used in this thesis to fabricate novel hydrogels is also employed to synthesize reactive polymer coatings onto magnetic nanoparticles. A platform that can be used for conjugation of hydrophobic molecules, their magnetic transport and finally their release under particular environment was also developed.

3. HOOKED ON CRYOGELS: A CARBAMATE LINKER BASED DEPOT FOR SLOW DRUG RELEASE

The materials in this chapter have been adapted from the following article: Aydin, D.; Arslan, M.; Sanyal, A.; Sanyal, R. Hooked on Cryogels: "A Carbamate Linker Based Depot for Slow Drug Release", *Bioconjug. Chem.*, Vol. 28, No. 5, pp.1443–1451, April 2017.

3.1. Introduction

Over the past decade, hydrogels have attracted a lot of interest due to their widespread applications in areas such as drug delivery, tissue engineering, diagnostic sensors and implant coatings [1, 3, 64-67]. Growing interest in these materials stems from their facile fabrication, low cost, chemical versatility and facile interfacing with various biological materials. In recent years, hydrogel coatings on implants and devices have been utilized as depots for slow release of proteins and drugs to facilitate the acceptance of these foreign objects in the body [68, 69]. Such polymeric materials in injectable forms, sheets or discs have been employed as depots for slow release of chemotherapeutic drugs as a postoperative step to eradicate any residual or latent cancerous cells that leads to recurrence of tumor [70]. Both physically and chemically crosslinked hydrogels can be employed as such reservoirs, where the drug can either be physically encapsulated or covalently attached. Chemically crosslinked hydrogels with covalently attached drugs through appropriate linkers can provide slow and extended release without undesirable burst release. Characteristics such as swelling, porosity and degradability of these hydrogels can be utilized to tailor the release profile of the therapeutic agent. The fabrication chemistry also has a profound effect on the physicochemical properties of the hydrogels and the structure-property relationship mostly shapes the preferred synthetic approach. While a wide range of fabrication methodologies such as radiation polymerization [71], azide-alkyne cycloaddition based 'click' chemistry approaches [6-8], Diels-Alder reaction [10, 11, 39, 72]. and Michael-type addition reactions [12] along with free radical photocrosslinking have been utilized to obtain functional hydrogels,

photopolymerization based techniques remain attractive due to their operational simplicity, high efficiency and temporal control over polymerization at ambient or physiological temperatures [14, 16, 34, 73].

Recent years have witnessed considerable focus on the linker chemistry utilized for conjugation of therapeutically active materials onto polymeric substrates [74]. Appropriate choice of linker allows tunability of release profiles in response to the surrounding biological environment. Stable yet cleavable linker chemistry is desirable to minimize premature release in a burst manner. Hydrolysable linkers containing the family of carbonyl based functional groups such as, esters, carbonates, carbamates and certain amides are among the most widely employed linkers for drug conjugation. Among these hydrolysable groups, carbamate based linkers allow slow release of covalently attached molecules and provide relatively stable linkages compared to their ester and carbonate counterparts, yet they are more labile than amides [75-80]. For example, a carbamate based linker chemistry was recently exploited by Hu coworkers in which they reported biodegradable multifunctional mixed micelles consisting of doxorubicin (DOX) conjugated to a diblock copolymer via carbamate linkages and demonstrated a pH-dependent drug release [81]. Shabat and coworkers reported a dimeric prodrug platform by using a double 1,4-quinone methide rearrangement. They synthesized the dimeric prodrug with the anti-cancer drugs doxorubicin, and camptothecin. A catalytic antibody 38C2 was used to trigger the release of the two drugs in an enzymatic environment [82]. In another study, Wang and coworkers designed a drug delivery system based on the carbamate linker where gold nanoparticles with a poly(ethylene glycol) (PEG) spacer was used to tether and thereafter release doxorubicin [83].

Herein, we outline the synthesis and evaluation of novel bulk hydrogels and cryogels containing N-hydroxysuccinimide (NHS) activated carbonate functional groups as reactive sites for attachment of drug molecules and enable their slow release through the hydrolysable carbamate linker. First, fabrication of bulk hydrogels with varying amounts of the amine-reactive activated carbonate containing monomer and hydrophilic PEG-based methacrylate monomer were carried out and these hydrogels were evaluated for their physical characteristics, drug conjugation and release efficiencies. As observed for most photo-polymerized PEG-methacrylate based hydrogels, low porosity of these materials was

evident from their limited swelling and poor drug release. Hence, in hope to obtain materials with slow yet higher overall release characteristics, cryogels were fabricated.

A family of highly porous reactive cryogels containing varying amounts of the NHS-based activated carbonate containing monomer were obtained. Functionalization of these cryogels with anti-cancer drug doxorubicin was carried out to demonstrate drug conjugation to the network and subsequently the release of the drug to aquatic medium. Finally, the efficacy of these drug loaded cryogels was evaluated through their in *vitro* cytotoxicity against MDA-MB-231 human breast cancer cells.

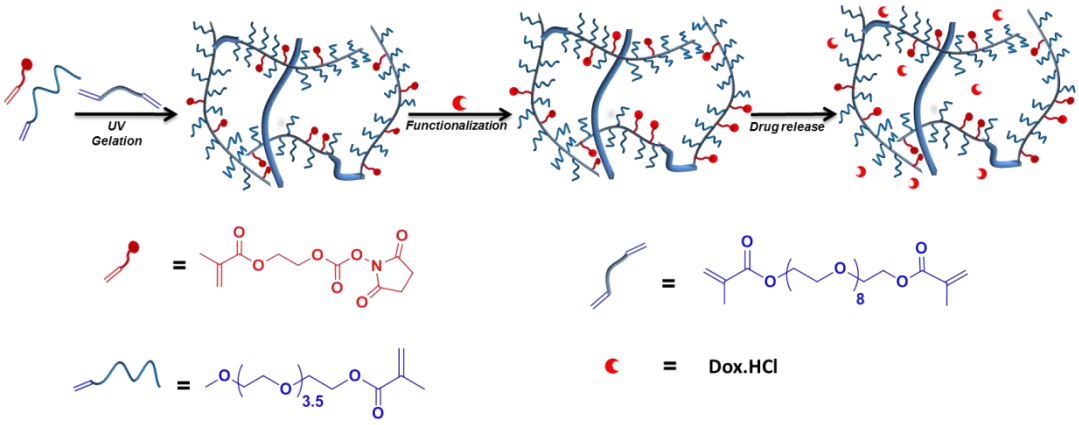

Figure 3.1. Schematic illustration of synthesis and functionalization of carbonate containing hydrogels and release of drug molecules from hydrogels.

3.2. Experimental Section

3.2.1. Materials and Instrumentation

Poly(ethylene glycol) methyl ether methacrylate (PEGMEMA, M_n = 300 gmol^{-1}, poly(ethylene glycol) dimethacrylate (PEGDMA, M_n = 550 gmol^{-1}) and 2-hydroxyethyl methacrylate (HEMA) were obtained from Sigma Aldrich and purified by filtering from activated aluminum oxide column prior to use. 2,2-dimethoxy-2-phenylacetophenone (DMPA), triethylamine (TEA), and *N*,*N*′-disuccinimidyl carbonate (DSC) were purchased from Sigma Aldrich. Anhydrous dichloromethane was obtained using the SciMatCo

purification system. Solvents were obtained from Merck and used as received without further purification unless otherwise noted. Synthesis of 2-(*N*-succinimidylcarboxyoxy)ethyl methacrylate (SCEMA) was undertaken according to previously reported procedure [84]. All photopolymerization reactions were performed at 365 nm using a handheld UV Lamp with a 100W spot bulb at a distance of 10 cm. UV-vis studies were performed using a Varian Cary 50 Scan UV-vis spectrophotometer. Elemental analysis data for hydrogels was obtained using a Thermo Electron S.p.A Flash EA® 1112 elemental analyzer. Infrared spectra of bulk hydrogels and cryogels were obtained using ATR-FTIR (Thermo Fischer Scientific Nicolet 380). For cytotoxicity experiments, human breast adenocarcinoma MDA-MB-231 cell lines were obtained from ATCC (Wesel, Germany). Cells were kept in the logarithmic phase of cell growth for the duration of experiments. The cells were maintained in RPMI-1640 culture medium (Roswell Park Memorial Institute) [Gibco, Invitrogen] supplemented with 10% fetal bovine serum [FBS] [Lonza], 100 U/mL penicilin 100 g/mL streptomycin and 0.25 g/mL amphotericin B at 37 ^{o}C, 5% CO_2, and 95% relative humidity. 4′,6-diamidino-2-phenylindole (DAPI) were obtained from Sigma-Aldrich. The cell internalization images were collected using Zeiss Observer Z1 fluorescence microscope connected to Axiocam MRc5 using a Zeiss Filter set 38.

3.2.2. Fabrication of Bulk Hydrogels

Hydrogels were obtained through photopolymerization of PEGMEMA and SCEMA monomers with PEGDMA crosslinker. A series of hydrogels obtained using PEGMEMA monomer with varying SCEMA content in the feed are presented in Table 1. A representative synthetic procedure for hydrogel (BH2) is as follows: a mixture of SCEMA (7.0 mg, 0.026 mmol), PEGMEMA (69.7 mg, 0.232 mmol), PEGDMA (7.12 mg 0.0129 mmol) and DMPA (3.32 mg, 0.0129 mmol) in dimethyl formamide (DMF) (40 μL) was prepared to a small vial and the mixture was sonicated for 10 seconds before placing the vial under a UV lamp (365 nm) for 60 min. After the gelation reaction, the bulk hydrogels were washed with DMF followed by tetrahydrofuran (THF) several times to remove all unreacted reactants. The hydrogels were dried in *vacuo* and the acquired cylindrical hydrogels of 1.5 mm diameter were cut into 1.5–2.0 mm thick slices

3.2.3. Swelling of Hydrogels

Swelling studies were conducted by sampling a circular piece of dried hydrogel in a vial containing distilled/deionized water at room temperature. At periodic time points, the increase in mass of hydrogel sample was recorded after removing the hydrogel from water and absorbing excess surface adhered water with a tissue paper. The water uptake percentage was obtained using the equation:

$$\text{percentage of swelling (\%)} = (W_{wet} - W_{dry}) / W_{dry} \times 100$$

where W_{wet} and W_{dry} are the weights of the hydrogels in their swollen and dried state, respectively.

3.2.4. Morphological Analysis Using Scanning Electron Microscopy (SEM)

SEM was used to characterize surface morphologies of obtained hydrogels and cyrogels. SEM images were obtained using an ESEM-FEG/EDAX Philips XL-30 (Philips, Eindhoven, and The Netherlands) instrument operating at an accelerating voltage of 10 kV.

3.2.5. Fabrication of Cryogels

Representative procedure for synthesis of cryogel CH2: Into a small vial containing a mixture of SCEMA (7.0 mg, 0.026 mmol), PEGMEMA (69.9 mg, 0.232 mmol), PEGDMA (141.65 mg, 0.258 mmol) and DMPA (3.30 mg, 0.01296 mmol), 1,4-dioxane (1.5 mL) was added and mixture was sonicated for 45 s. Then, the reaction vial was placed in a cryostat at -13 °C and exposed to UV irradiation (365 nm) at a distance of 10 cm for 90 m. After the gelation reaction the vial was taken out of the cryostat and thawed at room temperature. In order to remove all unreacted reactants, the cryogels were first washed with 1,4-dioxane followed by rinsing several times with THF. The cryogels cut into smaller dimensions of 1.5–2 mm thick slides and were dried in *vacuo*. Likewise, other cryogels were prepared using various dilutions with the same solvent to evaluate the effect of these parameters on the morphology of cryogels (Figure S2).

3.2.6. Conjugation of Doxorubicin to Bulk Hydrogels and Cryogels

Gels containing NHS-activated carbonate functional group were functionalized with doxorubicin. As a general procedure, gel sample (10 mg) was placed in a vial and a 1.5-fold excess of doxorubicin hydrochloride, corresponding to the carbonate groups in CH_2Cl_2 (2 mL) was added. After adding triethylamine, the reaction mixture was shaken in the dark at room temperature for 12 h. Solution was shaken at 100 rpm to facilitate the diffusion. After the reaction, gels were washed with excess dichloromethane to remove all non-conjugated drug. The drug loading was monitored by analyzing the doxorubicin concentration in the medium using a UV–vis spectroscopy.

3.2.7. Drug Release Experiments

Doxorubicin loaded gels (10 mg each) were put in acetate buffer (pH 5.4) or phosphate buffered saline (PBS, pH 7.4) solutions (4 mL) at 37 °C under 100 rpm mechanical shaking. 4 mL of release medium was periodically replaced with same volume of fresh buffer. By the help of a calibration curve, the concentration of drug in collected media was monitored spectrophotometrically using the absorbance of doxorubicin at 488 nm. The results were expressed in terms of cumulative release.

3.2.8. *In Vitro* Cytotoxicity Experiments

Cytotoxic activity of the cryogels was investigated over MDA-MB-231 human breast adenocarcinoma. Cells (5000 cells/well) were seeded in a 96-well plate in 100 μL appropriate culture medium and incubated at 37 °C for 24 h for cells to adhere completely. Cell adhered plates were treated with CH4 (5 mg) and CH4-DOX at 37 °C for 72 h. After the incubation, sample solutions were removed and wells were washed twice with PBS (100 μL). The amount of viable cells was determined using CCK-8 cell viability assay. By adding CCK-8 (10 %) to every well (total 60 μL) and incubation for 1 h, absorbance values at 450 nm were measured using a microplate reader. These experiments were done as triplicates.

3.2.9. *In Vitro* Cellular Internalization Experiments

Adenocarcinoma MDA-MB-231 human breast cells (50.000 cells/well) were seeded in a 24-well plate as triplicate in 1000 μL appropriate culture medium. Cells were incubated at 37 °C for 72 h with bare cryogel and DOX-conjugated cryogel. After incubation, wells were washed with 500 μL PBS solution twice and cells were stained with DAPI (1 μg/mL) at 37 °C for 30 min. Then, cells were washed with PBS three times and were fixed with 4 % formalin solution at 37 °C. The experiments were carried out in triplicate. Images of drug internalization within cells were obtained using fluorescence microscopy.

3.3. Results and Discussion

3.3.1. Synthesis, Characterization and Functionalization of Bulk hydrogels

A series of amine reactive bulk hydrogels (BH1-BH4) were synthesized using varying amounts of commercially available poly(ethylene glycol) methyl ether methacrylate (PEGMEMA) and the NHS-activated carbonate group containing monomer, where the later was synthesized according to our recent report [84]. Fabrication of hydrogels was carried out under UV irradiation (365 nm) in the presence of a photoinitiator 2,2-dimethoxy-2-phenylacetophenone (DMPA) and poly(ethylene glycol) dimethacrylate (PEGDMA) as a crosslinker (Figure 3.1).

Table 3.1. Bulk hydrogels fabricated via photocrosslinking.

Entry	Hydrogel	[SCEMA]:[PEGMEMA]	PEGMEMA (M_n gmol^{-1})	Gel Content[a] (%)
1	BH1	5 :95	300	92
2	BH2	10:90	300	89
3	BH3	20:80	300	95
4	BH4	30:70	300	92

[a] Calculated as (dry hydrogel weight/total weight of monomers and crosslinker) × 100.

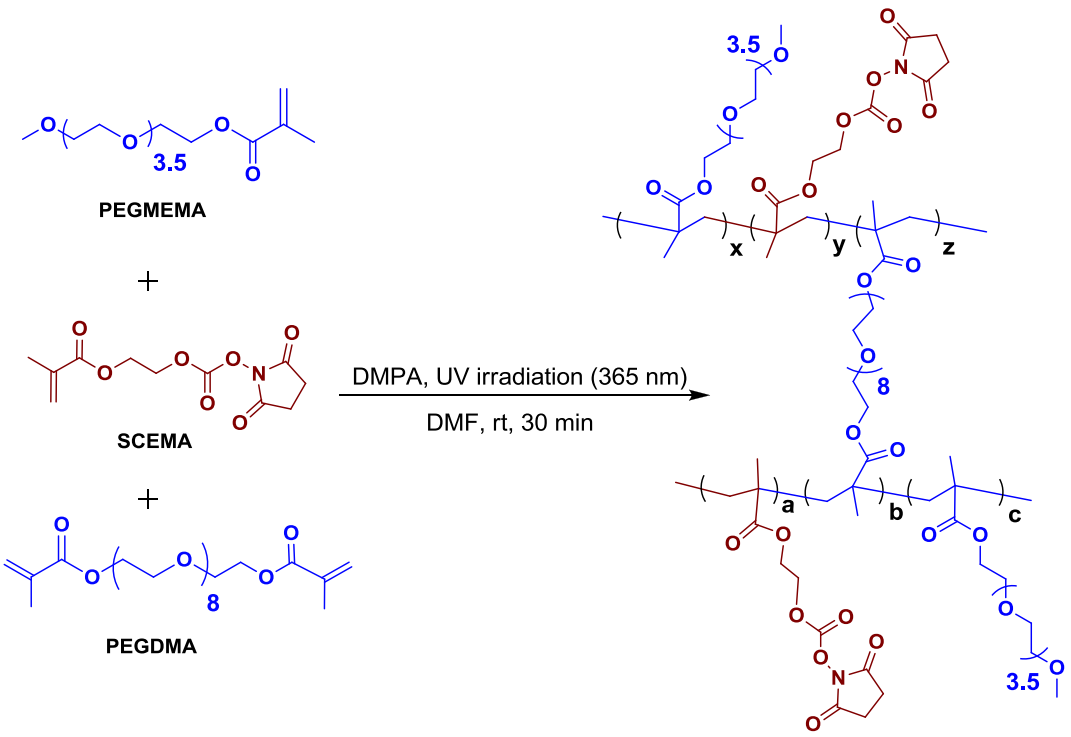

Figure 3.2. Schematic illustration of synthesis of carbonate-based reactive hydrogel.

In order to understand the relative incorporation of individual monomers in the hydrogels, the series of hydrogels with different monomer ratios were analyzed using elemental analysis. As expected, a proportional increment of nitrogen content was observed with an increase of the NHS-activated carbonate group in the hydrogels (Figure 3.3a). Additionally, the bulk hydrogels were also characterized using Fourier transform infrared spectroscopy (FTIR) to confirm the increasing amount of carbonate groups in the hydrogels. As expected, the FTIR spectra of hydrogels exhibited an increase in the intensity of the carboxyl bond stretching peak at 1812 cm^{-1} and 1789 cm^{-1} due to the increment of carbonate monomer (Figure 3.3b).

The swelling capacities of the prepared gels were investigated by recording their water uptake as a function of time till the hydrogels showed constant weight. It was observed that gels reach equilibrium swelling within a few hours and the equilibrium swelling values were consistent with the amount of the poly(ethylene glycol) unit in the hydrogels. Generally, all gels showed an increase in water uptake capacity with a decrease in the hydrophobic monomer content. Notably, hydrogel BH4 showed an increase in the swelling over time and surpassed BH3, presumably due to the increased hydrophilicity of

the newly formed hydroxyl groups upon release of relatively hydrophobic NHS units as resulted from the hydrolysis of the carbonate groups in aqueous environment (Figure 3.4).

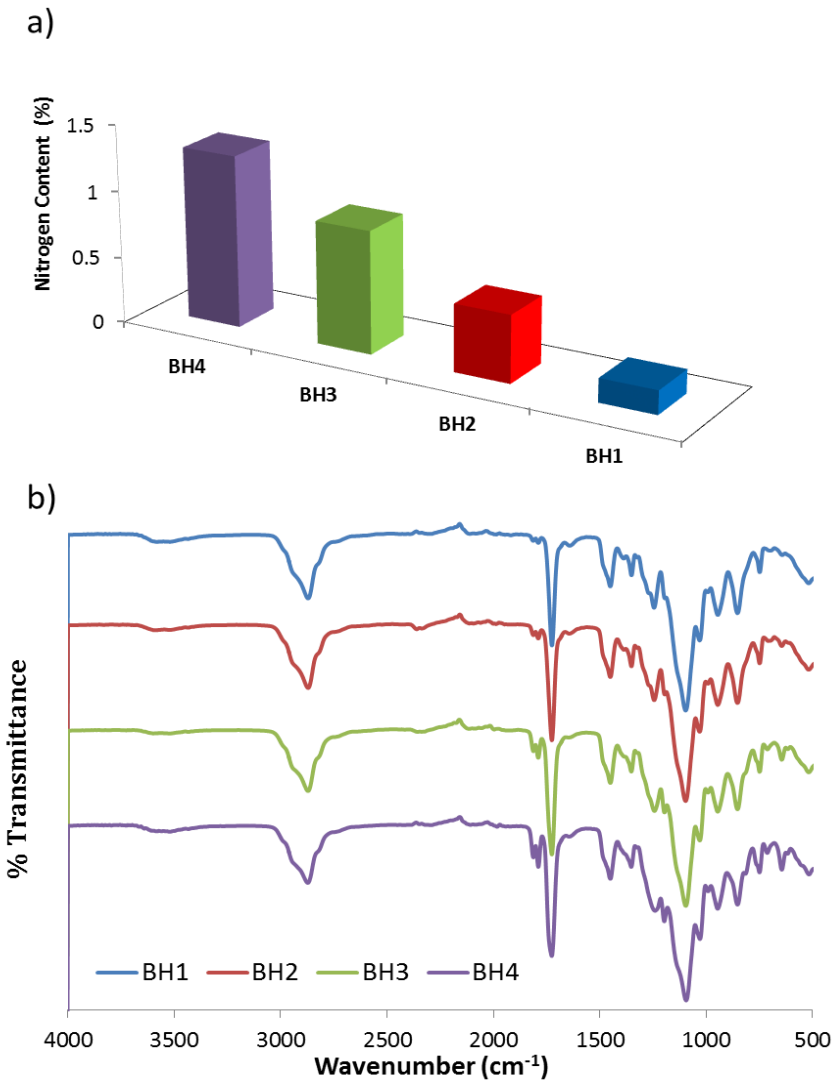

Figure 3.3. (a) Increase in nitrogen atom content of hydrogels with increase in the amount of carbonate monomer in the feed. (b) FTIR spectra of bulk hydrogels with increasing amount of reactive monomer.

Analysis of lyophilized samples of hydrogel BH3 obtained after immersion in aqueous media for 1 and 5 hours shows decrease and eventually complete loss of the infrared bands belonging to the succinimide group at 1812 and 1789 cm^{-1}, thus suggesting their hydrolysis (Figure 3.5).

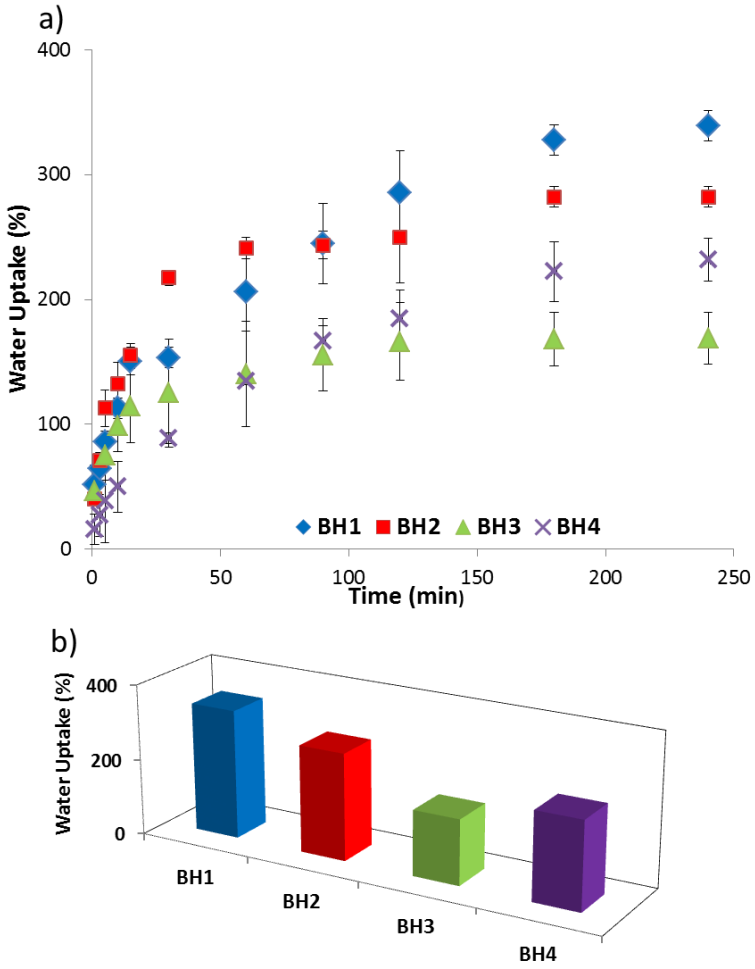

Figure 3.4. (a) Water uptake plots and (b) Comparison of water uptake capabilities with the variation of monomer ratio.

The drug conjugated bulk hydrogels were evaluated in terms of their release properties. As expected, a slow release of drug was observed under neutral conditions since the drug was connected to the hydrogel through a relatively stable, yet hydrolysable carbamate linker (Figure 3.7). Surprisingly, nearly no release of drug was observed for the hydrogels fabricated using conventional method. The maximum drug release over a period of a month was below 5 % under near neutral conditions. Only a slight increase in the drug release (up to 6 %) was observed under mildly acidic conditions (pH=5.4).

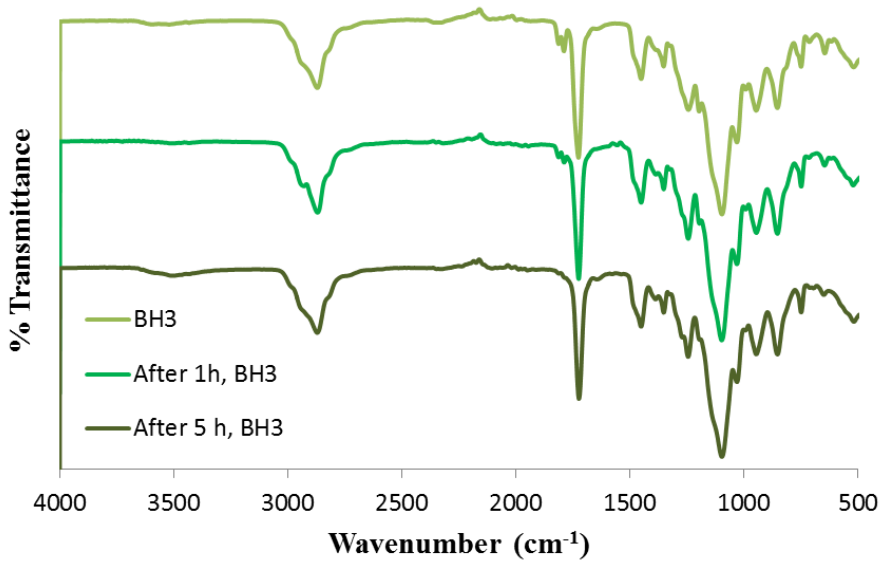

Figure 3.5. FTIR spectra of BH3 in water (after immersion in aqueous media for 1 and 5 hours).

In order to demonstrate the post-polymerization modification efficiencies of fabricated hydrogels, hydrogels with varying amounts of reactive carbonate group were functionalized with the anti-cancer drug doxorubicin (Figure 3.6). The amount of drug conjugation was determined using UV-vis spectroscopy by quantifying the amount of non-conjugated drug in the incubation medium, as well as the unbound drug rinsed from the hydrogels upon subsequent washing with solvents. The analysis revealed that the reactive hydrogels underwent efficient functionalization (75-85%) with the amine containing drug.

The reason for such a low release was evident upon examining the morphology of these hydrogels using SEM (Figure 3.8). The hydrogels obtained using conventional methods have non-porous rubber like microstructures. These slow releasing hydrogels can be useful for applications where such low levels of release over prolonged period suffices, but to increase their applicability one needs to design materials which will exhibit higher release. It was clear that the most important characteristics that one needs to improve in these hydrogels were their porosity and hence fabrication of reactive cryogels was explored.

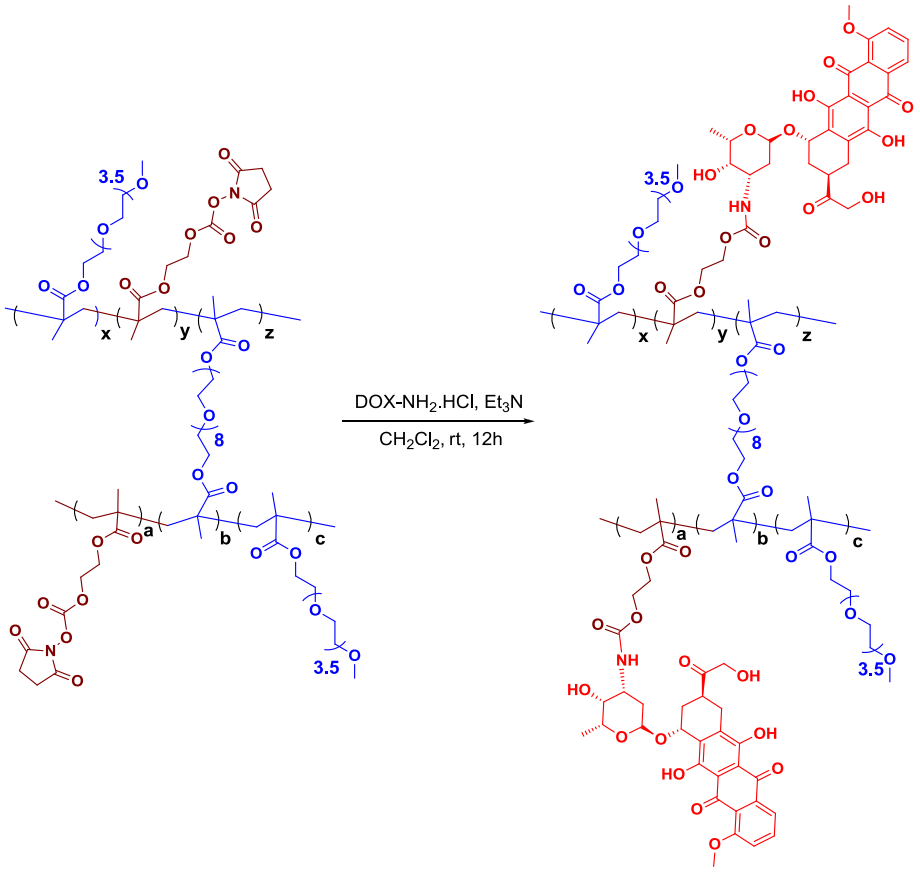

Figure 3.6. Schematic illustration of conjugation of doxorubicin to bulk hydrogels.

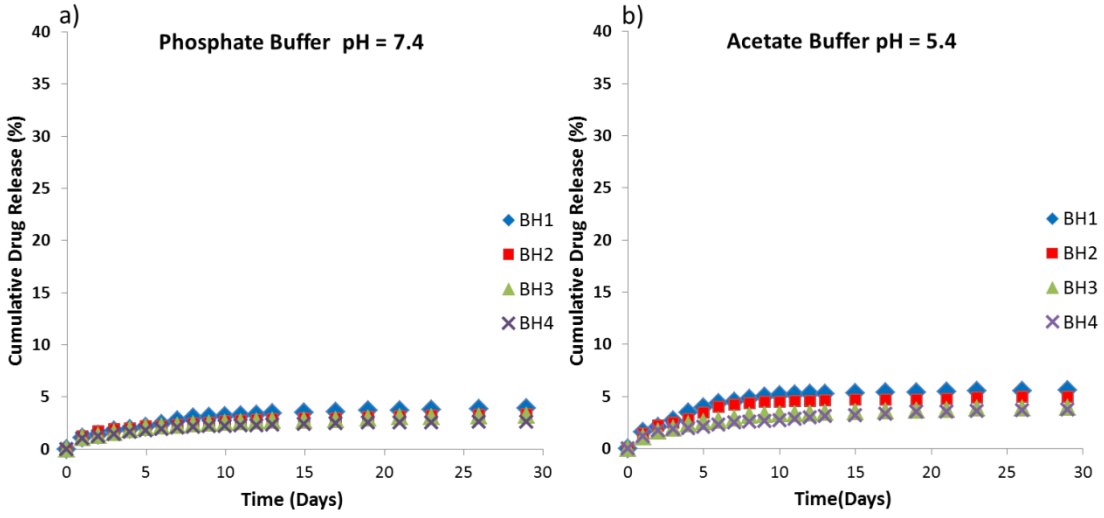

Figure 3.7. In vitro doxorubicin release profile from bulk hydrogels in (a) phosphate buffer pH: 7.4 and (b) acetate buffer pH: 5.4.

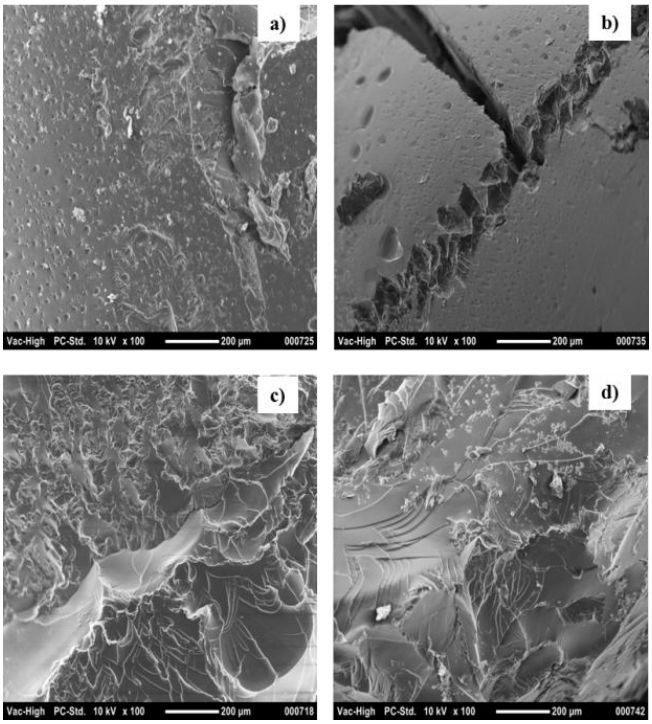

Figure 3.8. Representative SEM images of bulk hydrogels (a) BH1, (b) BH2, (c) BH3 and (d) BH4.

3.3.2. Synthesis, Characterization and Functionalization of Cryogels

As an alternative approach to obtain hydrogels with increased porosity, cryogels were synthesized using the monomers utilized above. Cryogels have been widely investigated for various biotechnological applications due to their highly porous structure, as well as superior mechanical behavior [81, 85]. Fabrication of cryogels was carried out at sub-zero temperatures, since during this process gelation proceeds around frozen solvent crystals that act as templates. Hence, the choice of solvent in cryogelation plays a critical role in determining morphology of gels. For the monomers involved, the best results were obtained upon using 1,4-dioxane as a solvent. Several trials by changing the monomer concentration and temperature were done to optimize conditions for obtaining highly porous cryogels with moderate to high conversions (70–82%) (Table 3.2, Figure A1). Comparison of hydrogel and cryogel samples fabricated using the same monomer composition demonstrated the distinct physical properties of two network system such as appearance, occupied volume and the porosity (Figure 3.9). A set of cryogels with varying

amount of the reactive carbonate monomer were obtained and characterized using FTIR spectroscopy to confirm the increasing amount of carbonate groups in the gels (Figure A2).

An increase in carbonate carbonyl band intensity was observed upon increasing the reactive monomer feed. The cryogels possessed a highly porous morphology as suggested by SEM analysis of the samples in their dry state (Figure 3.10). Furthermore, the cryogels exhibited rapid swelling and much higher equilibrium swelling capacity compared to the conventional bulk hydrogels (Figure 3.11).

Table 3.2. Cryogels fabricated via photo-crosslinking

Entry	**Cryogel**	**[SCEMA] : [PEGMEMA]**	**PEGMEMA (M_n gmol^{-1})**	**Gel Content[a] (%)**
1	CH1	5 :95	300	76
2	CH2	10:90	300	82
3	CH3	20:80	300	69
4	CH4	30:70	300	71

[a]Calculated as (dry hydrogel weight/total weight of monomers and crosslinker) × 100.

Functionalization of these porous scaffolds with doxorubicin proceeded with 69-80% efficiency under conjugation conditions similar to the previously described bulk hydrogels. Drug release studies from these cryogels tested in different pH conditions revealed a pH dependent release (Figure 3.12). As expected, because of the enhanced hydrolysis of carbamate groups in acidic medium, higher drug release was observed at lower pH.

When the release profile of the drug from cryogels was compared to those from the bulk hydrogels under acidic conditions, a seven-fold enhanced release was observed from the cryogels, suggesting the importance of the porous structure for effective hydrolysis of carbamate groups (Figure 3.12b). While higher release was observed for the more hydrophilic cryogels, all cryogels exhibited a sustained release without substantial initial burst.

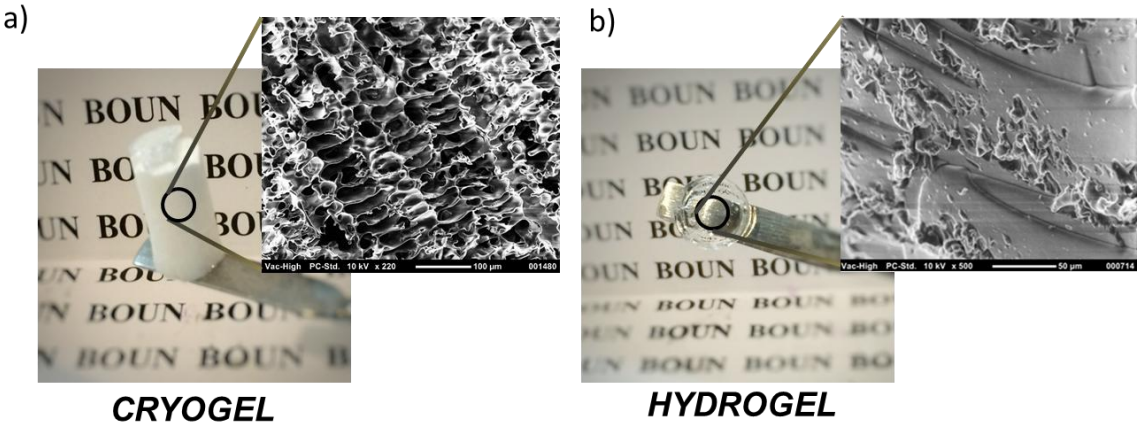

Figure 3.9. Illustrations of (a) cryogel (CH3) and (b) hydrogel (BH3), and their microstructures as deduced using SEM.

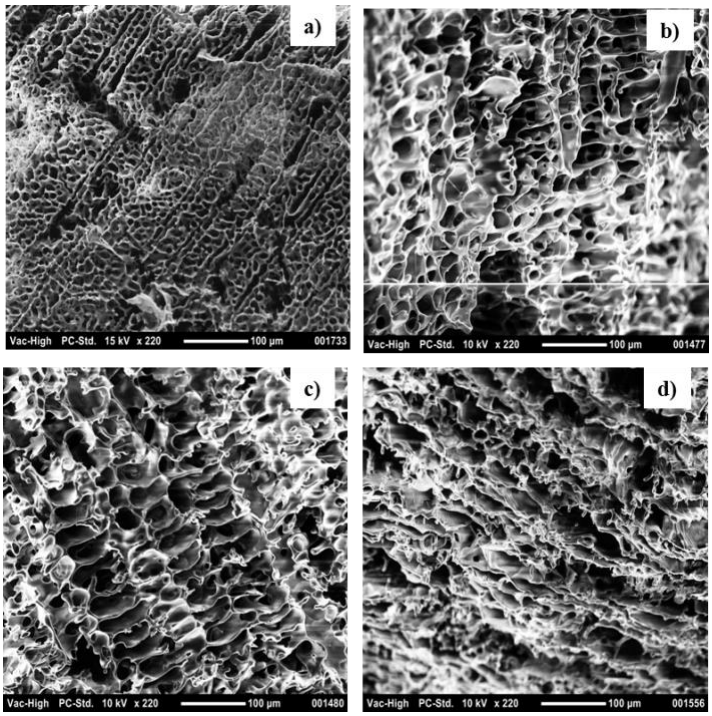

Figure 3.10. Representative SEM images of cryogels (a) CH1, (b) CH2, (c) CH3 and (d) CH4.

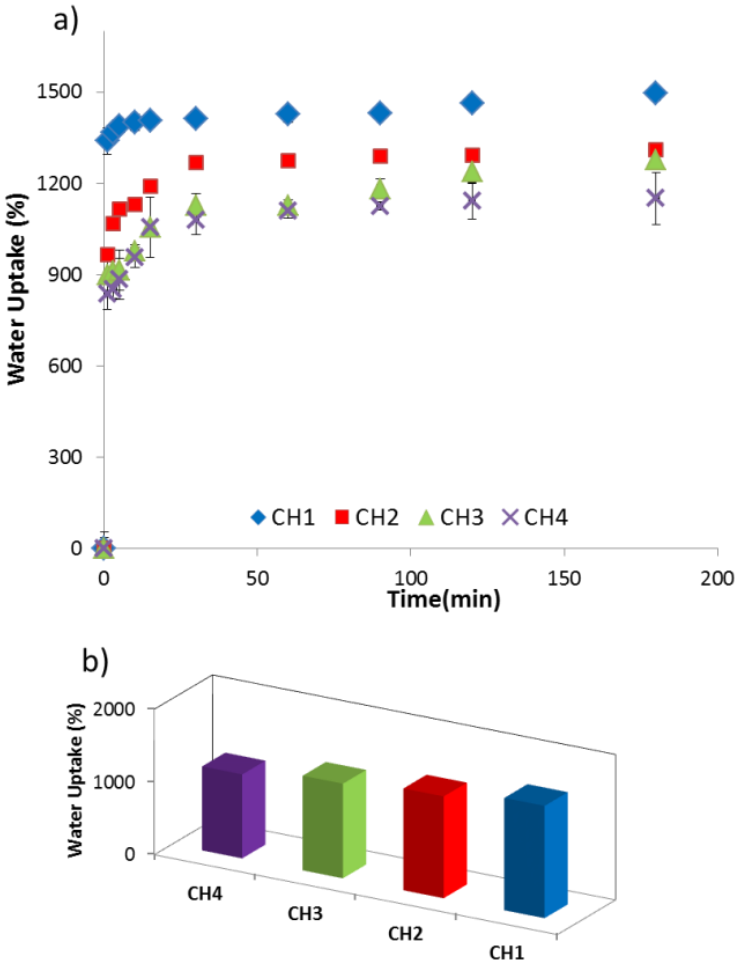

Figure 3.11. Effect of variation in monomer content on (a) water uptake profiles and (b) comparison of equilibrium water uptake capacity for cryogels.

As a next step, the effective release of the doxorubicin from cryogels was evaluated by in vitro cytotoxicity experiments. As a representative example, cryogel CH4 was reacted with doxorubicin and excess non-conjugated drug was washed off using copious amount of dichloromethane.

After drying the sample to remove traces of organic solvent, the drug conjugated cryogel was swollen in PBS and incubated with MDA-MB-231 human breast cancer cells. After 72 h incubation, cell nuclei were stained using a fluorescent dye, 4',6-diamidino-2-phenylindole (DAPI). It was clear from the micrographs that the drug released from the hydrogel was able to enter the nuclei of the cells (Figure 3.13a).

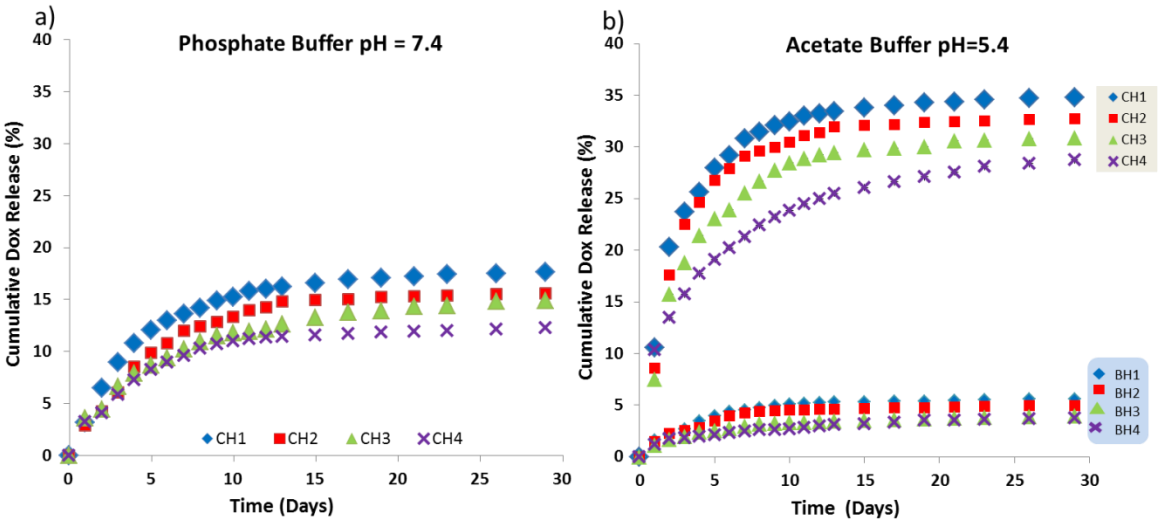

Figure 3.12. In vitro doxorubicin release profiles (a) from cryogels in phosphate buffer pH: 7.4 and (b) from cryogels and bulk gels in acetate buffer pH: 5.4. Release data from bulk gels are included here for comparison. Refer to appendix for plots with error bars (Figure A3 and A4).

Also, from the cell viability assay, it was evident that while the parent hydrogels did not pose noticeable toxicity to the cells, the drug conjugated hydrogels led to substantial cell death (Figure 3.13b). Overall, an effective release of the carbamate linked drug from the cryogel and successful passage to the cell nuclei leading to a loss of cell viability was observed.

3.4. Conclusion

Poly(ethylene glycol)-based conventional bulk hydrogels and cryogels containing amine-reactive functional groups were synthesized using photopolymerization. Hydrogels with varying amounts of amine reactive carbonate groups were prepared with high gel conversions. Although clear and transparent bulk hydrogels with high gel conversions were obtained within a short time; their poor water uptake capacities, non-porous microstructures and very poor drug releasing capabilities even under acidic environments, suggested their limited potential for utilization in biomedical applications.

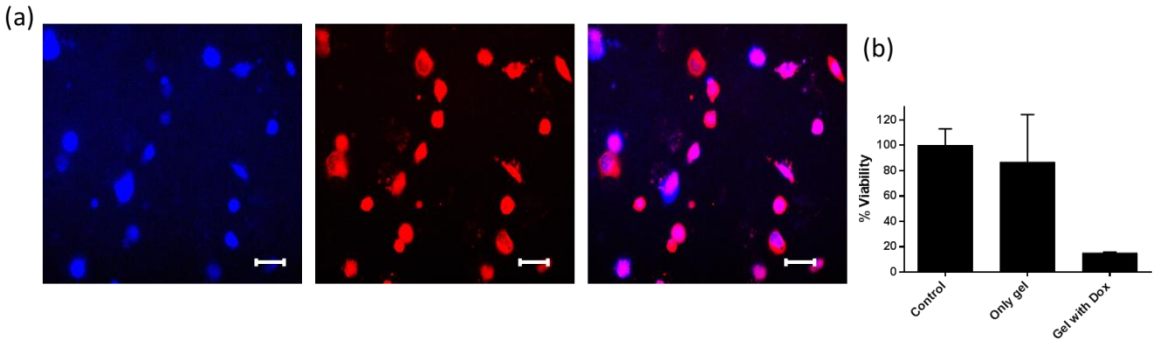

Figure 3.13. (a) Left image: MDA-MB-231 human breast cell nuclei stained with DAPI (blue). Middle image: Red fluorescence from internalized doxorubicin. Right image: Merged fluorescence image. Cells were incubated at 37 ^{o}C for 72 h. Scale bar = 50 μm.

To obtain substantial amount of drug release in a period of time, cryogels with highly porous microstructures were synthesized. The obtained cryogels were functionalized with the amine-containing anti-cancer drug doxorubicin through a hydrolysable carbamate bond formation. According to the release studies, much enhanced and sustained release of the doxorobucin from the cryogel at both physiological and mildly acidic conditions was observed. Release of the drug leading to loss of viability upon cellular internalization on a breast cancer cell line, MDA-MB-231 was also demonstrated. Overall, a novel class of cryogel that can serve as a depot for slow release of cytotoxic drugs was demonstrated through efficient fabrication of the highly porous amine-reactive scaffold, facile drug conjugation, and subsequent sustained drug release of drug to inhibit cell proliferation.

4. FABRICATION OF WELL-DEFINED POLY(ETHYLENE GLYCOL)-BASED HYDROGELS VIA THIOL-DISULFIDE EXCHANGE REACTION

4.1. Introduction

Delivery of protein has emerged as an important class of therapy since the introduction of recombinant insulin almost 25 years ago. At present there are more than 100 proteins that are approved for FDA for use in treatment of diseases or as component of diagnostic tools [86]. Increasing interest in utilization of proteins as therapeutic agents stems from their specificity and complex mode of action. Advances in biotechnological methods has enabled large scale production of proteins through expression in bacteria and yeast, and this method of production also reduces possible immunogenicity of these materials when compared to proteins obtained from animals. In spite of such attractive properties, application of proteins is challenging due to the delicate nature of these materials. Proteolytic and chemical decomposition and loss of stability upon administration often leads to loss of their biological efficacy. Conjugation or encapsulation with polymeric materials has been used as one of the major strategies to address this issue [39, 87-89]. In particular, hydrogels provide a protective matrix for encapsulation of proteins because of their ability to mimic the aqueous environment similar to present in our body [90, 91]. Judicious design of hydrogels also enables control over the release of proteins apart from just serving as a protective reservoir. Several reports in literature have demonstrated that varying the crosslinking density within the hydrogels allows tuning the release profile of encapsulated protein [67, 92].

Hydrogels formed using reversible crosslinking strategies allows their degradation on demand. The reversible linkage chemistry can be pH-sensitive [93, 94], thermoreversible [95], photocleavable [96], redox-sensitive [97], and enzyme cleavable [98]. Among these possible linkages, the disulfide cleavage based redox chemistry is particularly attractive due to its cleavage under mild conditions such as presence of naturally occurring thiol-based reducing agents like glutathione (GSH).

Recently, Wang and co-workers reported synthesis of hydrogels by crosslinking pyridyl disulfide containing hyaluronic acid with PEG-dithiol [9]. The hydrogel formation was efficient and the authors demonstrated encapsulation and release of proteins in presence of GSH. In another example, 8-arm containing dendrimers were appended with pyridyl-disulfide unit and subsequently mixed with 8-arm PEG to afford hydrogels. These hydrogels were used as injectable drug delivery system for ascending genitalinfections during pregnancy [99]. In the above mentioned examples and another related one [100], the crosslinking is random and hence the hydrogels lack a well-defined network structure. Interestingly, the highly efficient and specific chemistry of thiol-disulfide exchange reaction has not been employed for creation of hydrogels with well-defined network structure. It has been reported that hydrogels with well-defined network structures offer better control over both physical and chemical properties in these materials [72, 101]. The only example where disulfides have been incorporated into a well-defined network structure was reported in 2016, where Kong and co-workers synthesized well-defined disulfide bond containing hydrogels by the copper catalyzed click reaction between alkyne terminated 4-armed PEG and azide terminated disulfide bonds-containing poly(3-caprolactone). Disulfide bonds on the hydrogels were used to show reduced cleavability [102]. However the concern of using metal based catalyst for network formation because of toxicity concerns limits the adaptability of this approach for biomedical applications. Given the potential utility of thiol-responsive cleavable materials as an attractive biomaterial, new metal-free approaches toward their synthesis needs to be developed.

In this chapter, the thiol-disulfide reaction based approach towards fabrication of well-defined polymeric networks is explored. Judicious choice of polymer chain lengths should allow one to obtain networks with mesh sizes appropriate for encapsulation and release of a protein of any given size. Apart from the chain length, the chemical composition of the polymer can be used to control the release profiles. The presence of precisely and homogenously located disulfide linkages in the hydrogel can be expected to tune the release profile in the presence of varying amounts of thiol-containing molecules such as dithiothreitol. More importantly, complete release of the protein can be accomplished by dissolving the carrier on demand.

This approach also allows eventual degradation of carrier platform, which is often difficult to achieve under mild conditions. In summary, the study aims to create a novel and effective hydrogel system that can serve as a modular platform for protein encapsulation and release 'on demand'.

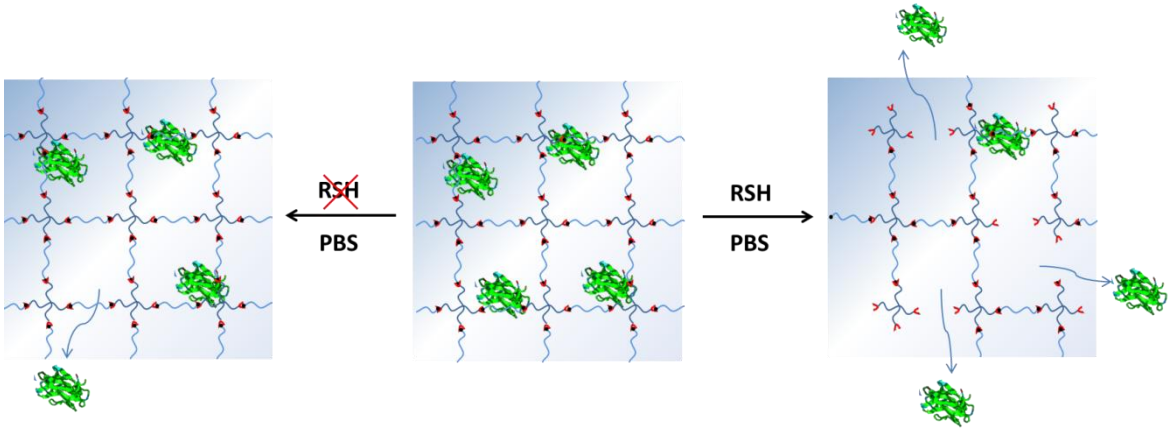

Figure 4.1. General scheme of release of FITC labeled dextran from hydrogels in presence and absence of RSH.

4.2. Experimental Section

4.2.1. Materials and Characterization

Poly(ethylene glycol)s (PEG 2K, PEG 4K, PEG 8K), (5,5'-dithio-*bis*-(2-nitrobenzoic acid), fluorescein isothiocyanate–dextran (20 kDa and 150 kDa), FITC labeled bovine serum albumin (BSA), fluorescein-5 maleimide and 4-dimethylaminopyridine (DMAP) were purchased from Sigma Aldrich. 1-Ethyl-3-(3-dimethylamino propyl) carbodiimide (EDCI) was obtained from Alfa Aesar. Anhydrous dichloromethane (CH_2Cl_2) and THF were obtained using the SciMatCo purification system. Other solvents and chemicals were obtained from Merck and they were utilized as obtained without further purification unless otherwise noted. Ultrapure water was obtained by using Milli-Q water purification System (Milli-Q system, Millipore, Billerica, MA, USA). PEG diacids [103, 104], pyridyldisulfide-containing alcohol [105] and 4-arm PEG thiol (10 kDa) [25] were synthesized and characterized according to reported protocols. ^{1}H NMR spectroscopy analyses were carried out employing a Varian INOVA400 at 400 MHz.

UV-Vis spectroscopy data were recorded on a Varian Cary 50 Scan UV-vis spectrophotometer.

4.2.2. Typical Synthesis of Bis-acid 2K PEG

Before usage, linear PEG diol (2.0 g, 1.0 mmol) was dried by azeotropic evaporation of toluene. Anhydrous PEG diol was dissolved in anhydrous THF (5 mL) and triethylamine (TEA) (0.42 mL, 2.99 mmol) was added to this solution under nitrogen atmosphere in an ice bath for 10 min. Then, succinic anhydride (0.34 g, 3.42 mmol) and DMAP (0.05 g, 0.40 mmol) were dissolved in anhydrous THF (5 mL) in a separate round bottom flask and was slowly added to the PEG containing solution at 0 °C. After stirring under nitrogen atmosphere for 20 h, the reaction mixture was evaporated under *vacuo*. The residue was dissolved in minimum amount of CH_2Cl_2 and precipitated in cold Et_2O. After filtration, bis-acid PEG was obtained as a white solid (2.13 g, 96 % yield). End group of other PEG diols with different molecular weights were converted to carboxylic acid by using similar protocol.

4.2.3. Synthesis of Bispyridyldisulfide PEGs

PEG 2K diacid (0.48 mmol, 3 g), pyridyldisulfide alcohol (1.44 mmol, 320.0 mg), EDCI (1.05 mmol, 202.0 mg) in the presence of DMAP (0.096 mmol, 11.0 mg) were dissolved in 10 mL of anhydrous CH_2Cl_2 and the reaction was stirred under N_2 atmosphere at room temperature for 18 h. After 24 h, reaction mixture was diluted with CH_2Cl_2 (100 mL) and extracted with saturated $NaHCO_3$ solution and dried over Na_2SO_4. After filtration, the solvent was removed *under vacuo*. Then, the residue was dissolved in minimum amount of CH_2Cl_2 and precipitated in cold Et_2O. The precipitate was dried under *vacuo* to yield a white solid (73 % yield). 1HNMR spectra of bispyridylsulfide-containing PEG (2 kDa) can be found in the Appendix (Figure A.5)

4.2.4. Representative Synthesis of Hydrogel via Thiol-Disulfide Exchange Reaction

The dipyridyldisulfide containing polymer (20 mg) were placed in a vial and dissolved in PBS (60 μL). In a separate vial, thiol-terminated tetra-arm PEG polymer (20

mg) in 60 μL PBS was prepared. After dissolving all chemicals, thiol-terminated tetra-arm PEG polymer solution was added to the dipyridyldisulfide containing polymer solution at 37 ^{o}C. Gelation took placed in 10 min, however to ensure formation of a well-defined system, gelation was allowed to proceed for 1 h. After gelation, gel was washed with excess amount of PBS and water to remove polymers/small molecules and then dried under vacuum for 24 h.

4.2.5. Determination of Free Thiol Groups

Free thiol groups in hydrogel were analyzed by using Ellman's reagent. 0.1 M sodium phosphate buffer solution (pH 8.0) with 1 mM EDTA buffer was prepared and freshly prepared hydrogel samples (5 mg) were rinsed in 2.5 mL of this solution. 4 mg of 5, 5'-dithio-*bis*-(2-nitrobenzoic acid) (DTNB) was dissolved in 4 mL of buffer solution and corresponding amount of Ellman's reagent was added into hydrogel solution. The mixture was placed at 37 ^{o}C in 200 rpm thermal shaking for 2 hours. Solution was analyzed via UV-vis spectroscopy. The concentration of free thiol groups in hydrogels were calculated by molar extinction coefficient of 2-nitro-5-thiobenzoic acid (TNB) (14,150 $M^{-1}cm^{-1}$) at 412 nm.

4.2.6. Morphological Analysis Using Scanning Electron Microscopy (SEM)

Surface morphologies of hydrogels are a by using scanning electron microscopy (SEM). Surface morphologies of dried hydrogels were analyzed using an ESEM Philips XL-30 (Philips, Eindhoven and The Netherlands) instrument operating at an accelerating voltage of 10 kV.

4.2.7. Swelling of Hydrogels

Disk-shaped lyophilized hydrogels were prepared to determine their swelling behavior. Circular pieces of dried hydrogels were put in a distilled/deionized water at room temperature.

At periodic time intervals, an increase in the mass of hydrogels was recorded. Measurements were continued until constant weight of hydrogels was obtained. The swelling capacity of hydrogels was calculated employing the equation;

$$\text{Swelling capacity (\%)} = (M_{swollen} - M_{dry}) / M_{dry} \times 100$$

where mass of swollen and dry hydrogels are $M_{swollen}$ and M_{dry}, respectively. Experiments were repeated in triplicate for every hydrogel sample.

4.2.8. Rheological Analysis of Hydrogels

Mechanical characterization of hydrogels was investigated by using Anton Paar MCR 302 rheometer. 15 mm diameter plate was used as test geometry with a gap of 1.5 mm between the plates. Time sweep and frequency sweep tests (0.1-100 Hz; 0.5% strain, 37 °C) were applied. Closed system was utilized to ensure lack of evaporation of water in hydrogel. Hydrogels swollen in water for 50 min were utilized for frequency sweep tests.

4.2.9. Degradation of Hydrogels

Cylindrical hydrogel samples (1.5 mm thick, 15 mm diameter) were incubated for in a thermal shaker (200 rpm at 37 ^{o}C) in aqueous medium containing 10 mM DTT (3 mL) to visual degradation and complete dissolution of hydrogels over time. Also, degradation studies with same procedures were examined by rheometry to determine degradation time of hydrogels. Additionally, degradation of hydrogel was investigated by conjugation of fluorescein maleimide to the hydrogel obtained using PEG 8K. Freshly prepared gel was placed in a glass vial in DMSO (3 mL) and amount of fluorescein-5 maleimide corresponding to free thiol groups was added onto the gel. After 2 h, the gel was washed with excess DMSO and water. The sample was divided into two pieces. One of the gel pieces was placed into 0.5 mL of DTT (10 mM) in a vial and the other one into a vial containing PBS solution. After waiting until dissolution of the hydrogel immersed in DTT solution, photograph of the vials was taken under UV illumination (365 nm).

4.2.10. *In vitro* Cytotoxicity Experiments

Cytotoxic activity of hydrogels was investigated on L929 mouse fibroblast cells cultured in RPMI 1640 media supplemented with 10% fetal bovine serum (FBS). 6000 cells/well were seeded in a 96 well plate as quadruplicates and incubated at 37ºC for 12 h. Cells were treated with hydrogels (1 mg/well) at 37ºC for 48 h. After incubation, sample solutions were removed and wells were washed with PBS (100 µl) twice. CCK-8 assay was performed to determine cell viability. Briefly, cells were incubated with 10% CCK-8 solution (100 µl/well) for 1h and absorbance at 450 nm was measured using a microplate reader. GraphPad Prism software was used for viability calculations.

4.2.11. Encapsulation of FITC-Labeled Dextran and BSA

Two different FITC-labeled dextran (20 kDa and 150 kDa) and a BSA polymer (66 kDa) were dissolved in distilled water (1 mL) to obtain 1mg/mL of FITC labeled dextran and BSA (66 kDa) solutions. The dipyridyldisulfide containing polymer (20 mg) in PBS (60 µL) and of FITC-dextran or BSA stock solution (50 µL) were added to this vial. In a different vial, 20 mg of thiol-terminated four-arm PEG was dissolved in PBS (60 µL). FITC-labeled dextran or BSA and dipyridyldisulfide containing polymer mixture was added into thiol-terminated four-arm PEG solution and it was sonicated for 1 min at 37 ^{o}C to obtain homogenous mixture.

4.2.12. FITC-Dextran and BSA Release Studies

Release studies of FITC-labeled dextran and BSA from hydrogels were studied by using UV-vis spectroscopy. Hydrogels containing FITC-labeled dextran and BSA were incubated in 1 mL of PBS solution at 37 ^{o}C. At specified sample collection times, 1 mL of PBS solution was removed and replaced with 1 mL of fresh PBS solution. The amount of FITC-labeled dextran and BSA release from hydrogels was monitored using UV-vis spectroscopy at 494 nm. The cumulative release of FITC-labeled dextran and BSA was calculated by using a calibration curve of FITC-labeled dextran and BSA.

4.3. Results and Discussion

4.3.1. Synthesis and Characterization of Hydrogels

The syntheses of hydrogels were carried out by mixing the dipyridyldisulfide containing PEG polymers with tetra-arm PEG-thiol based crosslinkers. The gelation reaction was carried out in PBS at 37 ^{o}C. While the gelation occurred within few minutes, gelation was continued for another hour to maximize the end group reactions of the two complementary reactive groups (Figure 4.2).

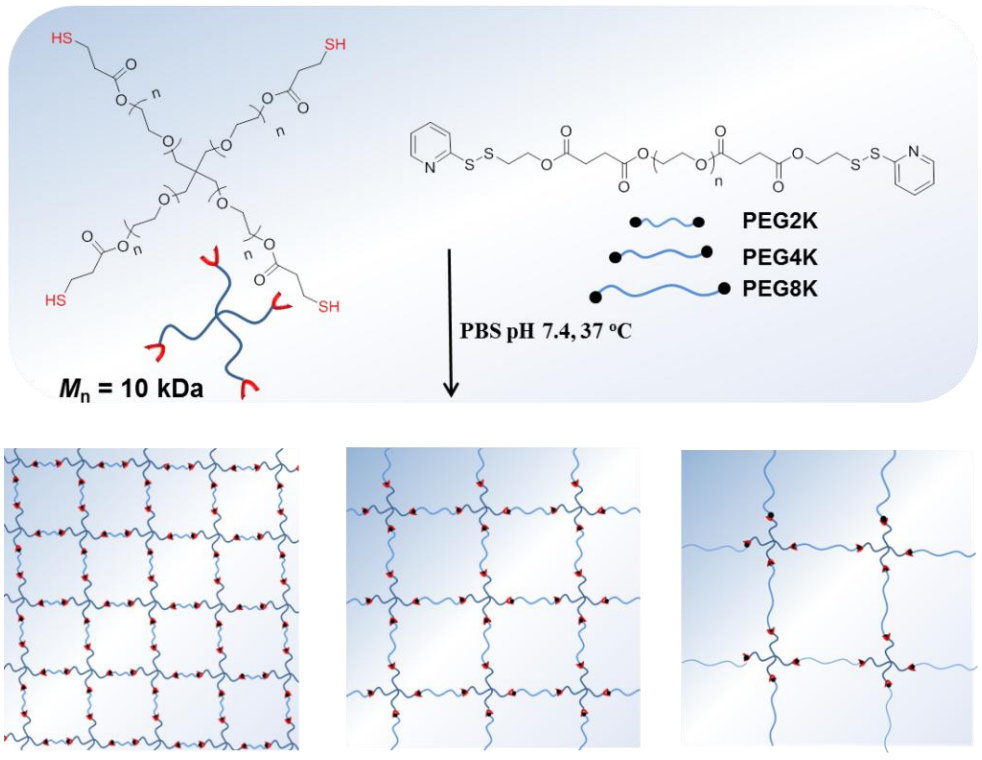

Figure 4.2. Schematic illustration of hydrogel formation via thiol-disulfide exchange reaction.

As a first step, PEG-based polymers with pyridyldisulfide end groups were synthesized (Figure 4.3). End groups of PEG polymer were converted to carboxylic acid via reaction with succinic anhydride in presence of Et_3N as base. These carboxylic acid terminated PEG polymers were modified with pyridyldisulfide-containing alcohol. Esterification reaction using EDCI in the presence of DMAP were used for attaching the pyridyldisulfide groups to chain ends of the PEG polymers. Three different linear PEGs (2

kDa, 4 kDa and 8 kDa) with different molecular weights were used to obtain hydrogels with different mesh sizes. Hydrogels were obtained with high conversions (>85%), and as a next step end group conversions were determined to understand the efficiency of thiol-disulfide exchange based chain-end couplings (Table 4.1).

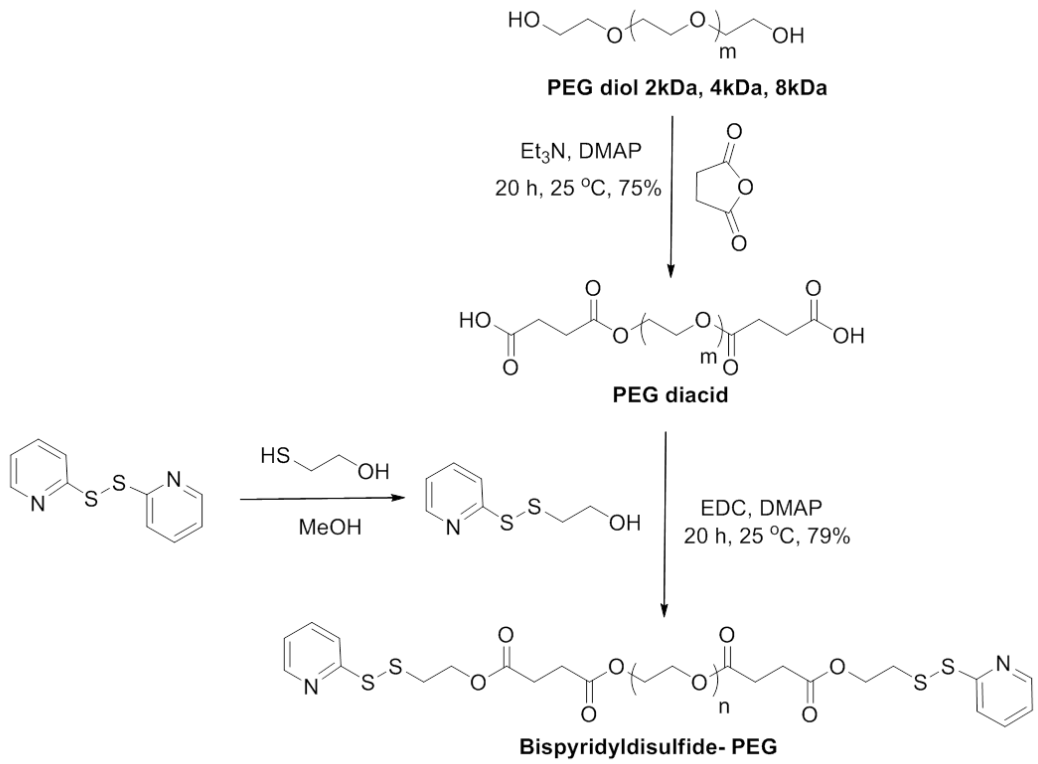

Figure 4.3. Synthesis of pyridyldisulfide linear PEG polymers.

The consumption of thiol groups in hydrogel was characterized by determining the amount of residual thiol groups by treatment with 5,5'-dithio-bis-(2-nitrobenzoic acid) (DTNB, Ellman's reagent). In the presence of free thiol groups, DTNB gives yellow colored TNB, detectable by UV-vis spectroscopy due to its characteristic absorbance. Using standard molar extinction coefficient of TNB, amount of free thiol groups in the gel can be easily quantified. It was observed that percent of free thiol groups in P8K were around 18 % whereas the sulfhydryl groups in P2K were almost around 16 %. Hence, one can conclude that all PEGs participated with similar efficiency toward hydrogel formation.

Table 4.1. Hydrogels with different chain length of PEG polymers and their gel conversions and the amount of thiol consumed.

Entry	Hydrogel	Polymer	Gel Conversion[a] (%)	Thiol Consumption[b] (%)
1	P2K	PDS-PEG$_{2000}$	86.50	84.02
2	P4K	PDS-PEG$_{4000}$	89.02	82.70
3	P8K	PDS-PEG$_{8000}$	85.46	81.91

[a] Calculated as (dry hydrogel weight/total weight of polymer)× 100. [b] Thiol amount utilized for 5 mg hydrogel / calculated thiol amount in 5 mg hydrogel sample (Data in triplicate).

Morphology of hydrogels was examined using SEM (Figure 4.4). All hydrogels exhibited highly porous structure as expected. Next, the swelling behaviors of all hydrogels were analyzed via gravimetric analysis (Figure 4.5). Utilization of polymers with longer hydrophilic chains exhibited higher water uptake capacity. Importantly, comparison of hydrogel networks made using PEG with different chain lengths provides us information about the effect of differences of crosslinking structure on water uptake. All gels reached constant swelling capacity within 45 min. Interestingly, PEG 2K based hydrogel, one with highest crosslink density exhibited maximum equilibrium swelling. It could be expected since the highest crosslinking also leads to the presence of maximum amount of hydrophilic PEG polymers in the hydrogel.

To understand viscoelatic behaviors of hydrogels, rheological behaviour of hydrogels prepared with different polymers lengths were investigated. Hydrogels swollen to equilibrium state were analyzed by using frequency sweep test. As expected for crosslinked networks, G′ values were higher than the G″ values. While hydrogels fabricated with shorter PEG chains possessed higher storage modulus, PEG 8K hydrogels had slightly lower storage and loss modulus values compared to the others (Figure 4.6).

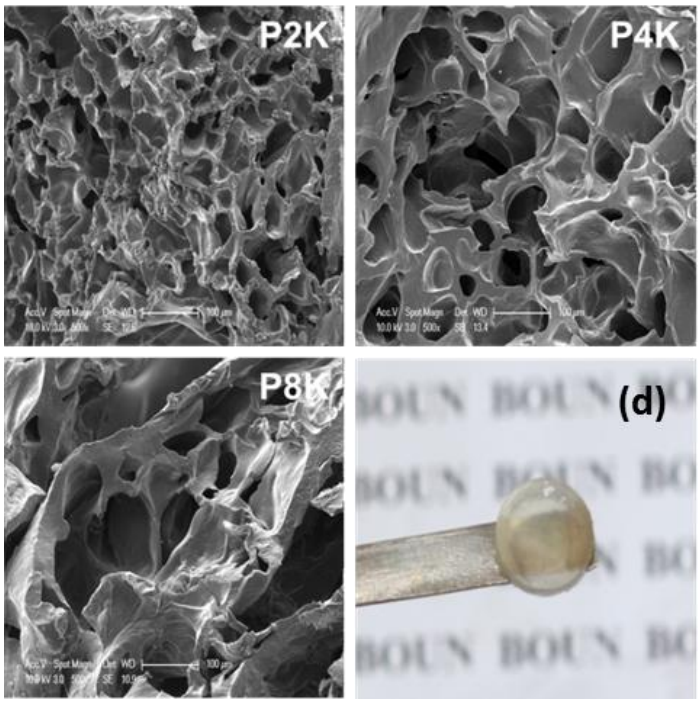

Figure 4.4. SEM images of well-defined hydrogels (P2K, P4K and P8K) and (d) photograph of P4K hydrogel. Scale bars are 100 μm.

4.3.2. Degradation of Hydrogels

As mentioned before, disulfide bonds undergo rapid degradation of hydrogel network structure in presence of thiol-containing molecules to allow to release of macromolecules. Therefore, hydrogel degradation was compared in presence of PBS buffer solutions (pH: 7.4) with and without the reductant dithiothreitol (DTT) at 37 ^{o}C. First, a disk shaped fluorescent dye conjugated hydrogel was synthesized by reaction of fluorescein-maleimide with the residual thiol groups in the hydrogel. After removal of unbound dye from the hydrogel, the dye conjugated hydrogel piece was cut in two pieces. One of the pieces of hydrogel was placed in the PBS solution at 37 ^{o}C, and the other one was immersed 10 mM DTT solution at 37 ^{o}C. Within 2 h, complete degradation was achieved for a piece of hydrogel immersed in the DTT solution, however the hydrogel in PBS solution remained intact.

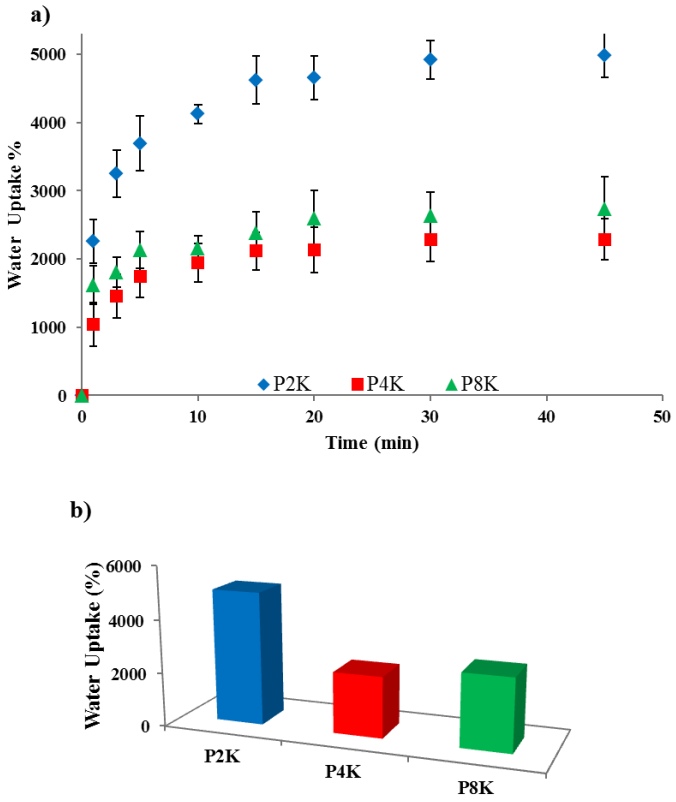

Figure 4.5. Swelling profiles and comparison of water uptake capabilities of hydrogels.

Upon degradation of the hydrogel, the polymer bound fluorescent dye was dispersed in the solution giving rise to a brightly fluorescent sulotion (Figure 4.7). As expected, for the vial containing the fluorescent hyderogel under non-reducing condition, the hydrogel remained intact and the fluorescence of the dye remained confined to the hydrogel.

In order to quantitatively show the hydrogel degradation, degradation was followed using rheometry. PEG8K based hydrogel was placed in 1 × PBS solution containing 10 mM DTT and PBS solution devoid of the thiol. Loss of storage modulus suggested degradation of the hydrogel in 1 × PBS solution containing 10 mM DTT, whereas hydrogel without reducing agent did not exhibit any change in modulus (Figure 4.8).

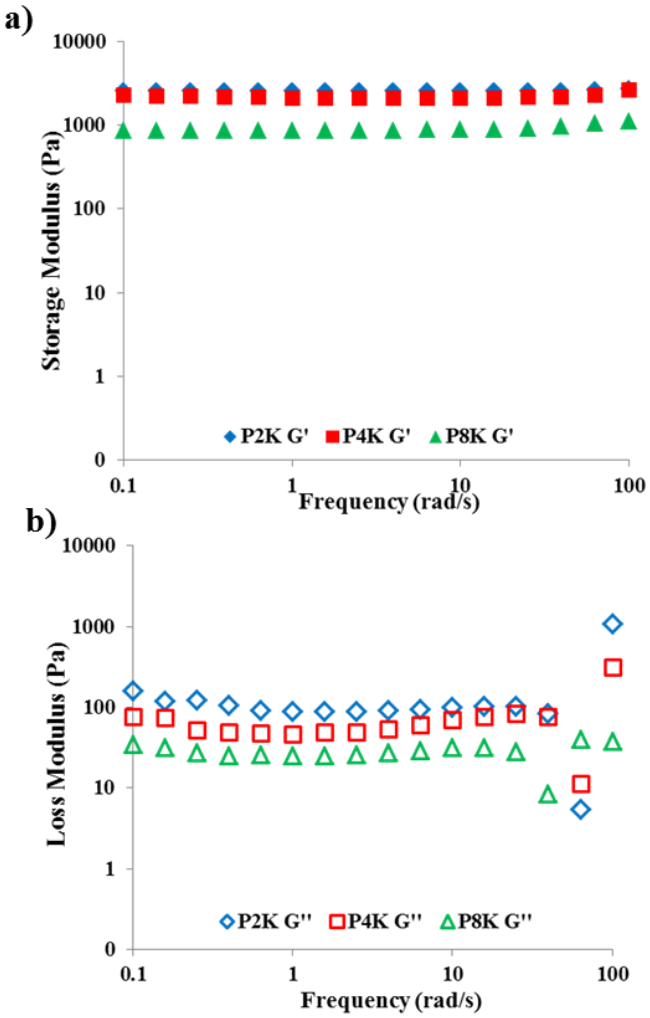

Figure 4.6. The frequency dependence of a) storage values and b) loss values of hydrogels.

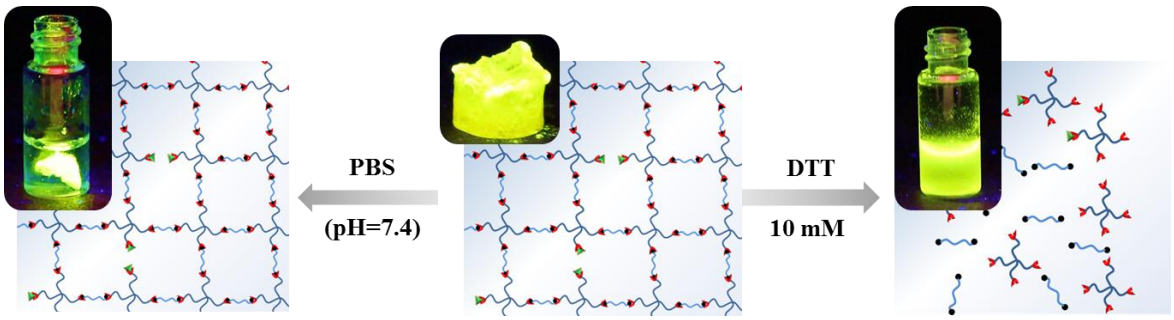

Figure 4.7. Photographs (under UV illumination (λex = 365 nm)) of hydrogels showing degradation in DTT (10 mM) and their stability in PBS.

In order to quantitatively show the hydrogel degradation, degradation was followed using rheometry. PEG8K based hydrogel was placed in 1 × PBS solution containing 10 mM DTT and PBS solution devoid of the thiol. Loss of storage modulus suggested degradation of the hydrogel in 1 × PBS solution containing 10 mM DTT, whereas hydrogel without reducing agent did not exhibit any change in modulus (Figure 4.8).

4.3.3. FITC-Labeled Dextran and BSA Encapsulation and Release Studies

In order to demonstrate the usage of these disulfide-cross-linked hydrogels in protein delivery, model studies were first carried out using FITC-labeled dextran polymers. These polymers were chosen with two significantly different molecular weights and thus possess would quite different hydrodynamic size when dispersed in water. FITC-labeled dextran polymers with two different molar masses of 20 kDa and 150 kDa were used for this purpose. The diffusion of FITC-dextran from hydrogel networks provides an estimate about differences in mesh sizes and thus permeability of macromolecules through hydrogel matrices. FITC labeled dextrans with molar masses of 20 and 150 kDa as a model macromolecule were encapsulated in hydrogel network and their release in 1× PBS solution with and without DTT was compared. Due to the presence of the fluorescent dye label, release of these polymers over time could be followed using UV-vis spectroscopy. FITC labeled dextrans were encapsulated in hydrogels during their formation and after removal of any physically attached polymers on the hydrogel surface with PBS buffer, hydrogels were immersed in PBS solutions to determine the release profiles of individual dextrans from the various networks. The release behaviors of encapsulated dextran was monitored by change of UV absorbance of immersion solution due to release of FITC-dextran at 494 nm. Due to smaller size, FITC-dextran (20 kDa) was expected to show faster release.

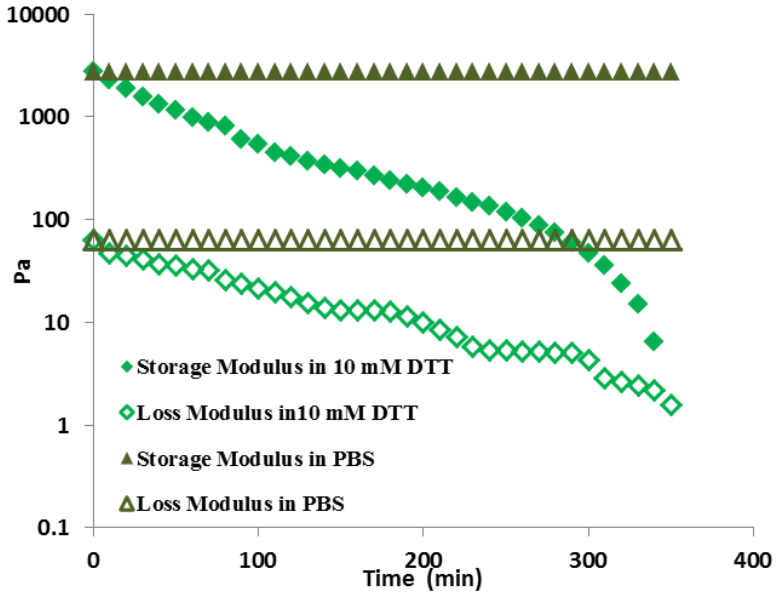

Figure 4.8. Differences of storage and loss modulus of P4K in the presence of DTT and PBS at 37 ^{o}C.

Furthermore, to control the effect of the PEG length on the dextran release, three sets of P2K, P4K and P8K encapsulated with the two different dextrans were compared. As shown in Figure 4.9a, in the release of 20 kDa dextran, it was observed that indeed initially there is a slight difference in the release profiles from the different hydrogels, more predominant for the PEG8K based hydrogel after 24 hours of incubation in PBS at 37 ^{o}C. After 24 h, with addition of DTT (100 mM), hydrogels demonstrated rapid release due to fast decomposition of the disulfide-crosslinked networks. Employing degradable hydrogels for controlled release studies is important since mild reducing agents are located in areas near various tumors. Therefore, to show the influence of the mild reducing agent on the dextran release, hydrogels were immersed in the DTT (10 mM) solutions. The release of dextran from all hydrogel samples significantly increased compared to that observed for only PBS. After 2 h, dextran release from P8K in the 10 mM DTT was about 90 % whereas only 18% of dextran had released in only PBS at pH 7.4 (Figure 4.9a and b). Tuning the release rate by exposure to various concentrations of DTT seems to be achievable.

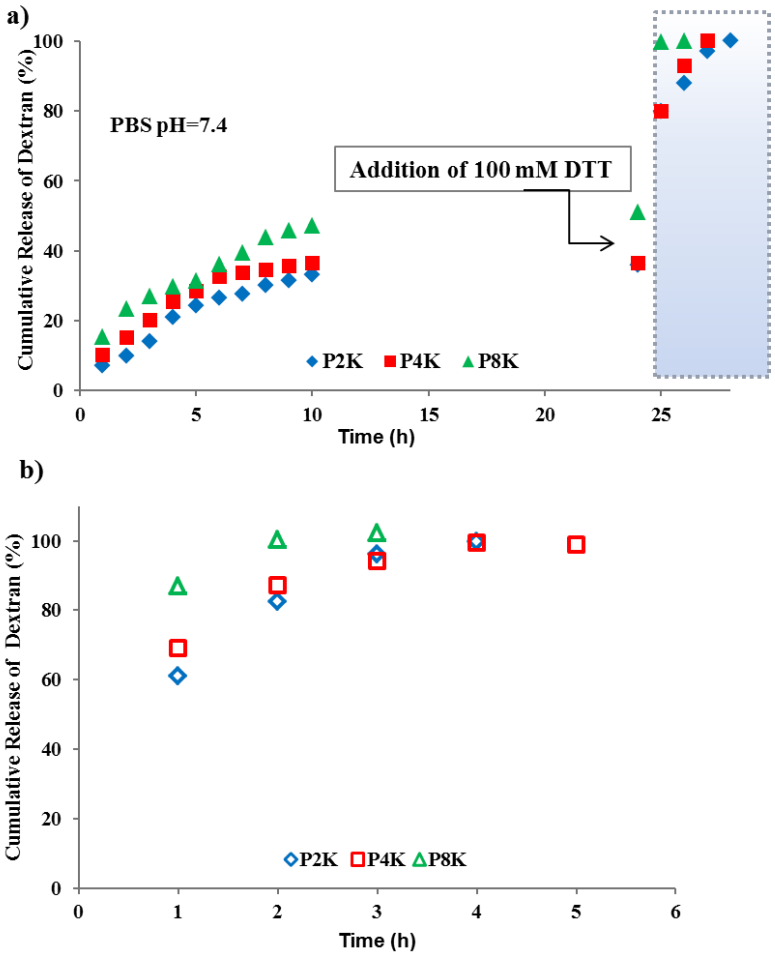

Figure 4.9. Cumulative release of FITC labeled Dextran (20 kDa) from hydrogels a) in PBS and b) in 10 mM DTT solution at 37 ^{o}C (plots with error bar Figure A.6a and b).

Thereafter, the effect of molecular weight of encapsulated molecule on diffusion from these networks was investigated. All release data were repeated for higher molecular weight of FITC labeled dextran (150 kDa). About 40 % of dextran release from hydrogels in only PBS was observed after 24 h (Figure 4.10a). However, much higher cumulative release of the dextran from hydrogels in case of DTT solution was obtained (Figure 4.10b). Limited dextran release from P2K in only PBS was obtained as expected and higher release profiles from P8K were observed. Notably, 100 % of dextran release from all hydrogels was able to accomplish in adding high concentration of DTT.

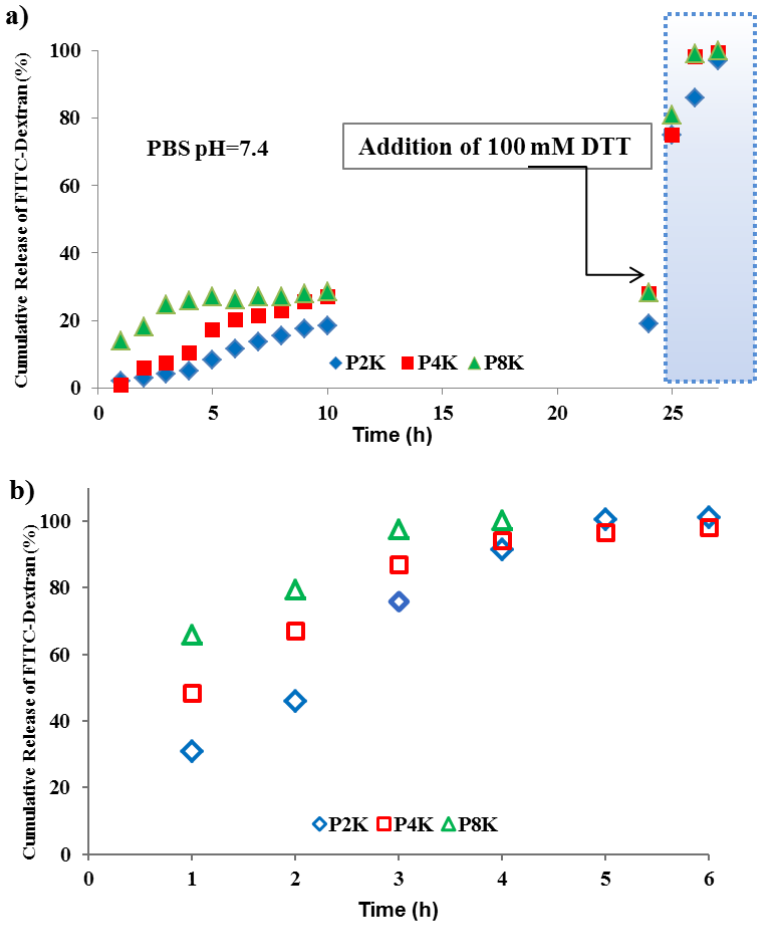

Figure 4.10. The release profiles of FITC labeled Dextran (150 kDa) from hydrogels a) in PBS and b) in 10 mM DTT solution.

After the investigation of release from these hydrogels using FITC-dextran as a probe, release of a protein, namely, FITC-labeled bovine serum albumin was undertaken. FITC-BSA was encapsulated in the different hydrogels during their formation, and then their release from these well-defined hydrogels was monitored. FITC-labeled BSA containing hydrogels were synthesized with same procedure, and then immersed in the PBS and DTT solution to monitor cumulative release of BSA. As expected, the cumulative release of FITC labeled BSA from hydrogels in PBS was lower than in the reducing environment as expected. The effect of the network structure was also apparent since P8K demonstrated slightly higher release than others because higher mesh size facilitates faster release of the protein from hydrogels (Figure 4.11a). Importantly, all proteins were rapidly released upon introduction of 100 mM DTT. Also, differences in release could be observed

at initial phases under mild reducing conditions but after a few hours they all became equal due to degradation of the network structure of the hydrogel (Figure 4.11b).

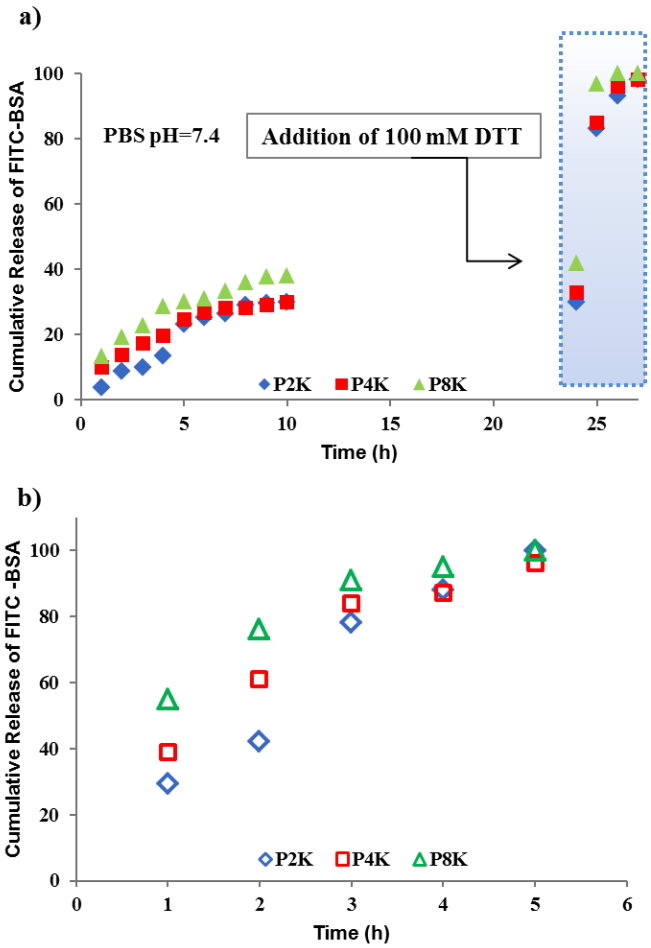

Figure 4.11. FITC labeled BSA release from hydrogels in the presence of a) PBS and b) DTT (Plots with error bars at Figure A.7a and b).

Since these materials are intended for use in biological applications, hence to understand their biocompatibility, cellular toxicity of these hydrogels were investigated using L929 fibroblast cell line. After 48 h, viabilities of cells were determined using 10 % CCK-8 assay (Figure 4.12). Lack of any significant toxicity with all of these hydrogels, makes them potential materials for biological applications.

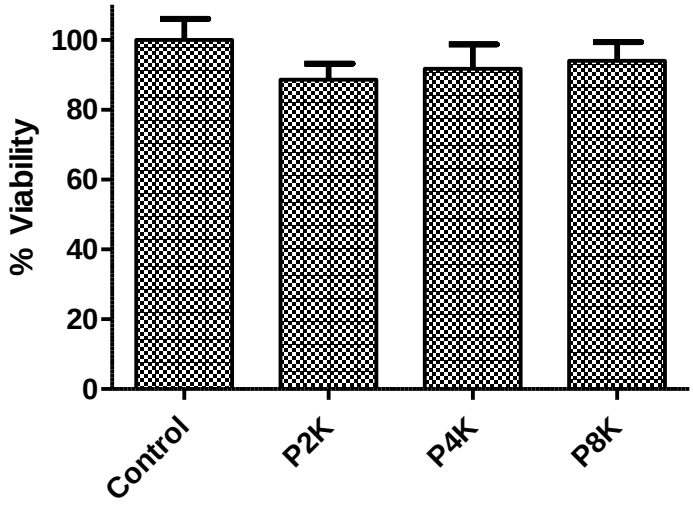

Figure 4.12. Cell viabilities of P2K, P4K and P8K on L929 fibroblast cell line.

Although not of direct interest in our context, but since the disulfide linkage chemistry has also been exploited to impart these materials with self-healing properties [106-110], we wanted to examine the potential of our hydrogels in this regard. One can envision the fabrication of compositit hydrogel materials by using self-healing of different components containing different proteins. In order to probe self-healing capability of the disulfide-containing hydrogel system reported here, cutting a hydrogel into two pieces and re-sticking them for recovery was investigated (Figure 4.13). In order to aid visualization, a red food coloring agent was added to one of the hydrogels. The freshly cut pieces of hydrogels were brought in contact by pressing them together with tweezers for a few minutes. Subsequent stretching of the hydrogel demonstrated that the two pieces were able to stick together quite efficiently within a few minutes. The self-healing process observed here is anticipated to originate from the reformation of the cleaved disulfide linkages. In order to verify this assumption, freshly cut hydrogel pieces were dipped in an aqueous solution of ethylmaleimide. Notably, hydrogel pieces did not stick to each other upon such a treatment. It can be argued that the thiol groups produced from the disulfide cleavage during scission reacts with ethylmaleimide and hence are no longer available for self-healing through recombination.

Although the focus of present work was to fabricate materials with rapid degradation on demand, this aspect of self-healability provides such materials with added advantage of maintaining their stability during wear and tear during their application, as well as open avenues for multicomponent systems.

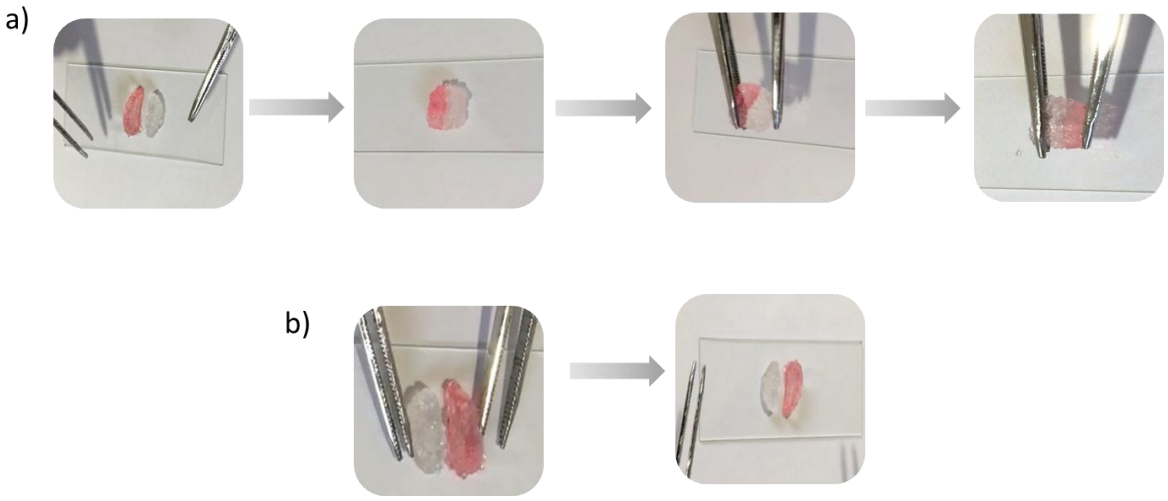

Figure 4.13. a) Self-healing characteristics of the disulfide-containing hydrogels and b) after thiol groups produced from the disulfide cleavage during scission reacts with ethylmaleimide

4.4. Conclusion

In summary, disulfide bond containing PEG based hydrogels with well-defined network structure were generated using thiol-disulfide exchange reaction. Hydrogels with different molecular weight of PEG were synthesized with high conversion. Hydrogel precursors were chosen such that well-defined structure could be obtained. For this purpose, an equimolar stoichiometry of thiol and disulfide functional groups was utilized. To understand the extent of well-defined network structure, the amount of free thiol groups in hydrogel were analyzed utilizing Ellman's method. Gel morphology in dry state, mechanical and self-healing behaviors, swelling and degradation rate of hydrogels were investigated. All gels showed highly porous structure and high swelling capacity. Degradation studies under varying amount of reducing agent showed successful cleavage of disulfide bonds, resulting in complete degradation of the hydrogels. Analysis of

diffusion of labelled polymers with different molecular weights and FITC-BSA protein in DTT containing PBS solution, as well as PBS were undertaken with all the different hydrogels synthesized in this work. Differences in release under neutral conditions and enhanced release in presence was observed from all hydrogels. Apart from control over the release of proteins, excellent cytocompatibility of these hydrogels demonstrate that they can be attractive candidates for biomedical applications like protein reservoirs.

5. DESIGN OF STIMULI RESPONSIVE DEFINED CYCLODEXTRIN CONTAINING HYDROGELS VIA THIOL-DISULFIDE EXCHANGE REACTION

5.1. Introduction

Over the past decades, hydrogels have emerged as attractive materials hence they can be easily prepared with low cost or can be readily modified with various (bio)molecules such of therapeutic importance. Therefore, they have gained growing popularity in biomedical applications, particularly in controlled drug release, design of novel biomolecular sensors or contact lenses and etc [1, 16, 90, 111, 112]. To describe their features, hydrogels can readily absorb huge amounts of water with the help of their hydrophilic porous structures while retaining their internal network structure and this behavior makes them ideal materials for abovementioned applications [62, 113, 114]. To date, various types of physically and chemically cross-linked hydrogels have been fabricated for drug delivery. In both types of hydrogels, loading of drugs in hydrogel matrix can be achieved either via physical encapsulation or chemical attachment. Physical drug encapsulation in hydrogels can be achieved by their entrapment within the voids in hydrogel and drug release can be controlled by diffusion, erosion and degradation mechanisms [115]. For the effective drug loading and release, it is beneficial to have well-defined hydrogels, since in such materials control over network structures can be designed in a predictable and controlled manner.

Well-defined network has homogenous and controlled mesh size as opposed to a random distribution of mesh sizes [116, 117]. This mesh size can be controlled by varying the polymer chain length (i.e. polymer molecular weight). For example when release of drugs with two different sizes through a well-defined network is compared, it can be expected that the release profiles can be tailored more effectively. This arises due to the homogenous distribution of mesh sizes. Apart from simple diffusion of drugs out of the hydrogels as a release mechanism, introduction of tailored degradation pathways in

hydrogels can be used to tune the release. Also, it may be desirable to remove or completely degrade the hydrogel once the drug release has finished. Hence design of hydrogels that can degrade in the presence of a biocompatible stimuli is highly desirable. In this thesis, as explained in previous chapter, exploration of disulfide chemistry is investigated. Hence it is of interest to design disulfide containing hydrogels, an issue which has been explored in previous chapter. However, a key challenge that remains in the area of drug delivery using hydrogels involve with the inherent challenge of solvation of hydrophobic drugs. Since drug molecules are most often synthesized using organic synthesis methodologies, many drug molecules are hydrophobic in nature. Indeed, many drugs in market are used as salt formulations to address this issue. Some drugs are not easy to convert into their salt forms. Hence, encapsulation of such drugs in hydrogels, as well as their subsequent release in the aqueous biological media in the body is quite difficult. The pharmaceutical industry has tried to address this issue by utilizing hydrophilic molecules like cyclodextrins as excipients. Addition of cyclodextrins improves the water solubility of some of the hydrophobic drugs through complexations. Hence integration of cyclodextrins into hydrogels has been investigated, as explained below. However, once drugs come out of the cyclodextrin's cavity, they are again encountered with the challenge of poor solubility in aqueous media. An approach where the drug molecules leave the hydrogel as a complex will keep the released drug solvated and thus preserve its bioavailability. The present chapter outlines an approach to design cyclodextrin-containing hydrogels with well-defined network structure, which will be capable to releasing cyclodextrin complexed drug molecules under glutathione based stimuli responsive conditions.

To date, several effective 'click' type reactions have been used to fabricate well-defined hydrogel networks. As mentioned in previous chapters, most of the earlier work involves their synthesis using copper catalyzed alkyne-azide cylcoadditions [118]. Due to potential concerns of residual metal impurities that may cause toxicity or decrease protein function/activity, utilization of metal-free reactions has gained popularity. Thiol-based conjugations used to date for making well-defined network structure includes the thiol-ene addition reaction promoted by UV irradiation [119, 120]. While many other thiol-addition reactions such as thiol-maleimide and thiol-vinyl sulfone reaction have also been used for making hydrogels [121], they are not readily degradable, as well as highly reactive groups like vinyl sulfone and maleimides can also react with amine groups to some extent and

thus capture a portion of the biomolecules permanently. As demonstrated in previous chapter, the pridyldisulfide-thiol exchange reaction can be effectively used in preparation of hydrogels and has degradable disulfide bonds that undergo cleavage in the presence of thiol-containing molecules [9, 99].

Cyclodextrins are cyclic oligosaccharides possessing hydrophobic inner cavity and hydrophilic outer shell. They have been commonly used in drug delivery applications because CDs make inclusion complexes with poorly water soluble drugs such as curcumin (CUR) so they improve the aqueous solubility of hydrophobic drugs [102, 122-127]. Hence, efforts have been focused on obtaining hydrogels containing CDs. In 2015, Lin and co-workers published a paper containing two types of cyclodextrin (CD)-PEG hydrogels using radical thiol-ene click reaction. One of them was obtained by multiarm PEG and βCD-allylether and the other one was formed by the reaction of β-cyclodextrin-thiol (βCD-SH) and multiarm PEG norborne. It was observed that thiol-norborne hydrogel has faster gelation kinetics and higher elastic properties than the others. To demonstrate β-CD drug loading capacity and sustained drug release, normal PEG and CD based hydrogels were loaded curcumin drug molecules. Although all gels possessed similar drug loading capacity, higher drug release in buffer solution was observed in PEG based hydrogels. This shows that CDs slow down the release of drug and thus provide a control over release. Indeed, all drug could be released from CD containing hydrogels upon treatment with DMSO [128]. A better trigger to release all drug would be definitely more attractive.

This chapter describes the design and synthesis of CD-containing well-defined hydrogels through thiol-disulfide exchange reaction (Figure 5.1). In this approach, we synthesized pyridyldisulfide containing homo-bifunctional PEGs with different molecular weight and a heptavalent thiol-functionalized β-CD crosslinker (β-CD$(SH)_7$). By the help of the thiol-disulfide exchange reaction between pyridyldisulfide and β-cyclodextrin crosslinker in the presence of acetic acid as a catalyst, well-defined hydrogels were obtained with high gel conversions. It was shown that the equilibrium swelling behaviors of these hydrogels can be controlled by changing the molecular weight of pyridyldisulfide containing PEGs. Also, hydrogels were characterized with rheology to ascertain their mechanical behaviors. After characterization, the solubilizing effect of cyclodextrin on curcumin (cur), a hydrophobic drug was investigated under physiological conditions. The

release of water insoluble drug was slow and release was found to be depended on composition of the hydrogels. As another approach, hydrogels were degraded by disulfide bonds cleavage using glutathione as a reducing agent and higher drug release was obtained. Finally, cytotoxicity and the efficacy of the drug loaded hydrogels were investigated by using U87 human brain cancer cells.

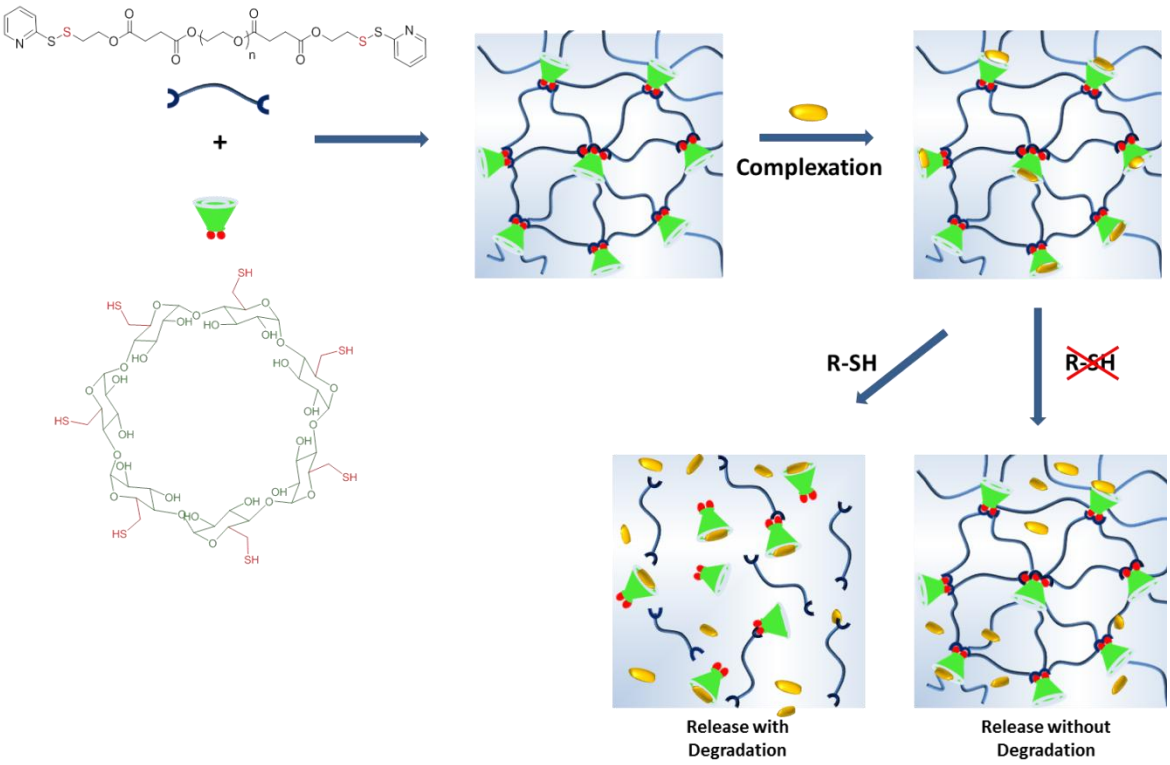

Figure 5.1. Schematic illustration of synthesis and complexation of cyclodextrin based well defined hydrogels and release of drug molecules.

5.2. Experimental Section

5.2.1. Materials

Poly(ethylene glycol)s (PEG 2K, PEG 4K, PEG 8K), (5,5'-dithio-*bis*-(2-nitrobenzoic acid) and 4-dimethylaminopyridine (DMAP) were obtained from Aldrich Chemical Co and 1-Ethyl-3-(3-dimethylamino propyl) carbodiimide (EDCI) and β-cyclodextrin hydrate were obtained from Alfa Aesar. 2,2'-Dipyridyl disulfide was obtained from TCI Chemicals. Curcumin and L-glutathione reduced was obtained from Sigma-

Aldrich and L-dithiothreitol (DTT) was purchased from Fluka. Thiol functionalized β-cyclodextrin [129], PEG diacids [103, 104] and pyridyldisulfide alcohol [105] were synthesized according to reported procedures. Anhydrous dichloromethane and tetrahydrofuran were obtained from SciMatCo purification system and other solvents such as dimethyl formamide were purchased from Merck. Proton NMR spectral data were recorded on a Varian 400-MHz. The cell internalization images were taken utilizing Zeiss Observer Z1 fluorescence microscope connected to Axiocam MRc5 utilizing a Zeiss Filter set 38.

5.2.2. Representative Hydrogel Formation

Hydrogels were synthesized using PEG's with three different molecular weights. An exemplary procedure for preparation of hydrogels (CDP4K) as follows:, Dipyridyldisulfide PEG_{4000} (0.050 g, 0.011 mmol) was placed in a glass vial and dissolved in 100 μL of DMF and acetic acid (1.25 μL, 0.0219 mmol) was added onto polymer mixture. Calculated amount of β-cyclodextrin was added into another glass vials and 100 μL of DMF was added onto this solution. Thereafter, cyclodextrin solution was added into first vial containing the disulfide reagents. The molar ratio of pyridyldisulfide to SH was 1:1. The mixture was sonicated for 5 min at 37 ^{o}C. To ensure complete gelation and end group reactions, gelation was left for 10 h. After hydrogel formation, gels were washed with excess DMF, followed by water to remove all unreacted gel precursors. Finally, samples were lyophilized to obtain dry gels.

5.2.3. Calculation of Free Thiol Content in Hydrogels

Free thiol concentrations in the hydrogels were quantitatively calculated by using Ellman's assay [130]. Initially, Ellman's reaction buffer was prepared by using 0.1 M sodium phosphate, pH 8.0, and 1 mM ethylenediaminetetraacetic acid was added. 4 mg of 5,5'-dithio-*bis*-(2-nitrobenzoic acid) (DTNB), often referred as Ellman's reagent was dissolved in 1 mL reaction buffer. 2.5 mL of buffer of corresponding Ellman's reagent, was added onto a freshly prepared gel (5 mg) sample in a vial. Gels were incubated at 37 °C for 2 hours. Absorbance of 2-nitro-5-thiobenzoic acid (TNB) at 412 nm was measured to quantify the concentration of free thiol group content in the gels [131].

5.2.4. Swelling Studies

To describe water uptake capacity of hydrogels, dried hydrogels (50 mg) were weighted and placed into water bath (10 mL) at room temperature. At certain time intervals, hydrogels were taken out of the water and the excess of water was removed by the help of the filter paper. Swollen gels were weighted to determine their swelling behaviors and the equilibrium. The swelling capacity of hydrogels was calculated by the weight ratio of the wet hydrogels to the dried hydrogels. Weight change was calculated by using this equation:

$$\text{Percentage of Water Uptake} = ((W_{wet} - W_{dry})/W_{dry} * 100),$$

W_{wet} refers to the wet weight of the hydrogels and W_{dry} refers to dry hydrogels. Experiments were repeated three times to determine average trends.

5.2.5. Morphological Characterization

Morphology of hydrogels was characterized with scanning electron microscopy (SEM). The cross sectional morphologies of dried hydrogels were acquired using an ESEM-Philips XL-30 (Philips, Eindhoven, The Netherlands) instrument operated at 10 kV accelerating voltage.

5.2.6. Rheological Measurements

The rheological analysis of hydrogels was examined by using an Anton Paar MCR 302 rheometer, using a parallel plate (diameter, 15mm) setup, and gap between plates was set to 2.0 mm. Angular frequency and time sweep tests were acquired to analyze rheological behaviors. Tests were conducted at 37 ^{o}C by utilizing 0.5 % strain between 0.1-100 rad/s.

5.2.7. Drug Loading and Release Studies

Drug loading into hydrogel was accomplished by using a solution absorption method. The disk shaped hydrogel sample (5 mg) was soaked in 1 mL curcumin solution

(2 mg of curcumin) and the mixture was shaken (150 rpm) for 12 h at 25 ^{o}C to facilitate drug loading. The concentration of drug loaded into hydrogel was monitored by measuring the absorption intensity of the soaking solution at 425 nm using UV-vis spectrometry. Standard curcumin calibration curve was obtained to determine the amount of curcumin in the soaking solution.

Curcumin loaded hydrogels (5mg) were washed with excess ethyl alcohol and then water before placing in phosphate buffered saline (PBS, pH 7.4) solutions or 5 mM GSH solution in PBS (3 mL) at 37^{o}C under 100 rpm mechanical shaking. Periodically, 3 mL of release medium was removed and replenished with same volume of fresh PBS solution. By the help of a calibration curve, the cumulative drug release in collected media was determined spectrophotometrically.

5.2.8. *In Vitro* Cytotoxicity Experiments

Cytotoxic activity of the hydrogels was investigated via CCK-8 viability assay on U-87 MG human glioma cell line. U-87 MG cells (7000 cells/well) were seeded in a 96-well plate in 100 μL RPMI supplemented with 10 % fetal bovine serum (FBS) and incubated at 37 °C for 24 h for cells to adhere completely. Cell adhered plates were treated with CDP2K, CDP4K, CDP8K hydrogels (ca. 1 mg) and curcumin loaded CDP2K, CDP4K and CDP8K hydrogels (containing equal curcumin amount) at 37 °C for 8 h and 24 h. After the incubation, hydrogels were removed from wells and were washed with PBS (100 μL) three times. CCK-8 solution (10 %) was added to every well (total 70 μL) and after incubation for 3 h, absorbance values at 450 nm were measured using a microplate reader. Experiments were repeated three times. Results were obtained by GraphPad prism software.

5.2.9. Curcumin Internalization on U-87 MG

For the cellular internalization, U-87 MG glioblastoma cells (100 000 cells/well) were seeded in 12-well plate as triplicate in 1 mL of culture media (RPMI). The cells were incubated at 37 ^{o}C for 24 h. Curcumin-doped 8K hydrogels were added into the wells. After incubation for 24 h, hydrogels were removed from wells. Then, cells were washed

with PBS (500 μL) three times. Cells were fixed using 4% formaldehyde solution for 10 min at 37 ^{o}C. After being washed with PBS three times, cells were incubated at 37 ^{o}C for 15 min for DAPI nuclei staining. Cell images were collected using Zeiss Observer Z1 fluorescence microscope and processed with AxioVision software.

5.3. Results and Discussion

5.3.1. Hydrogel Preparation and Characterization

Cyclodextrin containing PEG based hydrogels with well-defined structures were prepared through thiol-disulfide exchange reaction of pyridyldisulfide functionalized PEG polymers with a heptavalent thiol-functionalized β-cyclodextrin crosslinker (β-CD$(SH)_7$) at room temperature. In all hydrogel mixtures, equimolar amounts of CD and pyridyldisulfide functionalized PEGs groups were present, because we aimed to obtain well-defined gels through one to one coupling of pyridyldisulfide groups with thiols on CD. However, it is possible that the hydrogel network formation deviates slightly from the well-defined structure, especially under some condition which is most likely due to the steric bulk of polymer chains and the potential of cyclizations and side reactions. So the characterization also includes assessment of reactive group consumption to obtain an idea about network formation efficiency. To further confirm the effect of molecular weight of the polymeric segment on hydrogel properties, dipyridyldisulfide modified PEGs with varying molecular weight of 2000, 4000 and 8000 gmol^{-1} were selected. Hydrogels with good gel conversions were obtained, as determined gravimetrically (Table 1). The gelation was evaluated via *in situ* rheometry and increasing polymer length was found to exhibit lower gelation kinetic. The concentration of free thiol from βCD-SH during network formation was performed to determine the concentration of free thiol in hydrogels using 5,5'-dithio-bis-(2-nitrobenzoic acid) (DTNB), often termed as Ellman's reagent. DTNB produces 2-nitro-5-thiobenzoic acid (TNB) after the reaction with the sulfhydryl group of β-cyclodextrin. The TNB species is a yellow-colored product and it has a distinct absorption at 412 nm. Thus the total number of free thiols present in the hydrogel can be determined measuring the amount of released TNB. The results presented in Table 5.1 clearly demonstrate that most of the thiols are consumed and a slight decrease in reaction efficiency is observed upon increase

in molecular weight (Table 5.1). Considering the fact that seven thiol groups are all concentrated at the lower rim of the CDs, a conversion above 80% is quite satisfactory.

Table 5. 1. Series of hydrogels forming different molecular weight of difunctionalized PEG bispyridyldisulfide and gel conversions of synthesized hydrogels.

Entry	**Hydrogel**	**Polymer**	**Gel Conv.[a] (%)**	**Thiol Consumption (%)**
1	CDP2K	PEG 2K	91(±4.24)	86.30
2	CDP4K	PEG 4K	90(±5.39)	85.60
3	CDP8K	PEG 8K	87(±2.39)	81.50

[a] Calculated as (dry hydrogel weight/total weight of polymer and βCD-SH) × 100 (Data in triplicate).

After crosslinking of hydrogels, the swelling behavior of hydrogels was investigated to determine the equilibrium degree of swelling. For this purpose, freeze dried hydrogel samples with similar dimensions were immersed in water and expected to reach the equilibrium degree of swelling. To achieve good precision, three measurements were carried out on hydrogels of similar dimensions acquired from different gel samples. As expected for such hydrophilic networks, all hydrogels demonstrated fast swelling kinetics. Increase in equilibrium swelling values was consistent with increase in the molecular weight of PEG polymer in the hydrogels (Fig 5.2(a) and (b)).

The obtained hydrogels had a translucent appearance in their wet state (Figure 5.3 a). The interior morphology of the dry gel samples was examined by using scanning electron microscopy (SEM). SEM images of prepared hydrogels as shown in Figure 5.3 shows the morphology of hydrogels in their dried states. All hydrogel networks possessed a homogeneous porous structure. As expected, macroporous structure of hydrogels increases upon increase molecular weight of PEGs utilized during the synthesis.

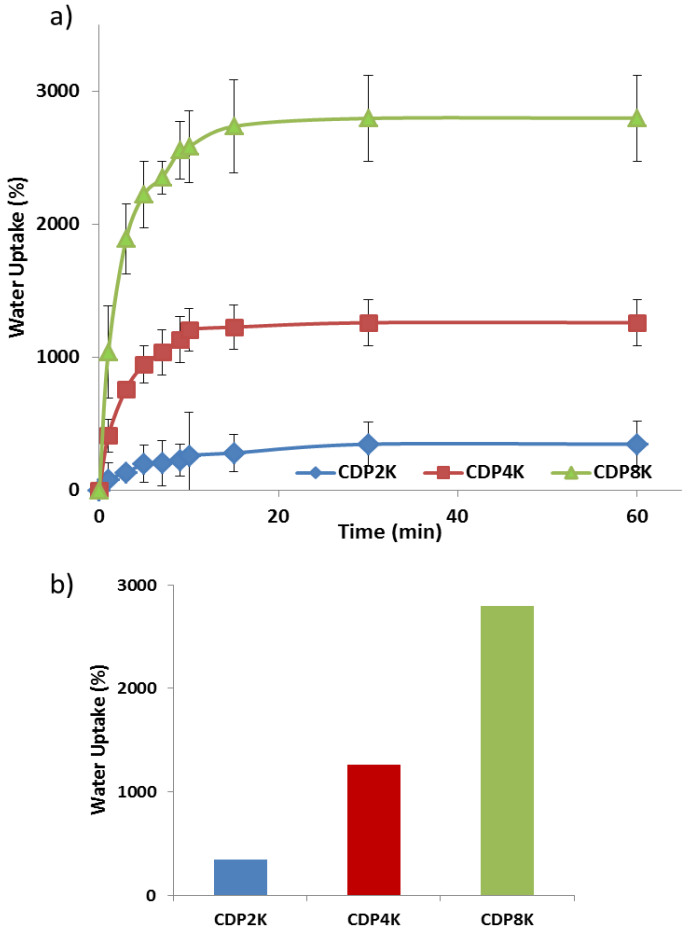

Figure 5.2. (a) Water uptake plots of time-dependent swelling of hydrogels with the varing of PEG chain length. (b) Comparison of maximum water uptake values of hydrogels.

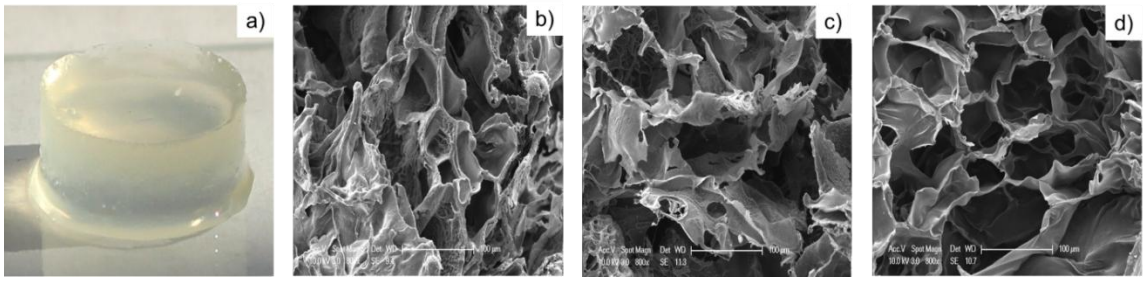

Figure 5.3. (a) Photograph of representative hydrogel sample (a) in wet state. Representative ESEM images of freeze-dried hydrogels: (b) CDP2K, (c) CDP4K and (d) CDP8K.

To follow the gelation process, estimate the gelation time and final elastic modulus for hydrogels with varying polymer molecular weight, time sweep tests were performed by using strain of 0.5 and frequency of 10 rad/s^{-1}. Initially, the storage modulus (G′) could not be observed since it was too low to measure. It was observed that CDP2K quickly formed a gel reaching of its storage modulus of 5990 Pa in 24 min as indicated by the crossover of the storage and loss modulus. As expected, the gelation kinetics of CD8K was slower than the other hydrogels, yielding a hydrogel with storage modulus of 2440 Pa in 54 min. It is interesting to note almost linear correlation of gelation time with molecular weight of used PEGs. It can be concluded that the difference at the gelation times results from increasing the polymer concentration i.e. increasing concentration of reactive end groups (Figure 5. 4). Also, it can be suggested that the longer chain lengths of higher molecular weight polymers find each other with more difficulty due to steric reasons.

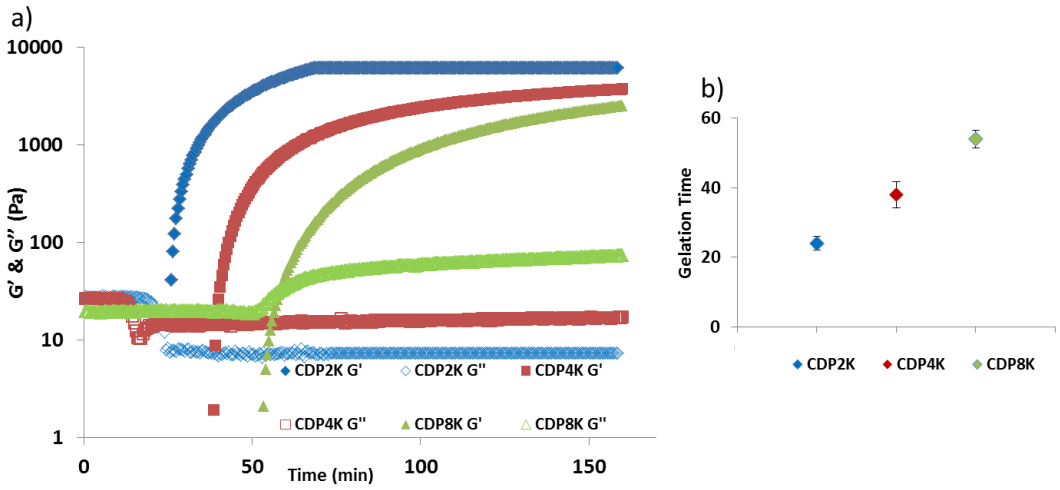

Figure 5.4. (a) Time sweep test for hydrogels with different molecular weight of polymer and (b) comparison of gelation time with different molecular weight of PEG.

To evaluate the effect of change in molecular weight of PEG chains on the physical behavior of the hydrogels, mechanical characteristics of hydrogels were determined by rheology. Generally for gel samples, strain sweep test, frequency test and time sweep test were monitored to obtain information about the variation in stiffness of hydrogels. By measuring of the strain test, the linear viscoelastic regions (LVE) of hydrogels were determined. For all samples, the storage modulus (G′, elastic component) is greater than the

loss modulus (G″, viscous behavior) in the whole frequency range of LVE, as expected for the presence of a stable crosslinked gel structure. When increasing strain (0.01 to 100%) was applied on hydrogels, a linear behavior was observed until 10 %. Hence, frequency sweep (from 0.01 to 100 Hz) test using strain value of 0.5 was carried out to investigate the stiffness behavior of hydrogels. A direct relationship between polymer molecular weight and storage modulus values was observed (Figure 5.5). For example, the P2CD hydrogel obtained by using the polymer with the lowest molecular weight shows highest stiffness, as expected due to highest crosslink density.

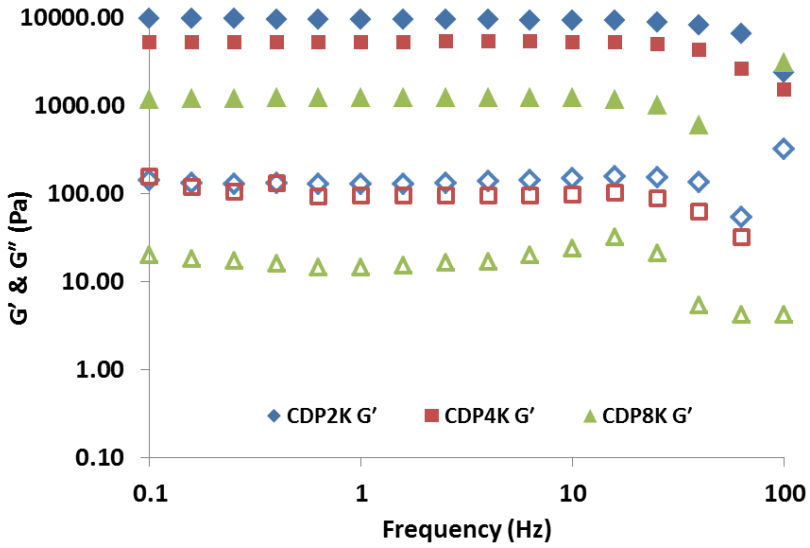

Figure 5.5. Frequency sweep test results of hydrogels. Solid and empty legends show storage and viscous elastic modulus respectively.

5.3.2. Degradation of Hydrogels

These hydrogels can be degradable under physiological conditions in the presence of reducing agents such as DTT and glutathione, since their network is composed of disulfide linkages. To study the rate of degradation of these hydrogels, disk shaped hydrogel samples were first immersed in phosphate buffered saline (PBS), and then immersed in various concentration of DTT (20 and 200 mM) and glutathione (20 and 200 mM) containing PBS solutions at 37 °C. As expected, the use of a reducing agent solution instead of a PBS increases the hydrogel degradation time Figure 5.6a. A degradation time

of 147, 117 and 11 min was observed for hydrogels CDP2K, CDP4K and CDP8K, respectively upon treatment with DTT (200 mM) solution.

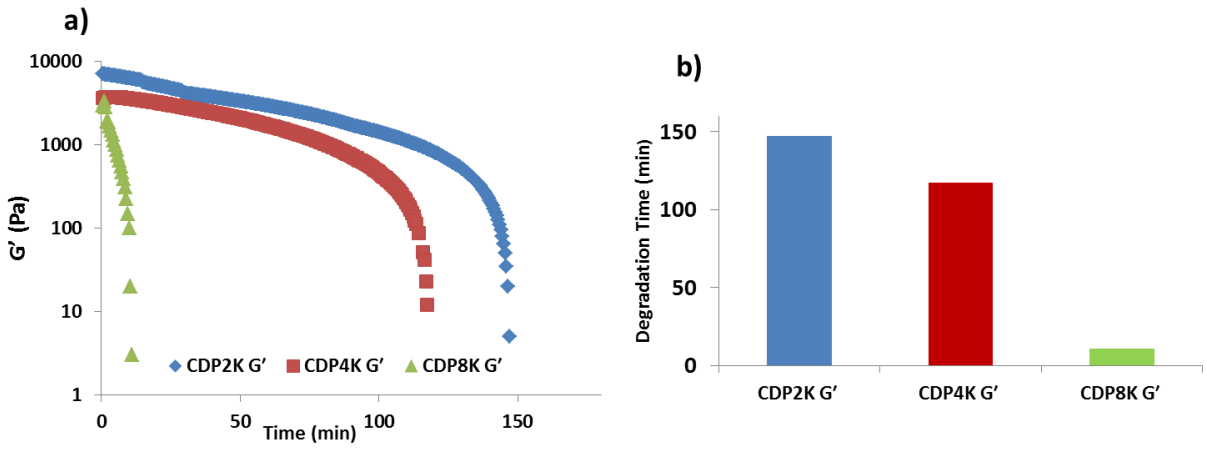

Figure 5.6. (a) Change in storage modulus for hydrogels in the presence of 200 mM DTT, (b) degradation time of hydrogels.

Such a decrease in degradation time upon increase of the PEGs molecular weight is expected since the hydrophilicity, overall swelling is higher of gels with longer PEG chains. Furthermore, most importantly, the number of crosslink density decreases upon increasing the molecular weight of PEG component. Similarly, degradation in glutathione, a naturally occurring thiol in our body, also exhibited similar trend. Figure 5.7a shows that degradation rates for CD2K and CD8K in 200 mM glutathione concentration in PBS at 37 °C are slower than the results obtained with DTT in PBS solution. Figure 5.7a shows that by increasing the PEG molecular weight from 2K to 8K, the hydrogel degradation time decreases almost twenty times due to lower number of disulfide linkages and higher swelling capacity. The disulfide bond cleavage observed in the presence of 20 mM DTT and glutathione are shown in figure 5.7b. As expected, degradation with glutathione is slower than the degradation with DTT since DTT has one more thiol group than glutathione, and has higher reactivity. Briefly, the degradation rate of CD hydrogels can be controlled by the concentration of the reducing agent and the chain length of the PEG polymer. Importantly, these networks can be completely degraded by using mild and biocompatible reducing agents.

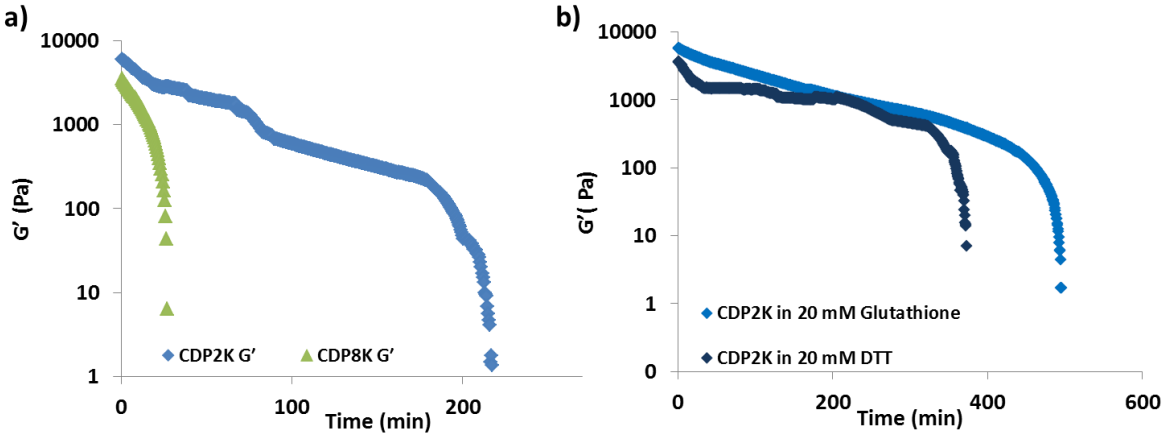

Figure 5.7. (a) Degradation of CDP2K and CDP8K with 200 mM glutathione, (b) the differences of degradation time of CDP2K in 20 mM glutathione and 20 mM DTT.

5.3.3. Drug Loading and Release Studies

To investigate the potential of β-CD and to control drug release from PEG based hydrogels, curcumin (cur), a hydrophobic drug was chosen. Hydrogels prepared as disks were immersed in curcumin solution for exemplary drug loading studies. It was found that the swollen hydrogel disks could be loaded with curcumin until equilibrium after 24 h of immersion. Immersion was monitored by the UV-vis spectroscopy since curcumin is a chromophore which exhibits a broad and relatively high molar extinction coefficient at 425 nm in methanol. Therefore, the beginning and final concentration of curcumin was determined to calculate the amount of drug absorbed by hydrogels. As expected, the amount of curcumin loaded in hydrogels was affected by the amount of β-cyclodextrin in the hydrogels. The higher the β-CD content, the more curcumin was loaded in the hydrogel. This could be attributed to the formation of inclusion complexes between the β-CD groups and hydrophobic curcumin molecules. *In vitro* release study of curcumin from hydrogels was carried out to evaluate the cumulative drug release. Hydrogels loaded with the drug were rinsed with distilled water to remove surface adhered drugs and then immersed in pH 7.4 PBS at 37 ^{o}C. At periodic time points, an aliquot of the release medium was replaced with fresh solution, and then the curcumin released in aliquot was analyzed by using a UV-vis spectrophotometer. According to Fig. 5.8a, in the first 1h, a burst release of curcumin was observed in all gels, where the reason for the burst release could be due to release of curcumin that is adsorbed in the voids of the hydrogel. It was

clear that when the polymer molecular weight increased, more curcumin was released from the gel at a higher rate. An increase in the CD content of the hydrogel decreased the amount of released drug, even at the burst stage. This can be due to higher amount of complexed drugs than free drugs within the hydrogel matrix. Over the course of first 72 h, 65% of loaded curcumin for CD8K was released in PBS. On the other hand, in the same time interval the fraction of curcumin released from CDP2K and CDP4K in PBS were about 50 and 56%, respectively. From the results presented in Figure 5.8, the release profile for all samples became constant after 72 h. However, to confirm the presence of the bound curcumin and observe the expected full drug release, all sets of hydrogels were treated with DMSO. This treatment confirmed that all of the curcumin remaining in the hydrogels was completely released (Figure 5.8a).

The release of drug from hydrogels was evaluated in the presence of the degrading agent like GSH. As expected, because of the cleavage of disulfide bonds with 5 mM GSH, higher drug release was obtained in the presence of reducing agent. After 72 h, it was observed that all hydrogels showed nearly quantitative drug release in the presence of 5 mM GSH (Figure 5.8b).

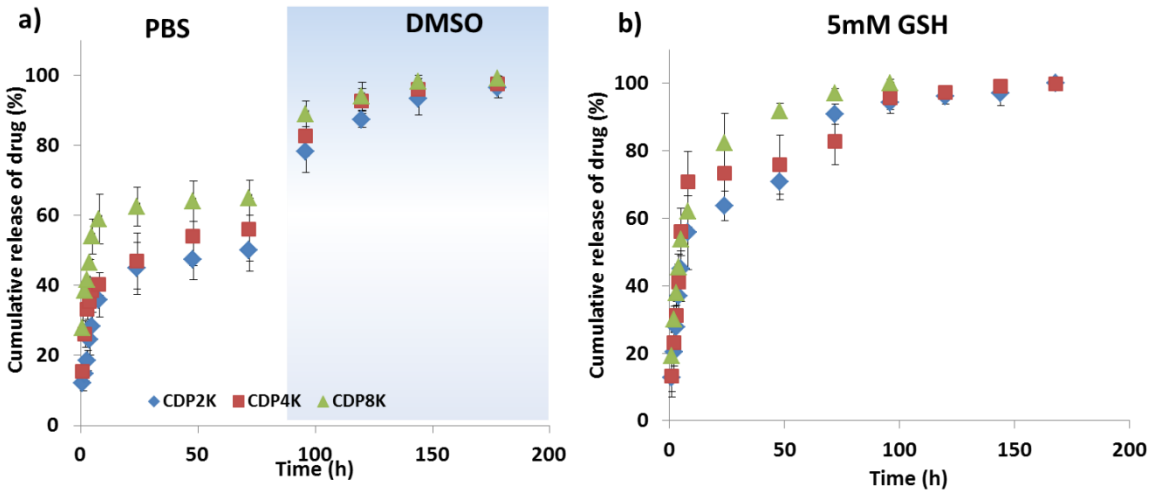

Figure 5.8. Cumulative release of curcumin from hydrogels in (a) PBS and then DMSO and (b) 5 mM GSH.

To address the suitability of these hydrogels for biological applications, cytotoxic profiles of hydrogels CDP2K, CDP4K, CDP8K and drug loaded versions were investigated. Curcumin was encapsulated within the three series of hydrogels. Afterwards, hydrogels with and without encapsulated curcumin were rinsed with water to get rid of loosely adhered species. All hydrogels were incubated with U-87 MG human glioma cells. From the cell viability assay, hydrogels without drug show over 90% cell viability after incubation for 8h, while cell viabilities of drug loaded hydrogels decreased 50 %. Free curcumin showed significant cell toxicity as expected. After 24 and 8 h incubation, any significant difference in cell viability between CDP2K, CDP4K and CDP8K hydrogels was not notable (Figure 5.9 (a) and (c)). However, there was significant differences in cell toxicity for drug loaded hydrogels. Although all of them contained same amount of drug, CDP8K hydrogels resulted in viability as low as 20 % and 10% after 8 h and 24 h, respectively (Figure 5.9 (b) and (d)). The cell viabilities were almost double and quite comparable for the hydrogels formulated with PEGs with lower molecular weight. These results can be expected since the drug release from higher molecular weight PEG was also significantly higher than the other two. These results indicate non-toxic behavior of parent hydrogels, as well as their ability to release encapsulated drugs to effectively induce cell death, thus demonstrating the potentials as these materials for sustained drug delivery.

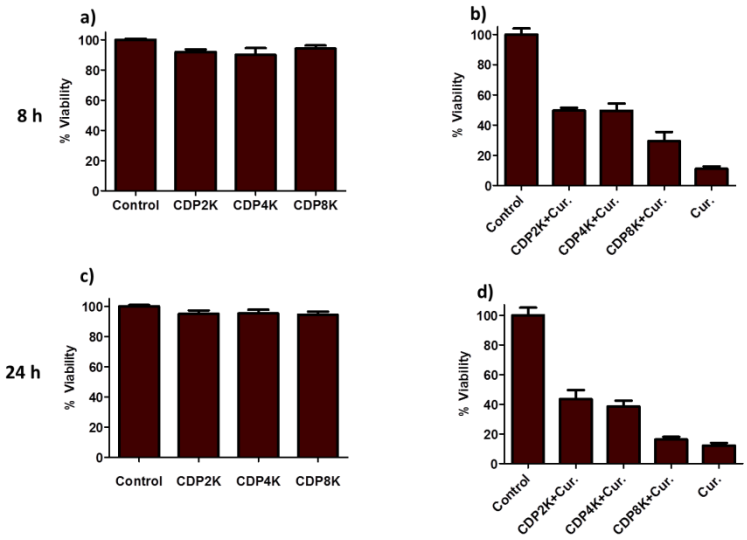

Figure 5.9. Cell viabilities of CP2K, CDP4K, CDP8K on U87 after 8 and 24 hours of incubation (a) and (c), and curcumin loaded CDP2K, CDP4K and CDP8K hydrogels (b, c). Cell viability was determined by CCK-8 assay.

As a next step, to evaluate the effect of disulfide linkages degradation in the CD-based hydrogel network cellular internalization of the drug loaded in CDP8K into U-87 MG human glioma cells was conducted. To show the GSH mediated payload release from CDP8K hydrogels, cell media was treated with 5 mM GSH. As a control experiment, equal drug amount loaded hydrogels were incubated in cell media without GSH. After incubation for 24h, cell nuclei were stained by utilizing a blue fluorescent dye, 4',6-diamino-2-phenylindole (DAPI) and results were analyzed using fluorescence microscopy. A significant increase in fluorescence intensity for cells incubated with 5 mM GSH was observed, while much lower fluorescence intensity was observed for cells devoid of GSH (Figure 5. 10). Cell internalization experiments demonstrate the critical role of thiol-induced hydrogel degradation on internalization of a hydrophobic drug.

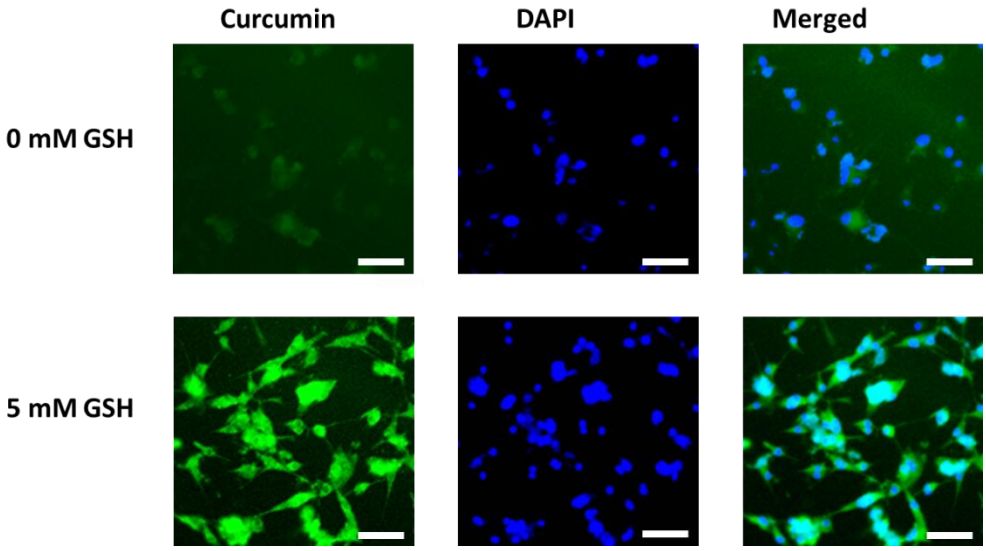

Figure 5.10. Internalization experiments of drug loaded CDP8K (1mg) in the presence of 0 mM and 5 mM GSH. Scale bar 50 μm.

5.4. Conclusion

We have designed and developed novel CD-containing well-defined PEG-based hydrogels by using crosslinking between heptathiol-derivative of β-CD and dipyridyldisulfide-terminated PEGs. Gelation was induced because of the thiol-disulfide exchange reaction between the thiol groups on CD and the activated pyridyldisulfide group

on chain ends of PEGs. These novel hydrogels were characterized in terms of their swelling properties, morphologies, rheological behaviors and degradation patterns. It was demonstrated that the molecular weight of the PEG component utilized had profound effect on both physical and chemical behavior of these hydrogels. Based on the formation of inclusion complex between β-CD and curcumin, we loaded the hydrophobic drug curcumin into β-CD containing hydrogels. Drug release profiles suggested prolonged and sustained release of the curcumin. In addition, release of curcumin was studied in presence of a thiol-based reducing agent, and a much enhanced release of curcumin from hydrogel was observed. Cytotoxicity of empty and drug loaded hydrogels were investigated using U-87 MG human glioma cells, and observed cytotoxicity data obtained was in good agreement with drug release profile. Furthermore, cell internalization studies of drug from hydrogels indicated that drug uptake by cells increased significantly in the presence of 5 mM GSH, thus highlighting the importance of the CD-containing degradable network structure in efficient delivery of the hydrophobic drug.

6. REVERSIBLE THIOL FUNCTIONALIZED HYDROGELS VIA PHOTOPOLYMERIZATION

6.1. Introduction

Past decades have witnessed a lot of effort in the design and fabrication of novel reactive crosslinked hydrophilic polymeric materials, often termed as hydrogels, for various biomedical applications. Hydrogels can absorb substantial amount of water while preserving their crosslinked network structures. This property enables them to mimic the biological environment and thus present themselves as biocompatible materials [65, 113]. For this reason, hydrogels have been widely used in biomaterial and pharmaceutical applications such as contact lenses, tissue engineering, drug release systems and biosensors. Additional reasons for utilizing hydrogels are their facile and low cost fabrication and chemical versalities [132-140].

Generally, fabrication of hydrogels is achieved by chemical or physical crosslinking.[7] Chemical crosslinking is often preferred to build hydrogel networks since it provides them higher mechanical stability. Based on the facile fabrication, photo-crosslinking based techniques have become a widely used method for preparation of these chemically crosslinked polymeric scaffolds [34, 90].

In recent years, reactive hydrogels have been extensively investigated because their modification with various biomolecules allow design of materials with increased functionality and wider applicability. Reactive hydrogels are usually synthesized using reactive monomers or polymers, which are afterwards reacted with biologically relevant molecules such as bioactive ligands, peptides etc. Conjugation of drugs and their release in a controlled manner can be achieved using various type of linker chemistry, therefore, hydrogels can also serve as attractive delivery agents [141, 142].

Hydrogel based materials can be used in post-operative drug releasing applications to eradicate residual cancer cells. Development of materials that will slowly release the

drug due to characteristic tumor environments are potential candidates for such use. We envision that perhaps the system can be made more effective if there are binding ligands on these materials that will attract cancerous cells preferentially. The same idea can be applied for developing anti-bacterial surfaces. Presence of a ligand that can attract the target cell or bio-organism like bacteria to the surface and then deliver the toxic agent would be an interesting and hopefully effective approach to increase the killing efficiency. Hence, it will need hydrogels where the cytotoxic agent is bound using a reversible, specifically cleavable chemistry, while the target attractive fragment is bound using a non-reversible linker (Figure 6.1).

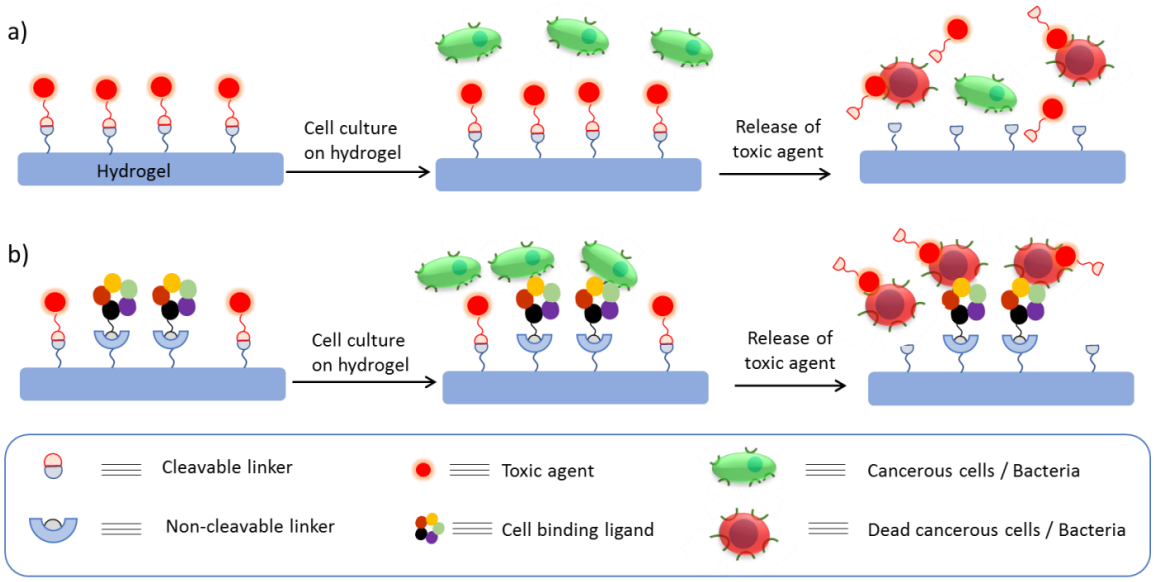

Figure 6.1. Schematic illustration of delivery of toxic agent with simultaneous attraction of target organism using reversible and non-reversible linkages.

As a model study to create the above mentioned hydrogel platform, dual-reactive hydrogels containing two different reactive groups, where the first group could irreversibly bind a fluorescent molecules into the hydrogel and the second group could release the reversibly bound molecules on demand (triggered by conditions of the medium) were fabricated (Figure 6.2). Maleimide group was chosen for irreversible dye attachment via Michael addition reaction, and pyridyldisulfide group was chosen for the binding of the compounds to be released through reduction. Although a system which does not use both linkage chemistry based on thiols, but uses an amine and thiol would be simpler, we

wanted to examine if we can make such a unique system that has potential to use two different thiols. Monomers containing these reactive groups can be used to obtain hydrogels via photopolymerization at room temperature. Effective functionalization of reactive groups in hydrogel network with fluorescent BODIPY-SH dye molecules was demonstrated and release study of the dye molecules from hydrogels in the presence of reducing agent was investigated. Cytotoxicity measurements demonstrated that these gels were not toxic. Although further studies will be needed to establish the validity of the system, these dual functional hydrogels bear potential for applications in targeted delivery.

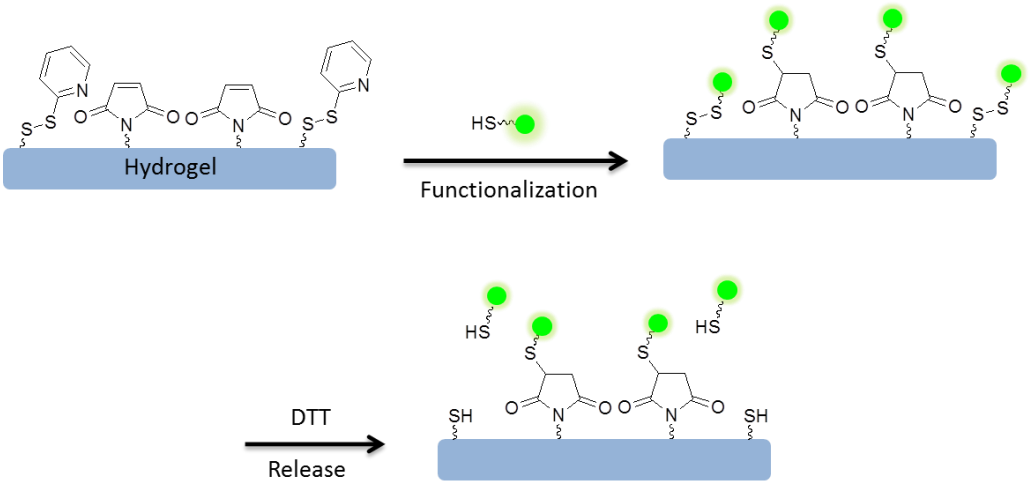

Figure 6.2. Thiol functionalized hydrogel formation and dye conjugation of the hydrogel.

6.2. Experimental Section

6.2.1. Materials and Characterization

2,2 dipyridyldisulfide was purchased from TCI chemicals. Poly(ethylene glycol) methyl ether methacrylate (PEGMEMA, Mn = 300 g mol^{-1}), 2,2-dimethoxy-2-phenylacetophenone (DMPA), L-glutathione reduced and poly(ethylene glycol) dimethacrylate (PEGDMA, Mn = 550 g mol^{-1}) were obtained from Sigma Aldrich and L-dithiothreitol (DTT) were purchased from Fluka. Methacryloyl chloride was purchased from Alfa Aesar. Furan protected maleimide monomer [28] and BODIPY-SH [143] were synthesized according to previous report. Photopolymerization reactions were performed at 365 nm using a handheld high intensity UV lamp with a 100 W spot bulb and 7° beam

width. UV-vis studies were carried out using a Varian Cary 50 Scan UV-vis spectrophotometer. FT-IR spectra of the hydrogels were performed using Thermo Fischer Scientific Nicolet 380. GraphPad Prism software was used to determine cell viability.

6.2.2. Synthesis of Pyridyl-Disulfide Alcohol

Pyridyldisulfide alcohol was synthesized according to reported procedures. Briefly, in a round bottom flask equipped with a magnetic stirrer, 2,2-dipyridyldisulfide (2 g, 9.08 mmol) was dissolved in methanol (5 mL) and acetic acid (0.13 mL, 2.27 mmol) was added into solution and the mixture was stirred under N_2. A solution of mercaptoethanol (0.32 mL, 4.54 mmol) in methanol (3 mL) was added dropwise to the reaction flask. The reaction was left to proceed for 4 h at room temperature. After the formation of alcohol, excess solvent was evaporated under *vacuo* to obtain a yellow liquid. The product was purified by column chromatography by using ethyl acetate and hexane (15:85) as eluent (80% yield).

6.2.3. Synthesis of Pyridyl-Disulfide Monomer

Pyridyldisulfide alcohol (1 g, 5.34 mmol) was dissolved in anhydrous DCM (5 mL) and triethylamine (0.74 mL, 5.34 mmol) was added to the solution. The mixture was cooled to 0 ^{o}C in an ice bath under N_2. Methacryloyl chloride (0.78 mL, 7.37 mmol) was added dropwise with continuous stirring into the mixture. The reaction was stirred in the dark at room temperature for 24 hours. Thereafter, extraction was done 30 mL with distilled water, then with $NaHCO_3$ (2x30 mL) and with brine (30 mL).Organic layer was collected and dried over anhydrous Na_2SO_4. The product was purified by column chromatography using ethyl acetate and hexane (18:82) [105].

6.2.4. Synthesis of Hydrogels

PEG based hydrogels were fabricated through photopolymerization of PDS and FuMaMA with PEGMEMA cross-linkers. For a representative hydrogel formation (H1): furan protected maleimide monomer (FuMaMA) (7.54 mg, 0.0259 mmol), pyridyldisulfide

monomer (6.6 mg, 0.0259 mmol), PEGMEMA (61.9mg, 0.207 mmol) and PEGDMA (14.2 mg, 0.0259 mmol) was placed in a glass vial and dissolved in DMSO (70 μL). A solution of DMPA (5 mg, 0.0194 mmol) in DMSO (10 μL) was added into the vial and sonicated for 10 min to achieve a homogenous mixture. The mixture was placed under UV irradiation for 45 min. After hydrogel formation, the bulk hydrogels were washed with DMSO followed by distilled water several times and to remove unreacted reagents. Hydrogels were lyophilized to obtain dry samples. As a control experiment, gel precursor without PEGDMA was prepared and exposed to UV irradiation. As expected, gelation was not observed under same reaction conditions in the absence of the crosslinker.

6.2.5. Swelling Studies of Bulk Hydrogels

A sample of dried bulk hydrogel was swollen in distilled/deionized water at room temperature. A moist filter paper was used to remove excess water, and then the weight change was measured periodically until gel sample demonstrated constant weight. The swelling ratio of gel sample was obtained from the following equation:

$$\% \text{ Swelling Ratio} = 100 \times (W_{wet} - W_{dry}) / W_{dry}$$

where, W_{wet} and W_{dry} are the wet and dry weight of the bulk hydrogels, respectively. The swelling behaviors of hydrogels were repeated at three times.

6.2.6. Scanning Electron Microscopy (SEM) Analysis of Hydrogels

Surface morphologies of dried bulk hydrogel samples were investigated with a scanning electron microscope (SEM) performed with an ESEM-Philips XL-30 (Philips, Eindhoven, The Netherlands) instrument at an accelerating voltage of 10 kV.

6.2.7. Rheological Measurements of Bulk Hydrogels

The mechanical behaviors of prepared bulk hydrogels were analyzed using an Anton Paar MCR 302 rheometer. Prepared hydrogels were analyzed by the help of the angular frequency and time sweep tests. The cylindrical disc shaped hydrogel samples (2 mm thickness) were immersed in distilled water and kept at room temperature till they reached equilibrium swelling capacity. For rheological measurements, a parallel plate

configuration with 8 mm diameter and 2 mm for gap, and 0.5 % strain between 0.1-100 rad/s was used.

6.2.8. Pyridothione Release from Bulk Hydrogels

Release of pyridothione from hydrogels was carried out by using GSH, was added as a reducing agent. Hydrogel samples (5 mg) were placed into 3 mL of glutathione solution (1.5-fold excess of glutathione corresponding to the pyridyl disulfide groups) in PBS at 37 ^{o}C. At several time points, solutions were removed out and analyzed by UV-vis spectrophotometer. Absorbance of pyridothione at 343 nm was measured and the release of pyridothione from hydrogels was calculated using the molar extinction coefficient of pyridothione.

6.2.9. Activation of Protected-Maleimide Functional Groups

Protected maleimide groups within the hydrogels were activated by heating the hydrogels in dry toluene (20 mL) at 110 ^{o}C for 10 h.

6.2.10. Conjugation of Hydrogels with Thiol-Containing Fluorescent Dye

Thiol reactive bulk H1, H2 and H3 hydrogels were functionalized via thiol-containing BODIPY-SH dye conjugation. Briefly, a disk shaped hydrogel (10 mg) was placed in a glass vial and BODIPY-SH molecule, corresponding to the maleimide groups within gel in 3 mL of THF was added to the vial. The mixture was stirred at room temperature for 24 h. After conjugation, dye conjugated hydrogels washed with excess THF and then water to remove excess dye.

6.2.11. BODIPY-SH Release from Bulk Hydrogels

BODIPY conjugated hydrogels (10 mg) were placed in 3 mL of DTT solution (10 mM in 1x PBS) in dialysis bag with MW cut-off 1 kDa. At periodic time intervals, 100 µL of release medium were collected and diluted with 3 mL of THF and then analyzed by UV-vis spectroscopy. The results were determined in terms of cumulative release.

6.2.12. *In vitro* Cytotoxicity Experiments

L929 cells cultured in RPMI 1640 media supplemented with 10% FBS were used for the experiment. 6000 cells/well were seeded in a 96 well plate as triplicates, 24 h before experiment. Hydrogel samples (1mg/well) were modified with glutathione to get rid of pyridothione groups and then these modified gels were added into each well and incubated at 37 ºC for 48 h. After incubation the gel was removed with medium and wells were washed with PBS twice. Cytotoxicity of hydrogels was analyzed via CCK-8 assay. Cell viability after incubation with PDS containing gels was calculated with respect to a control gel without PDS functional group via GraphPad Prism software.

6.3. Results and Discussion

6.3.1. Fabrication and Characterization of Bulk Hydrogels

PEG based hydrogels containing varying amounts of furan protected maleimide monomer, pyridyldisulfide and hydrophilic PEGMEMA monomer were synthesized under UV irradiation at room temperature for 45 min (Figure 6.3). PDSMA [105] and FuMaMa [28] monomers were synthesized according to literature, and gelation was achieved in the presence of PEGDMA as a crosslinker and DMPA as a photoinitiator. In order to give maleimide functionality to the hydrogels, a furan protected monomer was used in order to keep the maleimide units from crosslinking during gelation step. Transparent and soft hydrogels were obtained with a yield of 90%.

Hydrogel compositions and conversions of gelation are tabulated in Table 1. It is clearly seen that the conversion data of the hydrogels is as expected.

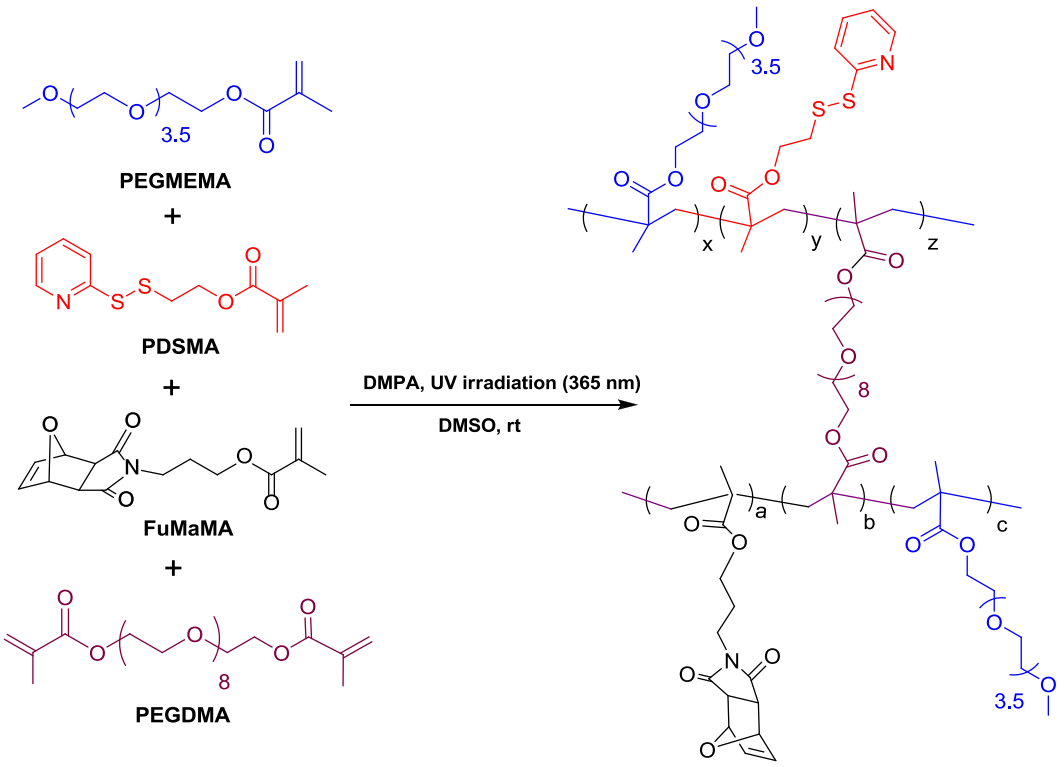

Figure 6.3. Synthesis of PEG based bulk hydrogels.

Table 6.1. Composition and conversions of bulk hydrogels

Sample	PEGMEMA (M_n g mol^{-1})	The ratio of monomer (PDSMA : FuMaMa : PEGMEMA) (%)	Conversion[a] (%)
H1	300	10:10:80	93
H2	300	20:10:70	90
H3	300	40:10:50	89

[a] Conversion (%) = (dry gel weight / total weight of monomers + crosslinker) × 100.

In order to examine the surface morphology of the hydrogels, scanning electron microscopy (SEM) was used. Dried hydrogel samples were analyzed using an accelerating voltage of 10 kV. Hydrogels did not show notably porous structure, they were nonporous rubber-like morphology, as expected for hydrogels with short PEG chains (Figure 6.4).

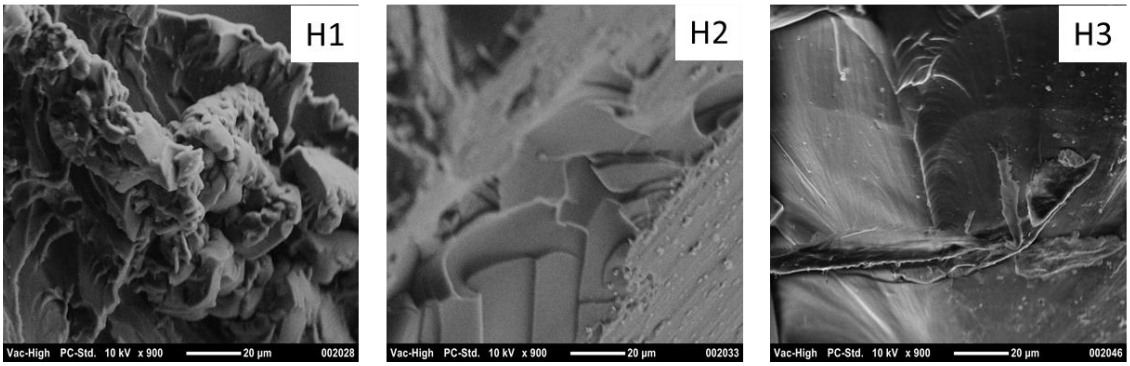

Figure 6.4. SEM images of bulk hydrogels.

Prepared hydrogels were evaluated in terms of their water uptake behaviors. Dried hydrogel samples were immersed in water and their water uptake capabilities were determined by gravimetric analysis. After hydrogels reached their maximum equilibrium degree of swelling within 90 min, % swelling capabilities of hydrogels were calculated. As expected, although all gels exhibited an increment in their swelling behaviors over time, the highest swelling capacity were observed for H1. Since swelling behavior of hydrogels depends on the hydrophilicity, highest water uptake capability belonged to the hydrogel H1 containing higher amount of hydrophilic PEG monomer (Figure 6.5).

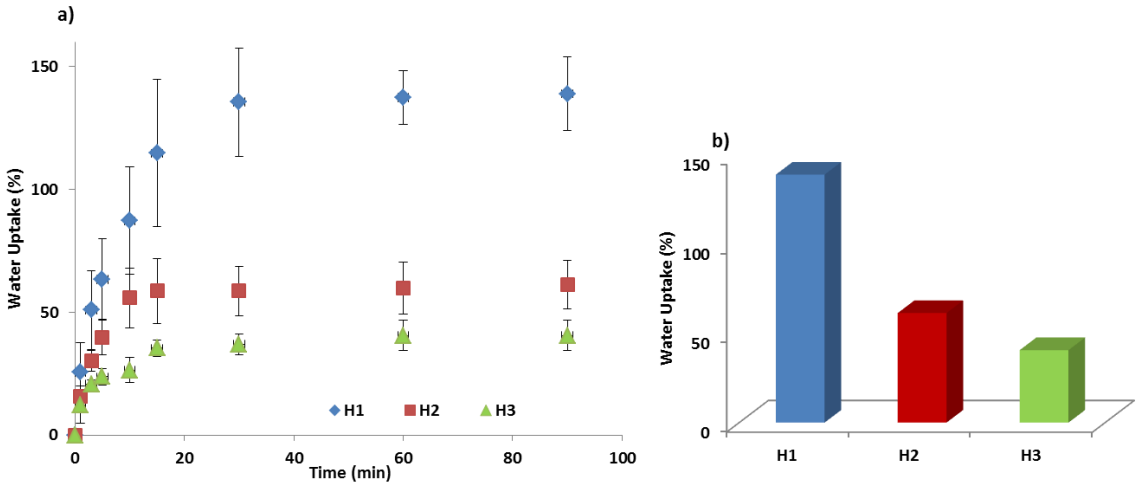

Figure 6.5. a) Water uptake profiles of bulk hydrogels and b) comparison of swelling behavior of hydrogels containing different monomer ratio.

The rheological behaviors of synthesized hydrogels were examined employing time sweep tests. Figure 6.6 shows the gelation time values of hydrogels. As expected, when UV illumination was not used, gelation was not observed. After 3 mins, gel mixtures were exposed to UV light, gelation took place in seconds. Also, G' values indicating lower PEG component for H4 was higher than other hydrogels.

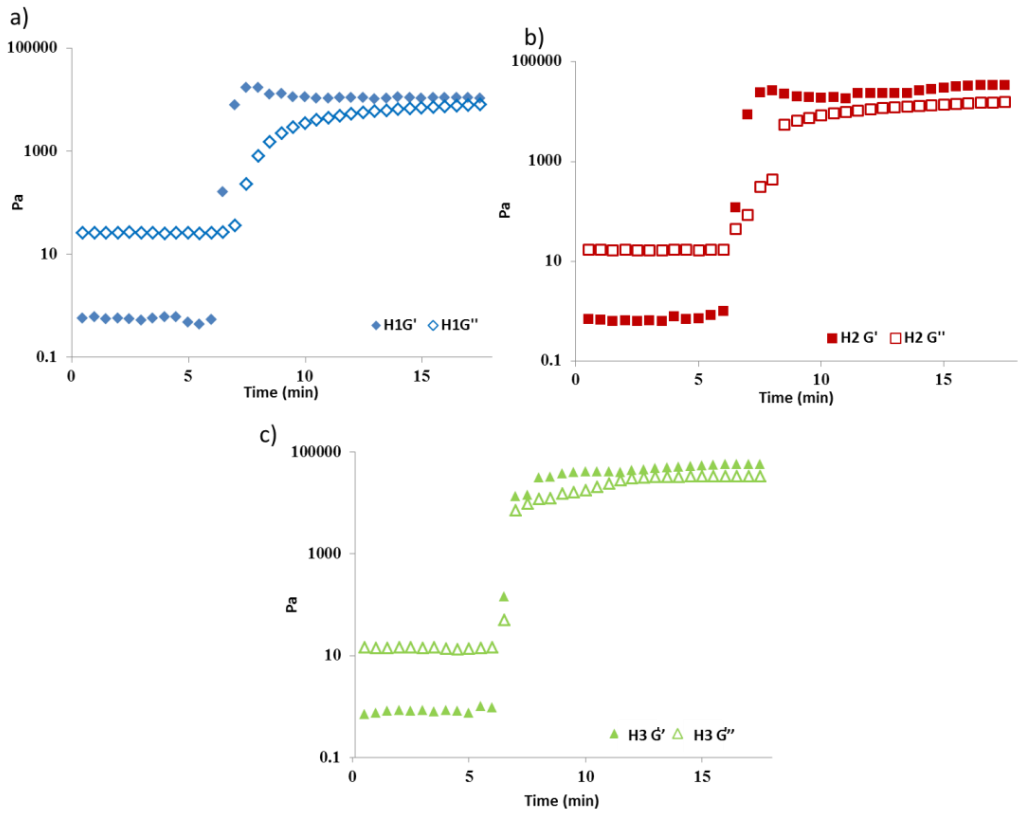

Figure 6.6. Time sweep test values of hydrogels. (a) for H1, (b) for H2 and (c) for H3.

Other rheological behaviors of bulk hydrogels were examined by dynamic frequency sweep tests. It was obtained that storage (G′) and loss (G″) modulus of water swollen hydrogels were ranging from 10^0 to 10^5. It was deduced that the increase in hydrophilic PEG monomer in the hydrogel leads to an increase in the storage modulus as expected (Figure 6.7).

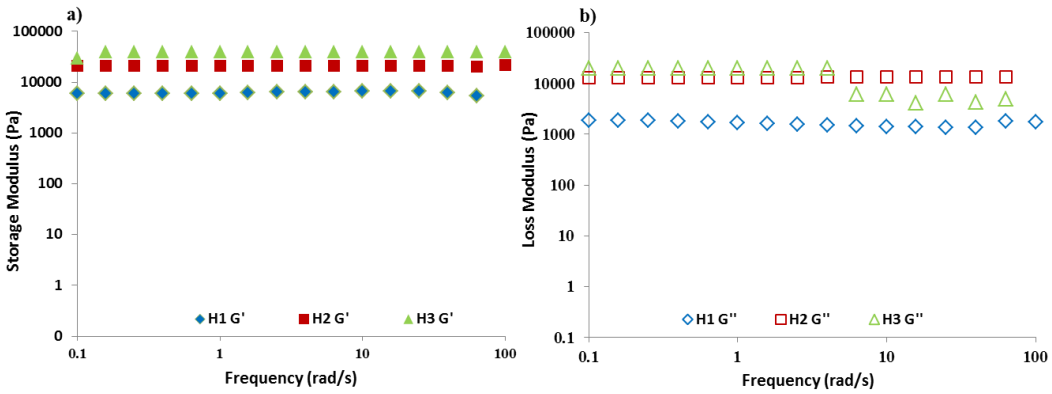

Figure 6.7. (a) Storage moduli and (b) loss moduli of hydrogel.

6.3.2. Activation of Maleimide Units in Hydrogels

After the characterization of hydrogels, removal of furan protecting groups was carried out via retro Diels-Alder reaction. Thermogravimetric analysis (TGA) was used to determine the presence of furan protected maleimide groups in the hydrogels, by probing the activation of the maleimide groups via loss of furan during rDA reaction. Thermogravimetric analysis (TGA) of the hydrogel (H1**)** showed a continuous weight loss starting from 60 to 180°C due to the release of furan molecules from the protected maleimide groups. From the clear weight loss observed in the TGA analysis, it can be easily concluded that furan protected monomers were incorporated in the hydrogels and they undergo deprotection upon heating (Figure 6.8).

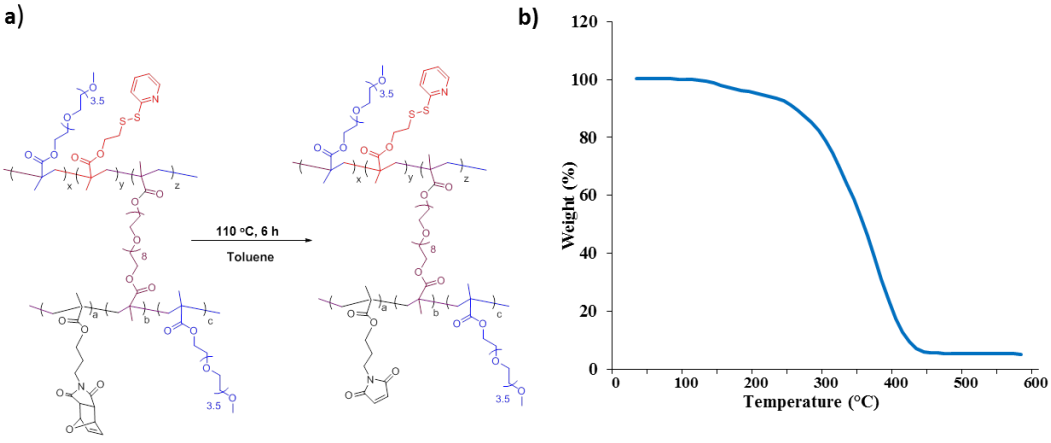

Figure 6.8. a) the retro Diels Alder reaction of hydrogel H1 and b) thermogravimetric analysis of hydrogel H1.

6.3.3. Release of Pyridothione from Hydrogels

Hydrogels H1, H2 and H3 contain varying amounts of pyridyldisulfide monomer, thus upon exchange reaction with thiol-containing molecules or reducing agent, varying amount of pyrido-2-thione fragment should be released (Figure 6.9).

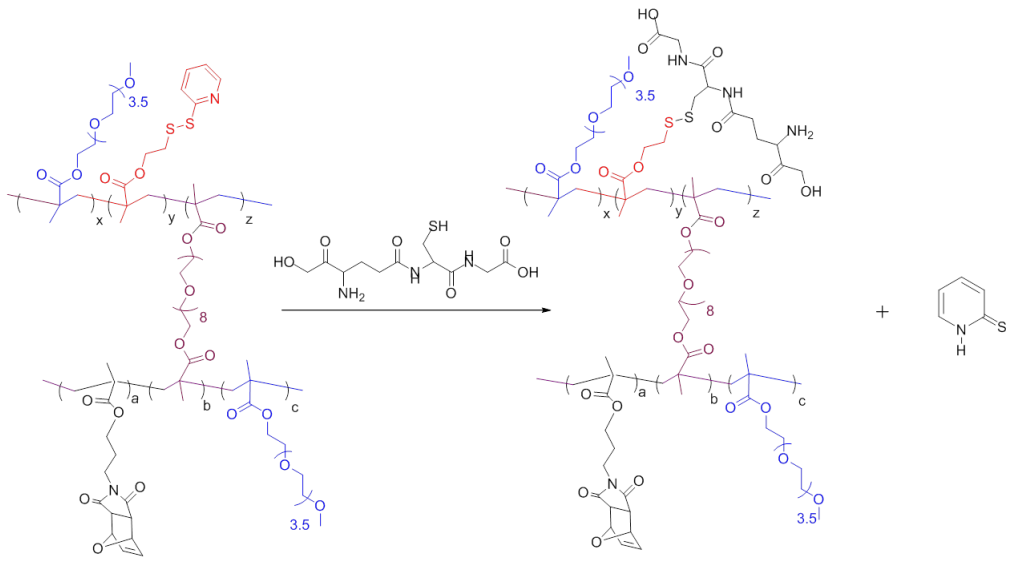

Figure 6.9. Pyridothione release from hydrogel in the presence of reducing agent (GSH).

Since pyridothione gives a characteristic absorbance peak at 343 nm, the cumulative release of pyridothione can be determined using UV-vis spectroscopy. Therefore, hydrogels were evaluated in terms of their pyridothione content by treating the gel samples with glutathione at 37 ^{o}C. By using molar extinction coefficient value of pyridothione at 343 nm, pyridothione release from hydrogels was calculated (Figure 6.10).

Figure 6.10 shows extent of pyridothione release from the hydrogels. It was observed that pyridothione release from H1 was around 93 % after 7 h, whereas the release from H3 after 6 hours was only 65 %. With increase of PEG monomer in the hydrogel, an increase in the release of pyridothione was observed. Almost 99% release of pyridothione from hydrogels was demonstrated after 24 h (Figure 6.10).

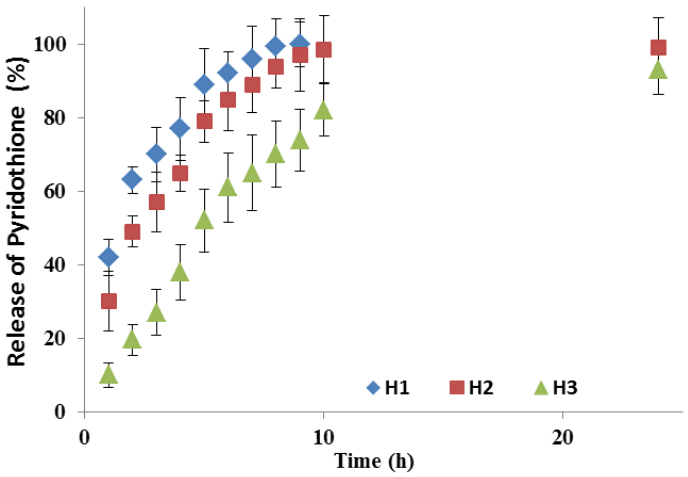

Figure 6.10. Pyridothione release from bulk hydrogels up to 24h.

6.3.4. Functionalization of Hydrogels and Release of Dye Molecules from Hydrogels

For various applications, efficient post-gelation functionalization is quite important for utilization of hydrogels. While functional group can be easily functionalizable when incorporated in soluble polymers, the slow diffusion of reactants and steric bulk can be expected to result in limited reactivity within hydrogels. Hydrogels synthesized in this study contain two different thiol-reactive groups which are maleimide and pyridyldisulfide. While the former is more reactive towards thiol-containing molecules through non-reversible conjugation, reaction of the thiol bearing molecules with the latter group is inevitable. Investigation of extent of reaction toward these groups need to be determined. Hence, functionalization of hydrogels was by attaching BODIPY-SH onto the functional groups in the gel matrix was probed (Figure 6.11).

For the functionalization, the amount of BODIPY-SH dye corresponding to maleimide functional groups in the hydrogel was used. Release of pyrido-2-thione is indicate the amount of BODIPY-SH conjugating to the disulfide unit. This information, indirectly, provides us an estimate of the comparative reactivity of BODIPY-SH toward the maleimide unit. By UV-vis analysis of released pyrido-2-thione, it was calculated that dye molecules react with 20 % of pyridyldisulfide groups in the H1 matrix (25 % for H2 and 38 % for H3 respectively) (Figure 6.12c).

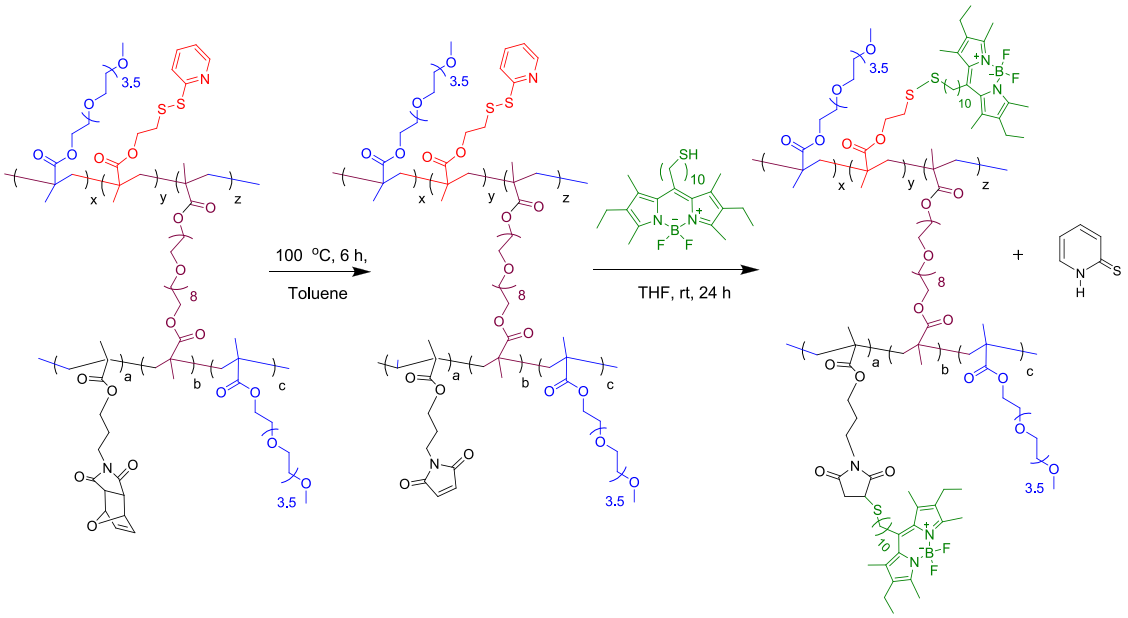

Figure 6.11. Conjugation of BODIPY-SH to hydrogel.

In other words, conjugation to maleimide units for hydrogels H1, H2 and H3 can be estimated at 80%, 75% and 62%, respectively. Hence while good selectivity of thiol-containing molecules toward maleimide group was observed for hydrogels with lower content of the PDS group, selective functionalization becomes challenging when the amount of this competing reactive group increases.

After modification with dye molecules, H1 was treated with DTT molecules to determine release behavior of it. The amount of BODIPY which is release from H1 was consistent with the amount of pyridine 2-thione (Figure 6.12d). Figure 7.12a and b show fluorescence images of H1 before and after treating with DTT. As expected, a slight decrease is observed but an overall green fluorescence is maintained.

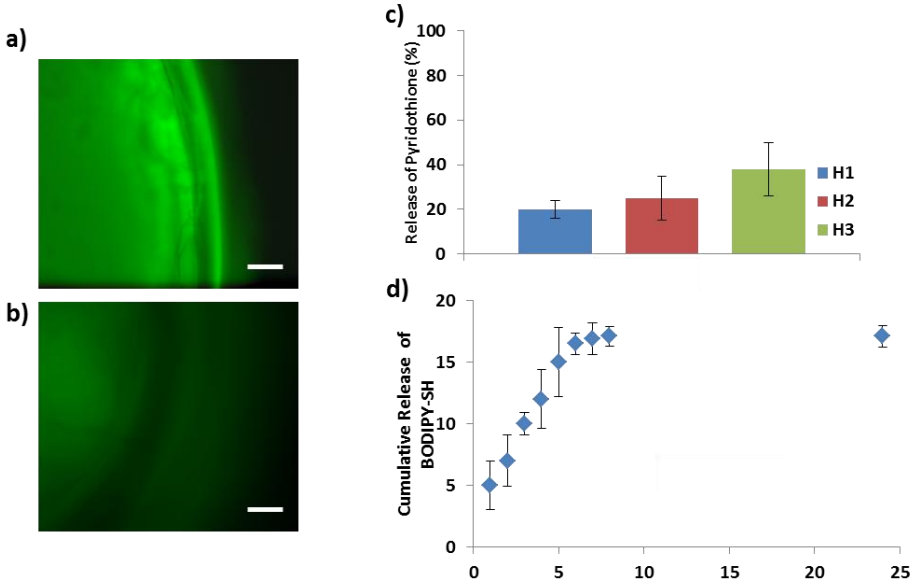

Figure 6.12. (a) Fluorescence image of dye conjugation H1 (b) fluorescence image of H1 after dye release from H1 and (Scale bar = 50 μm) (c) the release of pyridothione and (d) BODIPY-SH from hydrogels.

Since we want to adapt this study to biological application, cell cytocompatibility of the materials was tested. Prior the analysis, hydrogels were modified with GSH to remove the PDS groups to mimic an actual modified gel during usage. It was observed that after 48 h incubation, at least 90 % L929 fibroblast of cells were alive after incubation with the hydrogels (Figure 6.13).

6.4. Conclusion

In this project, the preparation of dual reactive hydrogels with good conversions is reported. Chemical composition, swelling and rheological behaviors of the obtained hydrogels were examined. Pyridothione release from gel matrix was investigated over time, and it was found that the release was dependent on the amount of PDS groups within the gel. The higher pyridothione release in the presence of the GSH was observed for H1 since H1 contains higher amount of the hydrophilic PEG monomer. Maleimide containing hydrogels were prepared using the furan protected maleimide monomer, where the thiol reactive maleimide groups were activated through the retro Diels-Alder reaction.

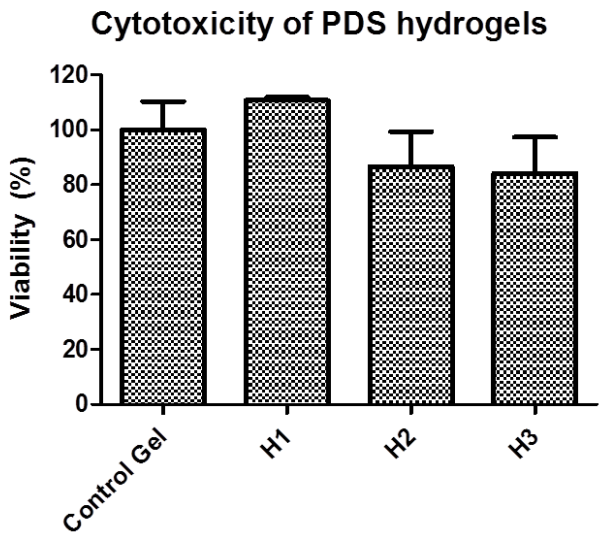

Figure 6.13. Cytotoxicty results of hydrogels on L929 fibroblast cell line.

Functionalization of these groups within hydrogels using fluorescent BODIPY-SH molecule revealed that while most of the thiol goes to maleimide for hydrogels with low PDS group content, the competition increases upon increasing amount of PDS in hydrogels. This was ascertained through monitoring release of pyrido-2-thione fragment, as well as conjugated BODIPY. The cyto-compatibility of the hydrogel with fibroblasts was found to be satisfactory. These results show that using the particular combination of these thiol-reactive groups, it is possible to create the system where there is both reversible and non-reversible conjugation. In future, potential of such system will be tested in vitro to gain further insight.

7. PREPARATION OF DISULFIDE GROUPS CONTAINING POLYMER BRUSH COATED MAGNETIC NANOPARTICLES AND THEIR APPLICATION IN RELEASE STUDIES

7.1. Introduction

In recent years, due to their unique physical and chemical properties, a lot of effort has been focused on developing novel magnetic nanoparticles for various biomedical applications such as magnetic resonance imaging (MRI), drug delivery, and hyperthermia based therapy [144-147]. Among magnetic nanoparticles, iron oxide nanoparticles (IONPs) are widely used in biological applications because they are non-toxic, environmentally safe and their particle sizes can be controlled [148-150]. IONPs can be coated with silica, oleic acid and polymers to provide them with a protective shell to prevent agglomeration and add other functional aspects [151, 152]. Polymer coated IONPs can be further modified with various molecules of interest via covalent or physical interactions with the functional groups on the coating. Covalent interactions in surface modification of IONPs are much more desired compared to non-covalent ones because of their higher stability [153].

Disulfide groups are mostly utilized for functionalization with biological molecules since they are easily modified with free thiol groups containing biomolecules forming a new disulfide bond. Since disulfide bond is easily cleavable in presence of a reducing agent, disulfide containing IONPs can be utilized as delivery agents in drug or protein delivery systems. Only a few reports are present in the literature where the disulfide chemistry has been coupled with the magnetic nanoparticle systems. Tarr and coworkers demonstrated the use of *N*-hydroxy succinimide functional silicone coated magnetic IONPs for the protein and peptide delivery system. These nanoparticles were modified with disulfide containing N-hydroxysuccinimide ester molecules to facilitate surfaces modification and modified silica@IONPs surface was further functionalized with peptide molecules via covalent interactions. Disulfide bond between nanoparticles and NHS linker was cleaved and separation of peptide from silica coated IONPs was achieved. Also, in particular, the pyridyldisulfide group is widely used for conjugation with free thiol containing molecules because it rapidly reacts with free thiol containing molecules through

thiol disulfide exchange reaction [154]. Recently, Zeng and co-workers reported another related example of pyridyldisulfide containing silica coated magnetic nanoparticles. Silica coated IONPs surface was firstly modified with pyridyl disulfide groups and these groups were then conjugated with thiol containing protein via thiol exchange reaction. Afterwards, formed disulfide bond was reduced by tris(2-carboxyethyl)phosphine (TCEP) to accomplish protein release from the NPs [155]. MNPs with reactive and biocompatible polymer coating plays an important role in applications. Especially, water soluble polyethylene glycol (PEG) is known as a biocompatible molecule and it can be utilized for biocompatible polymer coated nanoparticles. Polymerization on the nanoparticle surfaces can be achieved by reversible addition fragmentation (RAFT) polymerization method. Incorporation of disulfide containing groups to enable reversible functionalization with thiol-containing (bio)molecules would expand the utility of magnetic nanoparticles for various applications.

In this study, we report novel functionalizable polymer coated hydrophilic magnetic nanoparticles that contain thiol-reactive polymer brushes obtained using the “graft-from” approach. Structure and hydrodynamic size distributions of these nanoparticles were investigated. Afterwards, we explored functionalization of synthesized nanoparticles with a tripeptide glutathione (GSH) to understand the efficiency of functionalization. The reactive pyridyldisulfide groups were also employed for conjugation of a thiol-containing fluorescent dye through the thiol-disulfide exchange reaction under mild conditions. Disulfide bonds on the polymer coated NPs undergo cleavage upon exposure to dithiothreitol (DTT) and release of dye molecules from polymer coated NPs in a time dependent manner was investigated. Overall, a novel platform based on polymer coated magnetic nanoparticles for reversible conjugation of thiol containing (bio)molecules was established.

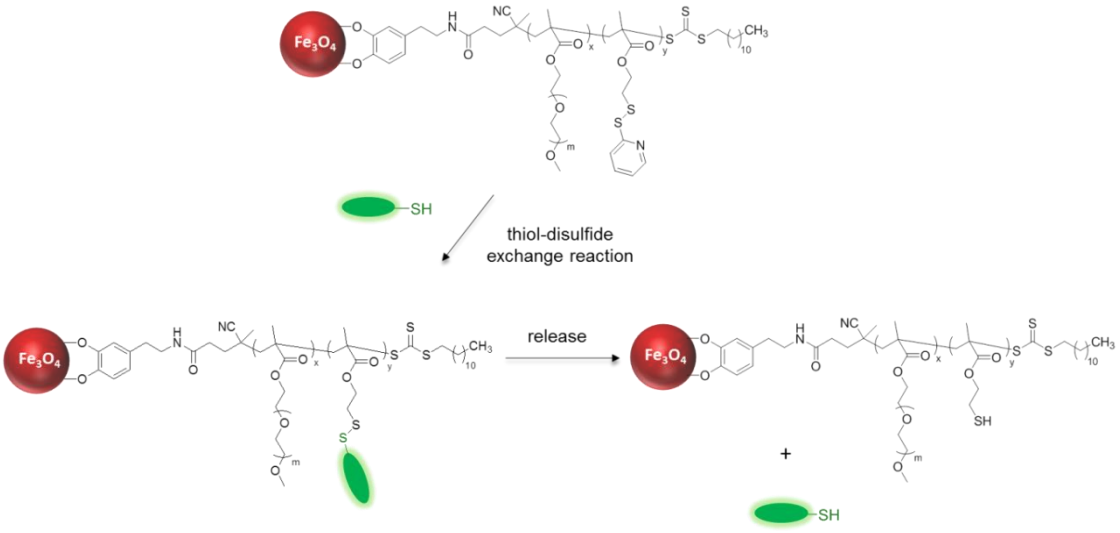

Figure 7.1. General scheme of functionalization thiol reactive polymer coated MNPs via cleavable disulfide bonds.

7.2. Experimental Section

7.2.1. Materials and Methods

Iron (III) chloride hexahydrate ($FeCl_3.6H_2O$), thionyl chloride, 1-dodecanethiol, Aliquot 336, triethylamine (TEA), oleic acid, 4-(dimethylamino)pyridine (DMAP), dopamine hydrochloride, and L-glutathione reduced were obtained from Sigma-Aldrich. 2,2'-azobis(2-methylpropionitrile) (AIBN) were purchased from Sigma and recrystallized from ethanol before use. Magnetic iron oxide NPs were obtained using thermal decomposition method according to previous reports (Figure 6.2). Pyridyldisulfide methacrylate (PDSMA) monomer [105] and BODPY-SH [143] were synthesized according to previous procedure. Poly(ethylene glycol) methyl ether methacrylate (PEGMEMA, Mn = 300 g mol^{-1},) and L-dithiothreitol (DTT) were purchased from Fluka. Organic solvents were obtained from Merck (Germany). Anhydrous dichloromethane, toluene and tetrahydrofuran were obtained from SciMatCo purification system. UV-vis analysis was collected using a Varian Cary 50 Scan UV-vis spectrophotometer. Infrared spectra of MNPs were performed employing ATR-FTIR (Thermo Fischer Scientific Nicolet 380). Dynamic light scattering analysis (DLS) of IONPs was performed on a

Malvern Zetasizer Nano ZS photometer. IONPs were visualized on LVEM5 microscope operated at 5 kV.

7.2.2. Synthesis of NHS Activated Chain Transfer Agent

CTA-NHS ester was synthesized according to reported previously reported protocol [156]. CTA (200 mg, 0.49 mmol) and NHS (72.04 mg, 0.63 mmol) were placed in a round bottom flask with a stir bar and dissolved in dry DCM (5 mL). EDCI (121 mg, 0.63 mmol) and DMAP (12.9 mg, 0.105 mmol) were added to the reaction. The mixture was stirred at room temperature under nitrogen atmosphere for overnight in the dark. After reaction is completed, excess solvent was evaporated under *vacuo*. Obtained product was extracted with saturated $NaHCO_3$ solution and DCM phase was collected. Then, aqueous phase was extracted with diethyl ether (3 x 30 mL), and then combined with DCM phase. Lastly, the organic phase was washed with distilled water (3 x 150 mL) and brine (3 x 150 mL) and dried over Na_2SO_4 and evaporated *in vacuo* to obtain pure product (160 mg, 87 %).

7.2.3. Synthesis of Dopamine Functionalized Chain Transfer Agent (Dopa-CTA)

Dopamine.HCl (75 mg, 0.395 mmol) was dissolved in MeOH, and triethylamine (TEA) (60 µl, 0.432 mmol) was added to this solution, followed by addition of CTA-NHS ester (159.5 mg, 0.32 mmol). Mixture was allowed to stir under protection from light for 24 h at room temperature. The solvent was evaporated *in vacuo*. Obtained product was dissolved in EtOAc and extracted with H_2O. Purification was done by column chromatography using ethyl acetate and hexane as eluent (3:1 v/v) to yield pure product (100 mg, 61 %).

7.2.4. Ligand Exchange Procedure

Dopa-CTA anchored Fe_3O_4 nanoparticles were obtained using a place exchange reaction. As a general procedure, oleic acid stabilized iron oxide NPs (50 mg) was placed in a vial and dispersed in $CHCl_3$ (5 mL). 5-fold excess of DOPA-CTA (250 mg) was added to this dispersion. The reaction mixture was sealed and stirred in the dark at 40 ^oC for 48 h under a nitrogen atmosphere. The solvent was removed under reduced pressure. The

nanoparticles were then redispersed in THF and precipitated in methanol. Precipitated magnetic Fe_3O_4 NPs were collected using an external magnet. Precipitation of the NPs was repeated until all unbound DOPA-CTA was removed, as confirmed by TLC analysis.

7.2.5. Surface Initiated RAFT Polymerization of PEGMEMA

Dopa-CTA anchored NPs, PEGMEMA (200 mg, 0.67 mmol) and AIBN (0.4 mg, 2.51 x 10^{-3} mmol) were added into a round bottom flask and dissolved in toluene (3 mL). The reaction mixture was purged with nitrogen for 15 min and placed in a pre-heated oil bath. Then, polymerization was allowed to proceed for 24 h at 70 ^{o}C. Polymer coated magnetic NPs were precipitated in cold diethyl ether and collected using a permanent magnet.

7.2.6. Surface Initiated Copolymerization of PDSMA and PEGMEMA via RAFT Polymerization

Representative procedure for 10% PDS-containing nanoparticles: Dopa-CTA anchored NPs (5 mg), PDSMA (17 mg, 0.067 mmol), PEGMEMA (180.9 mg, 0.603 mmol) and AIBN (0.4 mg, 2.51 x 10^{-3} mmol) were dissolved in toluene (3 mL) and purged with nitrogen for 15 min. Thereafter, the reaction mixture was placed in a preheated oil bath at 70 ^{o}C for 24 h. After surface initiated copolymerization of PDSMA and PEGMEMA on NPs (Fe_3O_4@PEGMEMA-PDS), the solvent was concentrated under reduced pressure and the mixture was precipitated in cold diethyl ether several times to remove excess unreacted monomers.

7.2.7. Pyridine 2-thione Release from PDSMA Containing Polymer Coated NPs

PDSMA containing polymer coated NPs (2 mg) and GSH solution (10 mM, 3 mL) were mixed in a glass vial and placed in a thermal shaker at 37 ^{o}C. At regular time intervals, absorption spectrum of the solution was collected by UV-vis spectrophotometer. The release of pyridothione was calculated by using molar extinction coefficient of pyridothione (8.08 x 10^3 $M^{-1}cm^{-1}$ at 343 nm) [147].

7.2.8. Conjugation of BODIPY-SH to PDSMA Containing Polymer Coated NPs via Thiol-Disulfide Exchange Reaction

10 % PDSMA coated magnetic Fe_3O_4 nanoparticles (10 mg) were mixed in 2 mL of THF and BODIPY-SH (0.5 mg) was added into this solution. After adding of 400 μL of CH_3COOH, the mixture was stirred at room temperature for 24 h. Unreacted dye was removed by precipitation of the dye conjugated nanoparticles in diethylether.

7.2.9. Release of BODIPY-SH from Polymer Coated Magnetic Iron Oxide Nanoparticles with Dithiothreitol (DTT)

The release of BODIPY-SH from polymer coated NPs was studied in the presence of reducing agent, DTT. For this study, dye attached polymer coated magnetic NPs (2 mg) were dispersed in 0.1 mL of H_2O and transferred into dialysis bag with MW cut-off 1 kDa. DTT (10 mM) in 1x PBS (pH: 7.4) (2 mL) was added into dialysis bag and released dye from the NPs was purified by dialysis against THF (because dye does not solve in PBS or water). Samples were taken from THF at certain time intervals to determine released dye and analyzed via a UV-vis spectrophotometer.

7.3. Results and Discussion

7.3.1. Modification of Chain Transfer Agent and Immobilization onto Fe_3O_4 Nanoparticles via a Place Exchange Reaction

Trithiocarbonate based chain transfer agent for RAFT polymerization was chosen because it is known to be suitable for methacrylate monomers [157]. CTA activation for esterification was carried out using NHS in the presence of EDCl as a coupling agent at room temperature (Figure 7.2). Then, NHS activated CTA was treated with dopamine for 24 h in the presence of TEA in chloroform. Dopamine contains catechol group, which is known to be an excellent anchoring group for metal oxides and metal surfaces [158]. Therefore, dopamine terminated chain transfer agent (DOPA-CTA) was synthesized for obtaining stable linkage of polymer chains onto the nanoparticle surface.

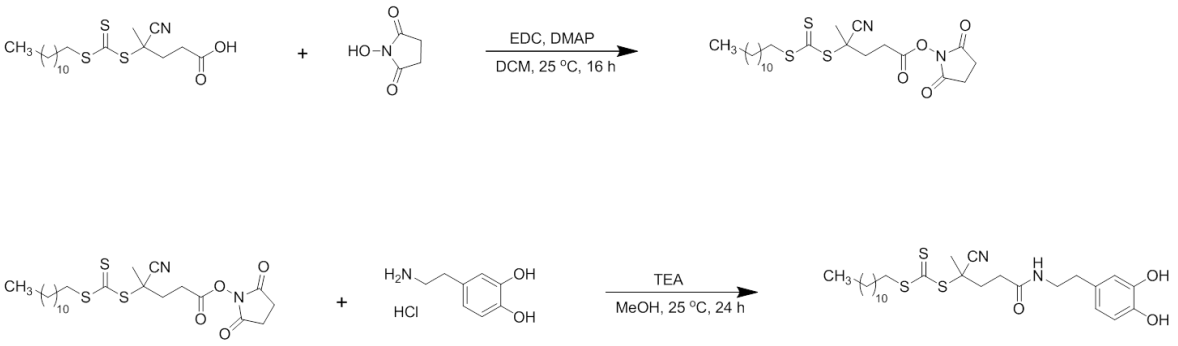

Figure 7.2. Preparation of dopamine terminated chain transfer agent.

Afterwards, immobilization of the DOPA-CTA on MNPs was achieved using a place exchange reaction in $CHCl_3$ at 40 ^oC for 48 h (Figure 7.3a). Non-tethered Dopa-CTA was removed by precipitating the magnetic nanoparticles in MeOH and centrifugation. Obtained CTA coated nanoparticles were kept in THF until further use to prevent aggregation of the nanoparticles. The successful coating step was monitored by FT-IR spectroscopy. Dopa-CTA coated nanoparticles showed a peak at 1649 cm^{-1} resulting from stretching vibration of amide carbonyl bond (Figure 7.3b).

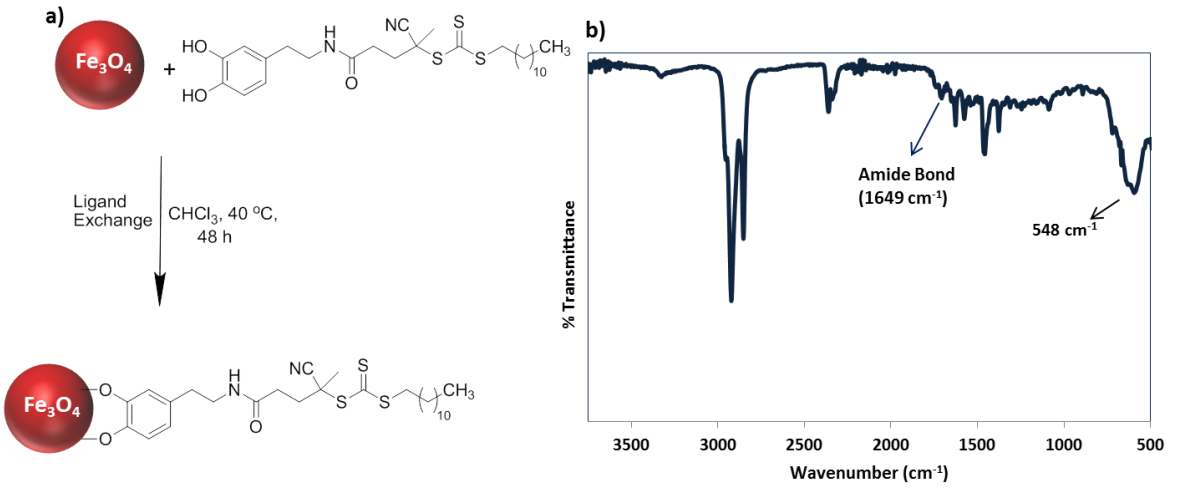

Figure 7.3. a) Immobilization of DOPA-CTA onto magnetic iron oxide nanoparticles b) FTIR spectra of Dopa-CTA coated iron oxide nanoparticles.

7.3.2. RAFT polymerization of PEGMEMA and PDS with Grafting-From Method

After DOPA-CTA immobilization onto magnetic NPs, thiol reactive pyridyldisulfide containing copolymers were grown from the surface using different amounts of hydrophilic PEG based poly(ethylene glycol) methyl ether methacrylate and the thiol reactive PDSMA monomer in toluene at 70 ^{o}C under nitrogen atmosphere for 24 h, yielding Fe_3O_4@PEGMEMA-PDSMA. Synthesis of this polymer coated NPs were synthesized using Fe_3O_4@CTA nanoparticles via surface initiated RAFT polymerization (Figure 7.4). The composition of nanoparticles coated with copolymers containing varying amount of the PDS group are given in Table 7.1.

Table 7.1. Nanoparticles obtained using RAFT polymerization from the NPs surface

Item	**Polymer**	**PDSMA : PEGMEMA(%)**
1	Fe_3O_4@PEGMEMA	0 : 100
2	Fe_3O_4@PEGMEMA-PDSMA1	10 : 90
3	Fe_3O_4@PEGMEMA-PDSMA2	20 : 80
4	Fe_3O_4@PEGMEMA-PDSMA3	40 : 60

FT-IR measurements were performed to analyze these nanoparticles. A band at 1730 cm^{-1} belongs to the carbonyl group of ester group in the PEGMA fragment. Compared to the FT-IR spectrum of PEGMEMA coated NPs, an additional peak at 1570 cm^{-1} belonging to pyridyl ring of PDS was observed for Fe_3O_4@PEGMEMA-PDS NPs (Figure 7.5). The intensity of the band increased with increasing content of the PDS functional group containing monomer.

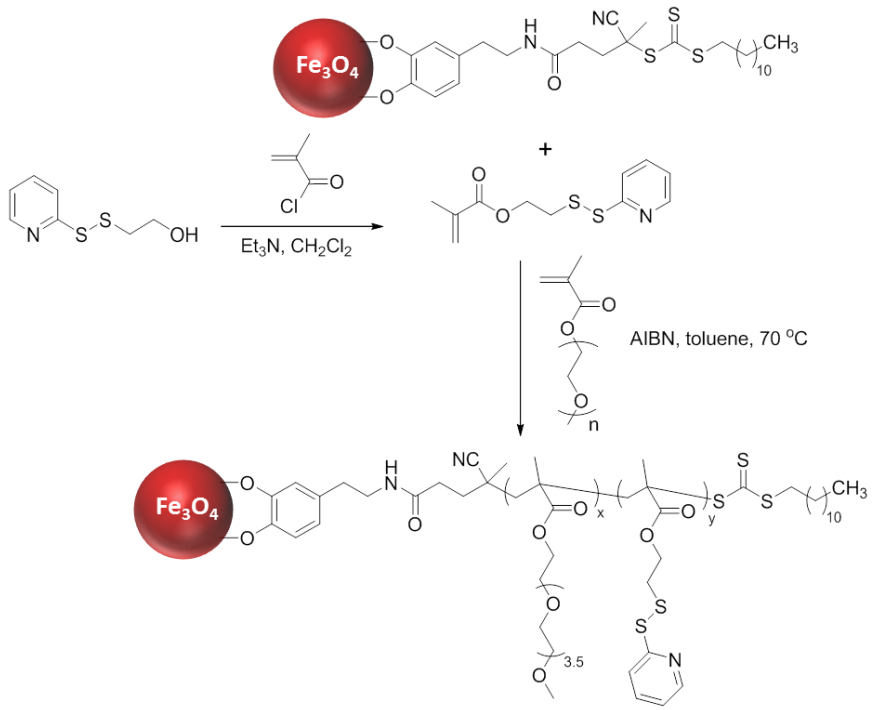

Figure 7.4. Synthesis of PDS-containing copolymer coated iron oxide nanoparticles.

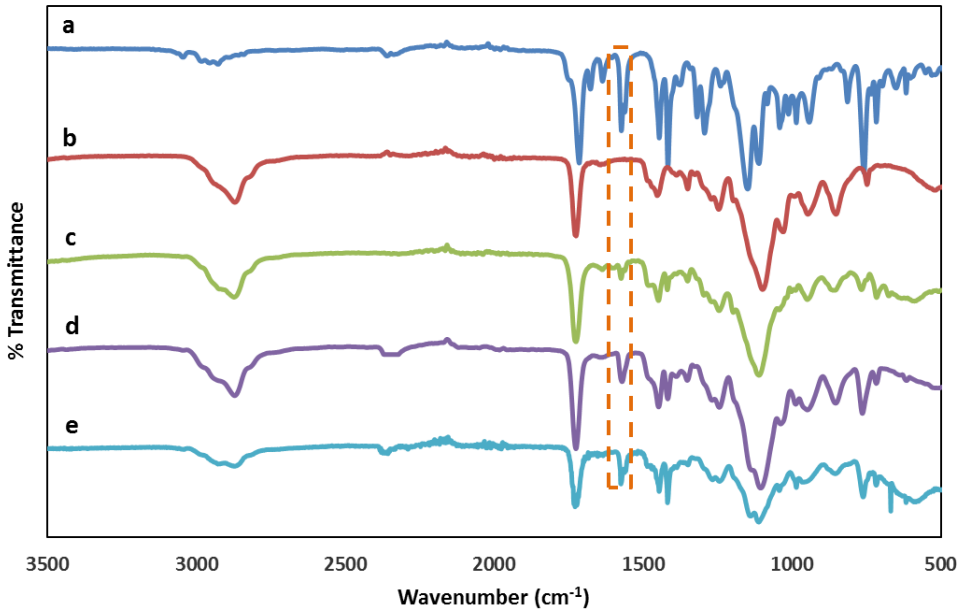

Figure 7.5. FT-IR spectra of polymer coated nanoparticles containing (a) PDSMA mon, (b) Fe_3O_4@PEGMEMA, (c) Fe_3O_4@PEGMEMA-PDSMA1, (d) Fe_3O_4@PEGMEMA-PDSMA2 and (e) Fe_3O_4@PEGMEMA-PDSMA3.

7.3.3. Dynamic Light Scattering Measurements of Polymer Coated NPs

To investigate hydrodynamic sizes of all MNPs, DLS were performed. Oleic acid coated MNPs and polymer coated Fe_3O_4 NPs were dispersed in chloroform. The size distribution of the magnetic NPs was shown in Figure 7.6a. The size of Fe_3O_4@OA found 6.0 nm whereas diameter of Fe_3O_4@CTA was 6.8 nm (Figure 7.6a and b). These results were expected since oleic acid and Dopa-CTA have almost same chain lengths. Hydrodynamic size of the polymer coated NPs was about 9 nm, indicating successful polymer growth from the surface (Figure 7.6c).

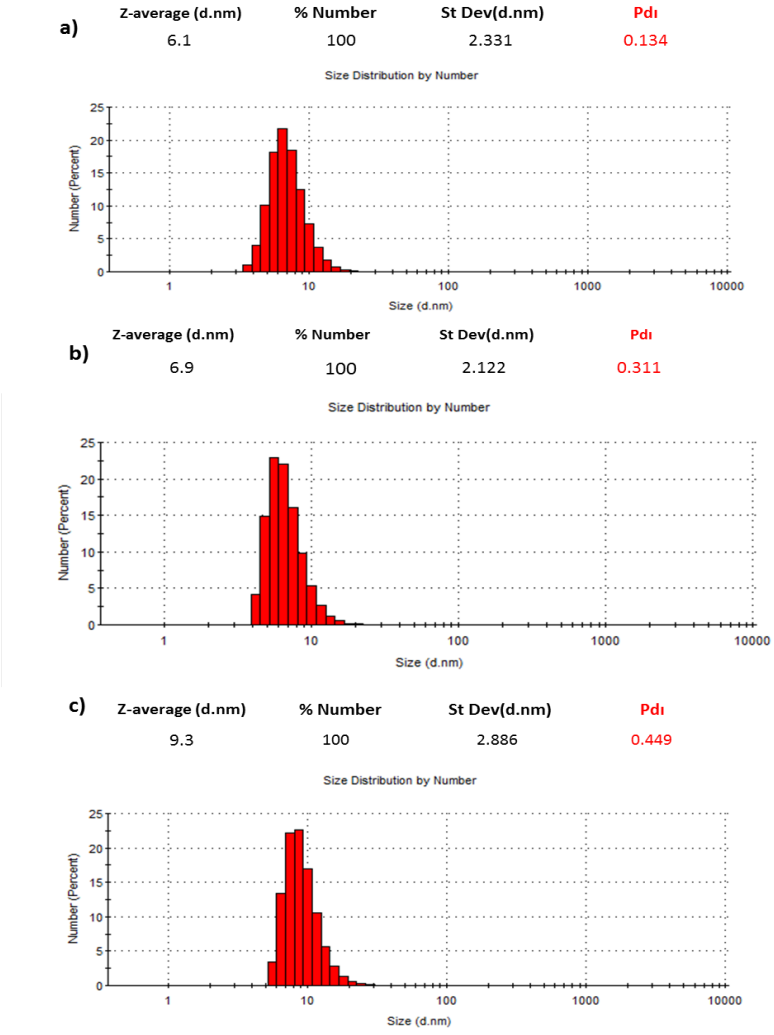

Figure 7.6. DLS size and histograms of (a) only oleic acid coated (b) CTA coated MNPs and (c) 10 % PDSMA monomer containing polymer coated MNPs (DLS size and histograms of (a) 20 % and (b) 40 % PDSMA containing polymer coated MNPs refers to Figure A.8).

7.3.4. Transmission Electron Microscopy (TEM) Images of Magnetic Iron Oxide NPs

Polymer coated NPs were investigated utilizing TEM. According to TEM images during polymerization process nanoparticles were not aggregated (Figure 7.7). This uniform structure of NPs is significant for utilization of the magnetic NPs in applications.

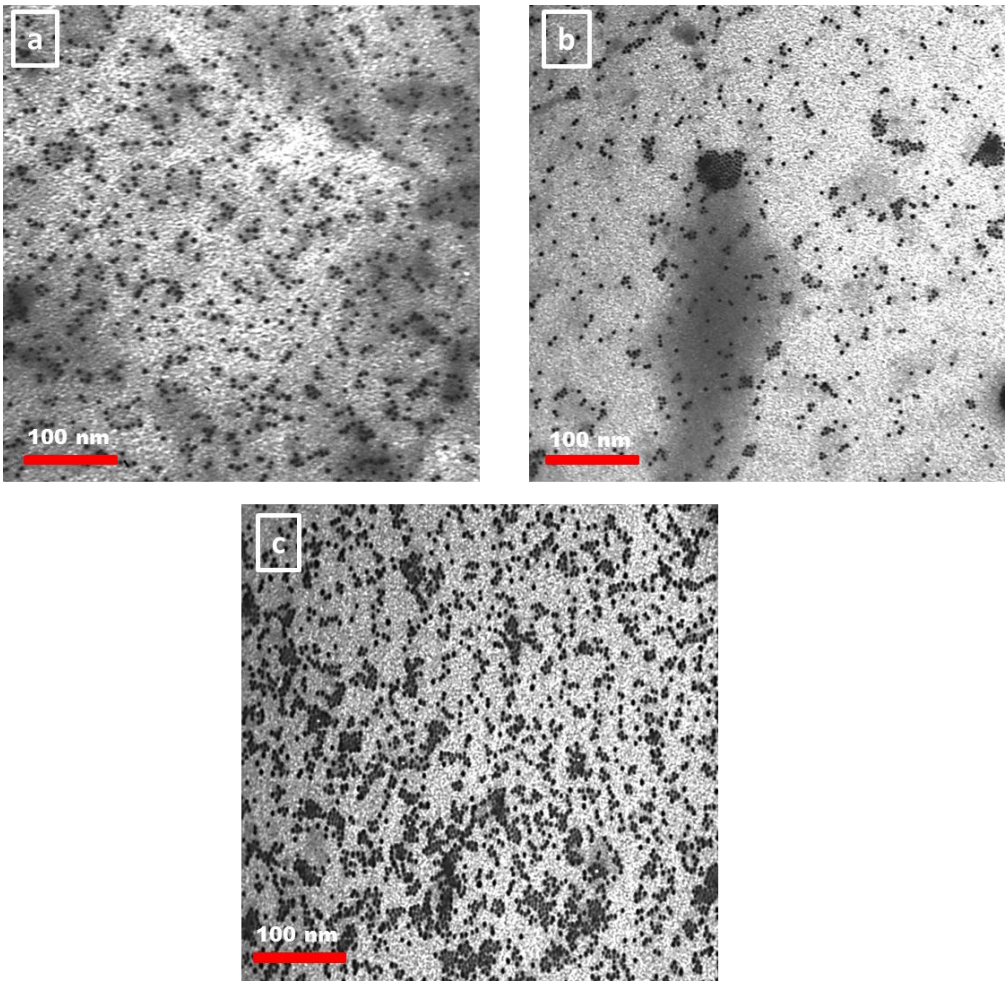

Figure 7.7. TEM images of (a) Fe_3O_4@PEGMEMA-PDSMA-1, (b) Fe_3O_4@PEGMEMA-PDSMA-2 and c) Fe_3O_4@PEGMEMA-PDSMA-3.

7.3.5. Conjugation of Pyridyldisulfide Containing Polymer Coated Magnetic Iron Oxide NPs with Glutathione (GSH)

To investigate the functionalization of PDSMA containing polymer coated MNPs, they were reacted with glutathione (Figure 7.8). The efficiency of functionalization is easy to determine since the released pyridine-2-thione fragment has a characteristic absorbance at 343 nm. Thus, the release of pyridine 2-thione from MNPs for the nanoparticles with different amounts of PDS group were analyzed by UV-vis spectroscopy. As expected, nanoparticles containing higher amounts of PDS monomer exhibited increased amount of PDS release (Figure 7.8).

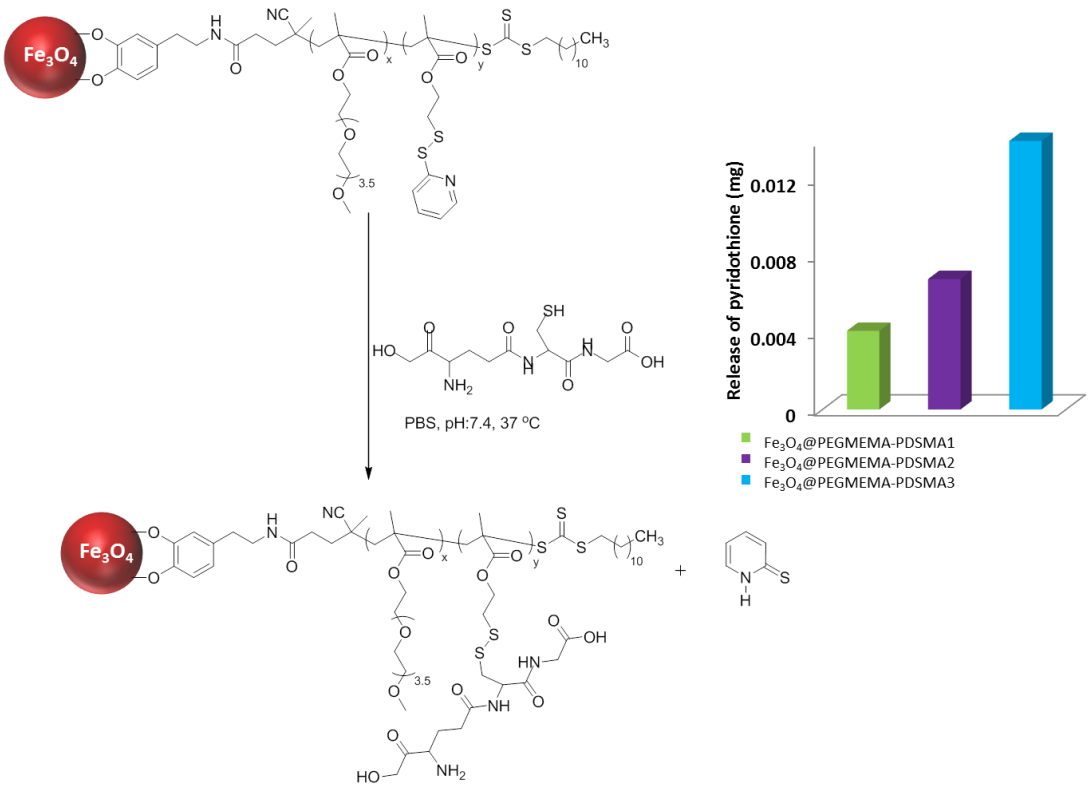

Figure 7.8. Conjugation reaction of PDS containing polymer coated NPs with GSH and associated pyridothione release profile from Fe_3O_4@PDSMA1, Fe_3O_4@PDSMA2 and Fe_3O_4@PDSMA3.

7.3.6. Functionalization of Copolymer Coated Magnetic Nanoparticles

Functionalization of thiol reactive polymer brush coated NPs (Fe_3O_4@PEGMEMA-PDSMA1) with BODIPY-SH was accomplished using pyridyldisulfide-thiol exchange reaction. For this purpose, BODIPY-SH was conjugated onto copolymer coated MNPs under mild conditions, leaving pyridine 2-thione groups on MNPs surface (Figure 7.9). Samples at different times were taken from the functionalization reaction and monitored by UV-vis spectrophotometer. Leaving pyridothione was analyzed by UV-vis spectrometer to identify the reaction time.

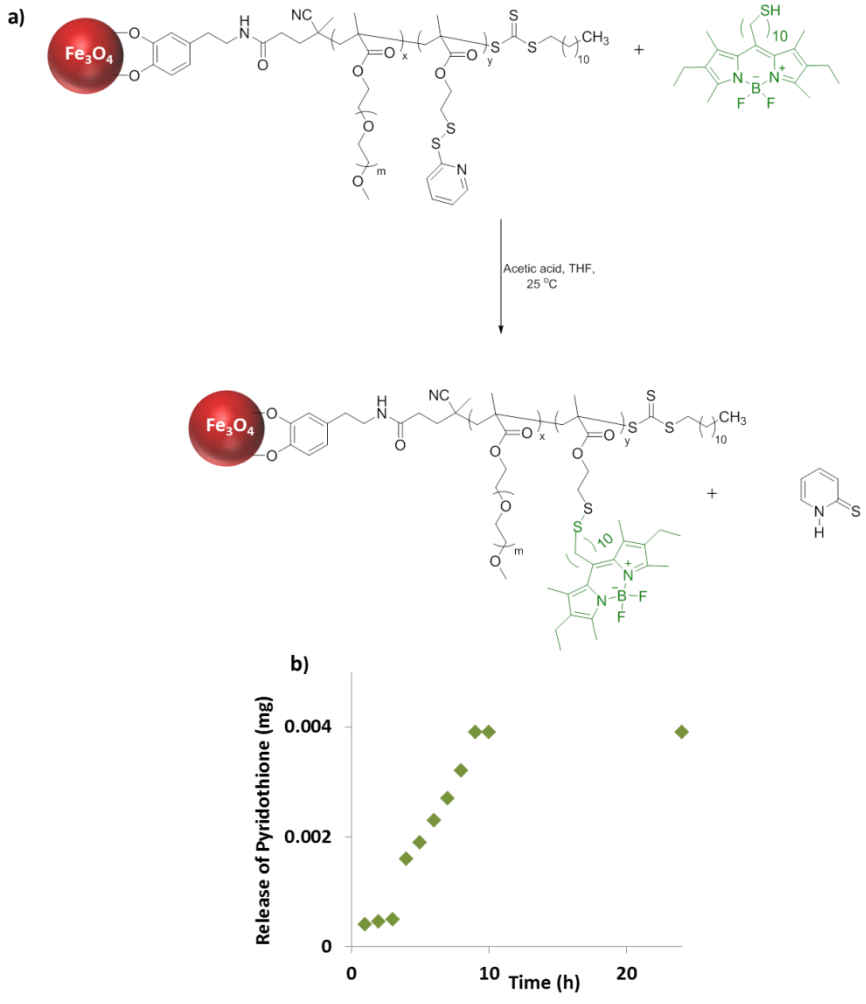

Figure 7.9. (a) Functionalization of polymer coated Fe_3O_4@PEGMEMA-PDSMA1 NPs with BOPIY-SH dye molecules. (b) Release of pyridothione from the NPs in THF after the dye attachment.

After the reaction, excess dye was removed by precipitating NPs in ether, since dye did not dissolve in water (Figure 7.10b-III) and NPs were collected by centrifugation. As a control experiment, polymer coated NPs without PDSMA monomers were reacted with BODIPY-SH under the same conditions. As expected, thiol containing dye did not react with PEGMEMA coated magnetic and so there was no fluorescence observed for thus treated nanoparticles in control experiment (Figure 7.10-I), while the dye functionalized NPs gave a strong fluorescence under UV illumination (Figure 7.10b-II). Dye conjugation to PDSMA coating MNPs by disulfide exchange reaction was also confirmed by UV-vis spectroscopy, and dye conjugated MNPs demonstrated an absorption spectra band at 525 nm resulting from the attachment of BODIPY onto the nanoparticles.

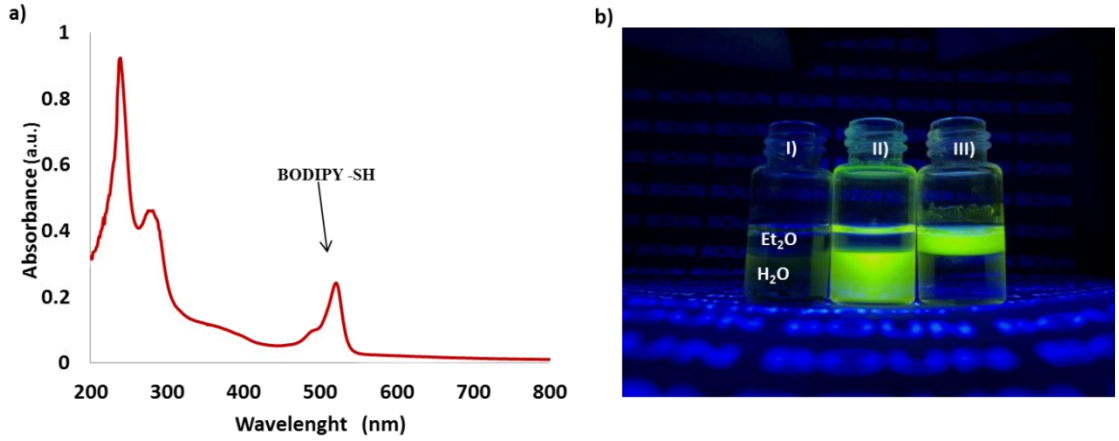

Figure 7.10. (a) UV-vis spectra of dye conjugated Fe_3O_4@PEGMEMA-PDS1 in THF, and (b) photographs of (I) control, (II) dye conjugated MNPs and (III) free dye under UV illumination.

7.3.7. BODIPY Release from Polymer Coated Nanoparticles

Since polymer coated nanoparticles were functionalized via thiol-disulfide exchange reaction, attached molecules can be released in the presence of a reducing agent such as DTT (Figure 7.11a). Dye release from the nanoparticle upon treatment with DTT was monitored using UV-vis spectroscopy (7.11b). The dye conjugated nanoparticle was dissolved in THF and confined inside a dialysis bag (MW cutoff 3.5 kDa). In the presence of DTT, the cleaved dye diffuses out of the dialysis bag into the outside solvent, while the

nanoparticles remain inside the dialysis bag. Over time, an increase in the amount of released dye is observed, as deduced from increase in absorbance observed in the UV-vis of the solution.

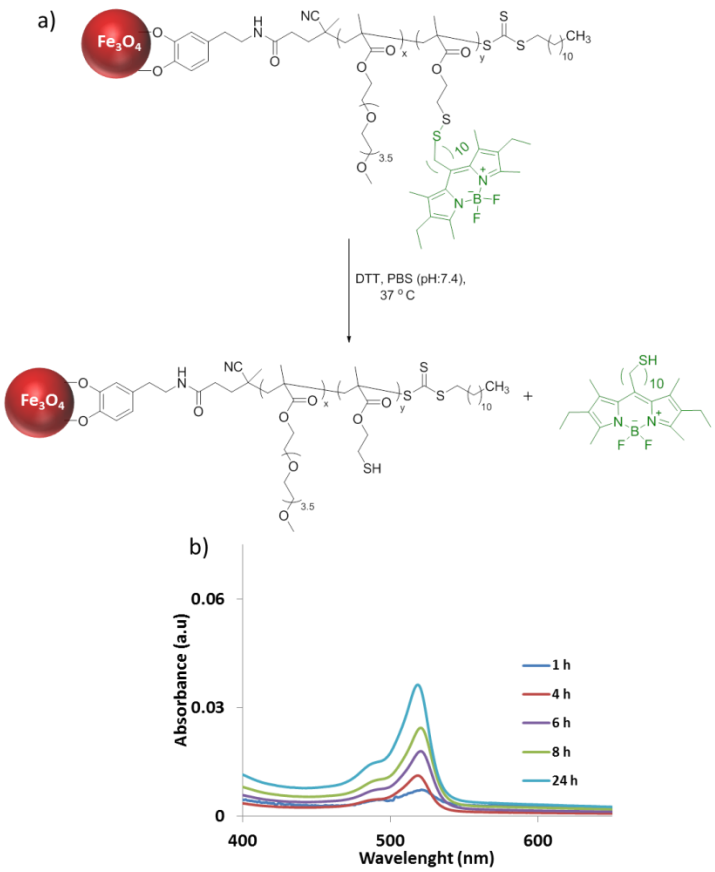

Figure 7.11. a) Relese of dye molecules from nanoparticles in the presence of DTT. b) UV-Vis spectra of BODIPY release from polymer coated MNPs in the presence of DTT.

7.4. Conclusion

Novel thiol-reactive polymer brush coated MNPs were synthesized by 'grafted from' method. To ensure robust attachment of the polymer chains on the nanoparticle surface, catechol based chelation chemistry was utilized. RAFT chain transfer agent containing the catechol group was synthesized and conjugated to oleic acid coated MNPs via place exchange reaction. Hydrophilic PEGMEMA and thiol-reactive PDSMA were used to grow polymers onto NPs surface. Change in solubility, as well as hydrodynamic size suggested successful formation of polymer chains on the NP surface.

Functionalization of the NPs was studied by using thiol containing molecules such as the tripeptide glutathione and fluorescent dye BODIPY. Successful cleavage of the conjugated dye from the NP in the presence of a thiol based reducing agent DTT was confirmed by UV-vis spectroscopy. Facile conjugation and cleavage of conjugated molecules from these biocompatible polymer coated hydrophilic MNPs makes them attractive candidates for various biomedical applications such as drug delivery.

8. CONCLUSION

In this dissertation, the design and fabrication of novel reactive interfaces such as hydrogels and polymer coated nanoparticles were investigated for applications related to the delivery of therapeutic agents. Randomly crosslinked hydrogels incorporating amine and thiol reactive groups that allow conjugation of various bioactive molecules in a releasable fashion were synthesized. Apart from using novel modes of conjugation and release from non-degradable hydrogel scaffolds, synthesis of a new class of degradable hydrogels with well-defined network structure was also established. Effective thiol-disulfide exchange reaction based strategies were employed to fabricate hydrogels where the crosslinked density could be varied and protein release profiles could be modulated. Importantly, very fast and complete degradation of these hydrogels to release the encapsulated protein was achieved. The power of thiol-disulfide exchange reaction was exploited to fabricate polymer coated magnetic iron oxide nanoparticles which could undergo facile functionalization with thiol-containing molecules and release them upon when exposed to reducing environments found in tumor tissues and cancerous cells.

In the first chapter of thesis, general information and recent examples related to functionalizable hydrogels were provided. The aim of this focused chapter was to provide the readers with an idea of current state of the art in these areas. Only a few closely related examples were chosen which addresses problems similar to ones investigated in this thesis, and thus in process highlight the shortcomings and challenges that needs to be addressed. In the second chapter, the specific goals of the research described in this thesis were summarized.

The third chapter describes the fabrication and evaluation of the novel reactive bulk hydrogels and cryogels containing activated carbonate functional groups as reactive sites for attachment of drug to enable their slow release through the carbamate linker. Fabrication of bulk hydrogels with varying amounts of amine-reactive *N*-hydroxysuccinimide-containing monomer and hydrophilic PEG-based methacrylate monomers were carried out and evaluated for their physical characteristics, drug conjugation and release efficiencies. As observed for most photo-polymerized PEG-methacrylate based hydrogels, low porosity of these materials was evident. Hence, to

obtain materials with slow yet higher overall release characteristics, cryogels were fabricated and functionalization of these hydrogels and cryogels with the anti-cancer drug molecules was carried out to demonstrate drug conjugation and their release.

The fourth and fifth chapters of the thesis describe a novel approach to fabricate degradable hydrogels with well-defined network structure using a thiol-pyridyl disulfide exchange reaction. Although this particular reaction has been extensively used in polymer functionalization, to date, it has not been evaluated to obtain well-defined network structures. Hydrogels were synthesized with high efficiencies and were completely degradable upon exposure to thiol-containing molecules such as GSH. Synthesized hydrogels are capable of encapsulating proteins or drug and their release under biologically relevant conditions. Also, the polymeric network structure within the hydrogel plays a very important role in efficient encapsulation and controlled release of proteins, hence the release behavior of encapsulated proteins from these hydrogels was investigated. From the lessons learned in the second chapter, the hydrogel design was modified to enable stimuli-responsive release of hydrophobic drug molecules in an efficient manner. The general problem of the poor solubility of the hydrophobic drugs was also addressed in our approach, which involved incorporation of CDs into hydrogels. As a platform that incorporates all these design aspects, synthesis of CD containing well-defined hydrogels through thiol-disulfide exchange reaction was investigated. Since CDs make inclusion complexes with poorly water soluble drugs such as curcumin (CUR) and improves their aqueous solubility, these degradable hydrogels acted as an effective drug delivery platform. *In vitro* studies demonstrated the advantages of using a thiol-responsive delivery system, since much higher internalization of drugs was observed from these hydrogels was observed in GSH concentrations similar to ones found in tumor tissues.

Lastly, in the sixth chapter of this thesis, fabrication of the dual functional hydrophilic polyethylene based hydrogels synthesized using photo-polymerization was demonstrated. The main aim of the work was to obtain hydrogels containing a reversible as well as a non-reversible linkage. Thus functional moieties used to attract cells and bacteria could be attached through non-reversible linkage, reversible linkages could be used to conjugate the cytotoxic or anti-bacterial agent. Maleimide groups were chosen for non-reversible attachment via the Michael addition reaction, and pyridyldisulfide group was

chosen for the conjugation of the compounds meant to be released. To demonstrate such functionalization, a fluorescent dye, namely BODIPY was utilized. After unmasking of the maleimide units, they were modified with thiol bearing dye molecules. It was observed that conjugation to the maleimide groups was higher than toward pyridyldisulfide group. However a little amount of the pyridyldisulfide groups also reacted with the dye via thiol-disulfide exchange reaction. Thus an effective hydrogel platform capable of undergoing dual functionalization with differential stability of conjugation was achieved.

The last chapter presented a method to synthesize novel functionalizable polymer coated hydrophilic magnetic nanoparticles that contain thiol-reactive polymeric coatings. A 'graft-from' approach was utilized to design pyridyl disulfide containing polymer coated magnetic nanoparticles, which could be functionalized with thiol-containing molecules. Since the appended molecules are conjugated to the polymeric coating through disulfide bonds, the conjugated molecules could be released in the presence of reducing agents such as glutathione.

In summary, this thesis discloses efficient utilization of organic transformations to design novel polymeric platforms. Various materials developed in this thesis demonstrate that the vast range of chemical bond stabilities can be used as a powerful handle to modulate their properties. Either the release of conjugated/encapsulated molecules or overall degradation of these hydrogels can be modulated. Furthermore, systems that combine aspects of degradation and release, as demonstrated for CD containing hydrogels can be developed. Importantly, the ease of preparation, effective modification and versatility of these materials are likely to make them attractive platforms for applications in various arenas of biomedical sciences.

REFERENCES

1. Peppas, N. A. A., J. Z. Hilt, A. Khademhosseini and R. Langer, "Hydrogels in Biology and Medicine: From Molecular Principles to Bionanotechnology", *Biomacromolecules,* Vol. 5, pp. 1345–1360, 2002.

2. Peppas, N.A., P. Buresa, W. Leobandunga and H. Ichikawa, "Hydrogels in Pharmaceutical Formulations", *European Journal of Pharmaceutics and Biopharmaceutics*, Vol. 50, No. 1, pp. 27–46, 2000.

3. Luo, Y., and M. S. Shoichet, "Light-Activated Immobilization of Biomolecules to Agarose Hydrogels for Controlled Cellular Response", *Biomacromolecules* Vol. 5, No. pp. 2315–2323, 2004.

4. Hennink W. E. and C. F. van Nostrum, "Novel Crosslinking Methods to Design Hydrogels", *Advanced Drug Delivery Reviews*, Vol. 64, pp. 223-236, 2012.

5. Kopecek, J., "Smart and Genetically Engineered Biomaterials and Drug Delivery Systems", *European Journal of Pharmaceutical Sciences*, Vol. 20, No. 1, pp. 1-16, 2003.

6. Yigit, S., R. Sanyal and A. Sanyal, "Fabrication and Functionalization of Hydrogels Through 'Click' Chemistry", *Chemistry an Asian Journal*, Vol. 6, No. 10, pp. 2648-2659, 2011.

7. Kaga, S., Gevrek, T. N., Sanyal, A., and Sanyal, R. "Synthesis and functionalization of dendron-polymer conjugate based hydrogels via sequential thiol-ene "click" reactions", *Journalof Polymer Science Part A Polymer Chemistry*, Vol. 54, pp. 926-934, 2016.

8. Crescenzi, V., L. Cornelio, C. Di Meo, S. Nardecchia and R. Lamanna, "Novel Hydrogels via Click Chemistry: Synthesis and Potential Biomedical Applications", *Biomacromolecules*, Vol. 8, No. 6, pp. 1844-50, 2007.

9. Choh, S. Y., D. Cross and C. Wang, "Facile synthesis and characterization of disulfide-cross-linked hyaluronic acid hydrogels for protein delivery and cell encapsulation", *Biomacromolecules*, Vol. 12, No. 4, pp. 1126–1136, 2011.

10. Tan, H., J. P. Rubin and K. G. Marra, "Direct Synthesis of Biodegradable Polysaccharide Derivative Hydrogels Through Aqueous Diels-Alder Chemistry", *Macromolecular Rapid Communications*, Vol. 32, No. 12, pp. 905–11, 2011.

11. Wei, H. L., Z. Yang, L. M. Zheng and Y. M. Shen, "Thermosensitive Hydrogels Synthesized by Fast Diels–Alder Reaction in Water", *Polymer*, Vol. 50, No. 13, pp. 2836–2840, 2009.

12. Zhu, W., L. Gao, Q. Luo, C. Gao, G. Zha, Z. Shen and X. Li, "Metal and Light Free 'Click' Hydrogels for Prevention of Post-operative Peritoneal Adhesions", *Polymer Chemistry*, Vol. 5, No. 6, pp. 2018-2024, 2014.

13. Zhang, J. T., S. W. Huang, J. Liu, and R.-X. Zhuo, "Temperature Sensitive poly[N-isopropylacrylamide-co-(acryloyl beta-cyclodextrin)] for Improved Drug Release", *Macromolecular Bioscience*, Vol. 5, No. 3, pp. 192–196, 2005.

14. Nguyen, K. T., and J. L. West, "Photopolymerizable hydrogels for tissue engineering applications", *Biomaterials*, Vol. 23, No. 22, pp. 4307-4314, 2002.

15. Park, E. J., T. N. Gevrek, R. Sanyal, and A. Sanyal, "Indispensable Platforms for Bioimmobilization: Maleimide-based Thiol Reactive Hydrogels", *Bioconjugate Chemistry*, Vol. 25, No. 11, pp. 2004-2011, 2014.

16. Yagci, Y., S. Jockusch, and N. J. Turro, "Photoinitiated Polymerization: Advances, Challenges, and Opportunities", *Macromolecules* Vol. 43, No. 15, pp. 6245-6260, 2010.

17. Egorov, T. A., A. Svenson, L. Rydén, and J. Carlsson, "A rapid and specific method for isolation of thiol-containing peptides from large proteins by thiol-disulfide exchange on a solid support", *Proc. Natl. Acad. Sci. U. S. A.* Vol. 72, pp. 3029-3033, 1975.

18. Singh, R., and G. M. Whitesides, "Thiol-disulfide interchange", In Supplement S: The Chemistry of Sulphur-Containing Functional Groups (eds. Patai S. and Rappoport Z.), John Wiley pp. 633–658, 1993.

19. Ryu, J.-H., R.T. Chacko, S. Jiwpanich, S. Bickerton, R.P. Babu, and S. Thayumanavan, "Self-Cross-Linked Polymer Nanogels: A Versatile Nanoscopic Drug Delivery Platform Supporting Info.", *Journal of the American Chemical Society*, Vol. 3, pp. 2-10, 2010.

20. Vanderhooft, J. L., B. K. Mann, and G. D. Prestwich, "Synthesis and Characterization of Novel Thiol-reactive Poly(ethylene glycol) Cross-linkers for Extracellular-matrix-mimetic Biomaterials", *Biomacromolecules*, Vol. 8, No. 9, pp. 2883--2889, 2007.

21. Chien, H. W., X. Xu, J. R. Ella-Menye, Tsai, W. B., and S. Jiang, "High viability of cells encapsulated in degradable poly(carboxybetaine) hydrogels", *Langmuir* Vol. 28, No. 51, pp. 17778-17784, 2012.

22. Savina, I. N., G. C. Ingavle, A. B. Cundy, and S. V. Mikhalovsky, "A simple method for the production of large volume 3D macroporous hydrogels for advanced biotechnological, medical and environmental applications", *Scientific Reports*, Vol. 6, pp. 1-9, 2016.

23. Plieva, F. M., I. Y. Galaev, and B. Mattiasson, "Macroporous gels prepared at subzero temperatures as novel materials for chromatography of particulate-containing fluids and cell culture applications", *Journal of Seperation Science,* Vol. 30, No. 11, pp. 1657-1671, 2007.

24. Ozmen, M. M., M. V. Dinu, and O. Okay, "Preparation of macroporous poly(acrylamide) hydrogels in DMSO/water mixture at subzero temperatures", *Polymer Bulletin,* Vol. 60, No. 2-3, pp. 169-180, 2008.

25. Lozinsky, V. I., I. Y. Galaev, F. M. Plieva, I. N. Savina, H. Jungvid, and B. Mattiasson, "Polymeric cryogels as promising materials of biotechnological interest", *Trends in Biotechnoogy,* Vol. 21, No. 10, pp. 445-451, 2003.

26. Akande, W., L. Makhalovska, S. James, S. Mikhalovsky, "Affinity Binding Macroporous Monolithic Cryogel as a Matrix for Extracorporeal Apheresis Medical Devices", *International Journal of Biomedical Materials Research,* Vol. 3, No. 5, pp. 56-63, 2015.

27. Erturk, G., B. Mattiasson, "Cryogels versatile tools in bioseparation", *Journal of Choromatography A.*, Vol. 1347, pp. 24-35, 2014.

28. Okay, O., V. I. Lozinsky, "Synthesis and structure Property Relationships of Cryogels", *Polymeric Cryogels,* pp. 103-157, 2014.

29. Kahveci, M. U., Z. Beyazkilic, and Y. Yagci, "Polyacrylamide cryogels by photoinitiated free radical polymerization", *Journal of Polymer Science Part A, Polymer Chemistry*, Vol. 48, No. 22, pp. 4989-4994, 2010.

30. Dispinar, T., W. Van Camp, L. J. De Cock, B. G. De Geest, and F. E. Du Prez, E. "Redox-Responsive Degradable PEG Cryogels as Potential Cell Scaffolds in Tissue Engineering", *Macromolecular Bioscience,* Vol. 2, No. 3, pp. 383-394, 2012.

31. Kim, Y., S. O. Ho, N. R. Gassman, Y. Korlann, E. V Landorf, F. R. Collart, and S. Weiss, “Efficient Site-specific Labeling of Proteins via Cysteines”, *Bioconjugate Chemistry*, Vol. 19, No. 3, pp. 786–791, 2008.

32. Salmaso, S., A. Semenzato, S. Bersani, F. Mastrotto, A. Scomparin, and P. Caliceti, “Site-selective protein glycation and PEGylation”, *Eur. Polym. J.* Vol. 44, pp. 1378-1389, 2008.

33. Wong, L., C. Boyer, Z. Jia, H. M. Zareie, T. P. Davis, and V. Bulmus, “Synthesis of versatile thiol-reactive polymer scaffolds via RAFT polymerization”, *Biomacromolecules,* Vol. 9, No. 7, pp. 1934-1944, 2008.

34. Meng, F., W. E. Hennink, and Z. Zhong, “Reduction-sensitive polymers and bioconjugates for biomedical applications”, *Biomaterials,* Vol. 30, No. 12, pp. 2180-2198.

35. Ding, Z., C. J. Long, Y. Hayashi, E. V. Bulmus, A. S. Hoffman, and P. S. Stayton, “Temperature Control of Biotin Binding and Release with A Streptavidin-Poly(N - isopropylacrylamide) Site-Specific Conjugate”, *Bioconjugate Chemistry,* Vol. 10, No. 3, pp. 395-400, 1999.

36. Beria, L., T. N. Gevrek, A. Erdog, R. Sanyal, D. Pasini, and A. Sanyal, “Clickable hydrogels for all: facile fabrication and functionalization”, *Biomaterials Science*, Vol. 2, No. 1, pp. 67-75, 2014.

37. Kosif, I., E. J. Park, R. Sanyal and A. Sanyal, “Fabrication of Maleimide Containing Thiol Reactive Hydrogels via Diels−Alder/Retro-Diels−Alder Strategy”, *Macromolecules*, Vol. 43, No. 9, pp. 4140-4148, 2010.

38. Brandl, F., N. Hammer, T. Blunk, J. Tessmar, and A. Goepferich, “Biodegradable hydrogels for time-controlled release of tethered peptides or proteins”, *Biomacromolecules,* Vol. 11, No. 2, pp. 496-504, 2010.

39. Leach, J. B., and C. E. Schmidt, "Characterization of protein release from photocrosslinkable hyaluronic acid-polyethylene glycol hydrogel tissue engineering scaffolds", *Biomaterials* Vol. 26, pp. 125-135, 2005.

40. Zustiak, S. P., and J. B. Leach, "Characterization of protein release from hydrolytically degradable poly(ethylene glycol) hydrogels", *Biotechnol. Bioeng.* Vol. 108, No. 1, pp. 197-206, 2011.

41. Altinbasak, I., R. Sanyal, and A. Sanyal, "Best of both worlds: Diels–Alder chemistry towards fabrication of redox-responsive degradable hydrogels for protein release", *RSC Adv.* Vol. 6, No. 78, pp. 74757-74764, 2016.

42. Vyas, A., S. Saraf, and S. Saraf, "Cyclodextrin based novel drug delivery systems", *Journal of Inclusion Phenomena Macrocyclic Chemistry,* Vol. 62, No. 1-2, pp. 23-42, 2008.

43. Rodriguez-Tenreiro, C., C. Alvarez-Lorenzo, A. Rodriguez-Perez, A. Concheiro, and J. J. Torres-Labandeira, "New Cyclodextrin Hydrogels Cross-linked with Diglycidylethers with a High Drug Loading and Controlled Release Ability", *Pharmaceutical Research*, Vol. 23, No. 1, pp. 121–130, 2006.

44. Peng, K., I. Tomatsu, A. V. Korobko, and A. Kros, "Cyclodextrin–dextran based in situ hydrogel formation: a carrier for hydrophobic drugs", *Soft Matter,* Vol. 6, pp. 85-87, 2010.

45. Uekama, K., F. Hirayama, and T. Irie, "Cyclodextrin Drug Carrier Systems", *Chemical Reviews*, Vol. 98, No. 5, pp. 2045–2076, 1998.

46. Liu, K. L., Z. Zhang, and J. Li, "Supramolecular hydrogels based on cyclodextrin–polymer polypseudorotaxanes: materials design and hydrogel properties", *Soft Matter,* Vol. 7, pp. 11290, 2011.

47. MacHin, R., J. R. Isasi, and I. Velaz, "β-Cyclodextrin hydrogels as potential drug delivery systems", *Carbohydrate Polymers*, Vol. 87, No. 3, pp. 2024-2030, 2012.

48. Arslan, M., T. N. Gevrek, R. Sanyal, and A. Sanyal, "Fabrication of Poly(ethylene glycol)-based Cyclodextrin Containing Hydrogels via Thiol-ene Click Reaction", *European Polymer Journal*, Vol. 62, pp. 426–434, 2015.

49. Boyer, C., V. Bulmus, P. Priyanto, W. Y. Teoh, R. Amal, and T. P. Davis, "The stabilization and bio-functionalization of iron oxide nanoparticles using heterotelechelic polymers", *J. Mater. Chem.* Vol. 19, pp. 111-123, 2009.

50. Bhat, R. R., Tomlinson, M. R., Wu, T., and Genzer, J. "Surface-Grafted Polymer Gradients: Formation, Characterization, and Applications", *Surface-Initiated Polymerization II (*Springer-Verlag, Berlin/Heidelberg), pp. 51-124, 2009.

51. Basuki, J. S., L. Esser, P. B. Zetterlund, M. R. Whittaker, C. Boyer, and T. P. Davis, "Grafting of P(OEGA) Onto Magnetic Nanoparticles Using Cu(0) Mediated Polymerization: Comparing Grafting "from" and "to" Approaches in the Search for the Optimal Material Design of Nanoparticle MRI Contrast Agents", *Macromolecules,* Vol. 46, pp. 6038–6060, 2013.

52. Na, H. Bin, G. Palui, J. T. Rosenberg, X. Ji, S. C. Grant, and H. Mattoussi, "Multidentate Catechol-Based Polyethylene Glycol Oligomers Provide Enhanced Stability and Biocompatibility to Iron Oxide Nanoparticles", *ACS Nano,* Vol. 6, pp.389-399, 2012.

53. Lu, X., R. Jiang, Q. Fan, L. Zhang, H. Zhang, M. Yang, Y. Ma, L. Wang, and W. Huang, "Fluorescent-magnetic poly(poly(ethyleneglycol)monomethacrylate)-grafted Fe3O4 nanoparticles from post-atom-transfer-radical-polymerization modification: synthesis, characterization, cellular uptake and imaging", *J. Mater. Chem*. Vol. 22, pp. 6965, 2012.

54. Matsuno, R., Yamamoto, K., Otsuka, H., and Takahara, A. "Polystyrene-Grafted Magnetite Nanoparticles Prepared through Surface-Initiated Nitroxyl-Mediated Radical Polymerization", *Chem. Mater.* Vol. 15, pp. 3–5, 2003.

55. Wang, W. C., Neoh, K. G., and Kong, E. T. "Surface functionalization of Fe3O4 magnetic nanoparticles via RAFT-mediated graft polymerization", *Macromol. Rapid Commun.* Vol. 27, pp. 1665-1669, 2006.

56. Schmidt, A. M. "The Synthesis of Magnetic Core-Shell Nanoparticles by Surface-Initiated Ring-Opening Polymerization of Caprolactone", *Macromol. Rapid Commun.* Vol. 26, pp. 93-97, 2005.

57. Wolski, K., A. Gruszkiewicz, M. Wytrwal-Sarna, A. Bernasik, and S. Zapotoczny, "The grafting density and thickness of polythiophene-based brushes determine the orientation, conjugation length and stability of the grafted chains", *Polym. Chem.* Vol. 8, No. 40, pp. 6250-6262, 2017.

58. Oz, Y., M. Arslan, T. N. Gevrek, R. Sanyal, and A. Sanyal, "Modular Fabrication of Polymer Brush Coated Magnetic Nanoparticles: Engineering the Interface for Targeted Cellular Imaging", *ACS Appl. Mater. Interfaces* Vol. 8, pp. 19813-19826, 2016.

59. Moad, G., E. Rizzardo, and S. H. Thang, "Radical addition–fragmentation chemistry in polymer synthesis. *Polymer,* Vol. 49, pp. 1079-1131, 2008.

60. Moad, G., E. Rizzardo, and S. H. Thang, "Living Radical Polymerization by the RAFT Process", *Australian Journal of Chemistry*, Vol. 58, No. 6, pp. 379, 2005.

61. Keddie, D. J., "A Guide to the Synthesis of Block Copolymers Using Reversible-Addition Fragmentation Chain Transfer (RAFT) Polymerization", *Chemical Society Reviews*, Vol. 43, No. 2, pp. 496–505, 2014.

62. Tasdelen, M. A., Y. Y. Durmaz, B. Karagoz, N. Bicak, and Y. Yagci, "A new photoiniferter/RAFT agent for ambient temperature rapid and well-controlled radical polymerization", *J. Polym. Sci. Part A Polym. Chem.* Vol. 46, pp. 3387-3395, 2008.

63. Willcock, H., and R. K. O'Reilly, "End group removal and modification of RAFT polymers", *Polym. Chem. 1*, Vol. 2, pp. 149-157, 2010.

64. Hoffman, A. S., "Hydrogels for Biomedical Applications", *Advanced Drug Delivery Reviews*, Vol. 54, No. 1, pp. 3-12, 2002.

65. Almany, L., and D. Seliktar, "Biosynthetic hydrogel scaffolds made from fibrinogen and polyethylene glycol for 3D cell cultures", *Biomaterials,* Vol. 26, pp. 2467-2477, 2005.

66. Wi, O., and D. LIM, "Hydrophilic Gels for Biological Use", *Nature,* Vol. 185, pp. 117-118, 1960.

67. Peppas N. A. and R. Langer, "New Challenges in Biomaterials", *Science*, Vol. 263, pp. 1715–1720, 1994.

68. Loh, X. J., S. H. Goh, and J. Li, "Hydrolytic degradation and protein release studies of thermogelling polyurethane copolymers consisting of poly[(R)-3-hydroxybutyrate], poly(ethylene glycol), and poly(propylene glycol)", *Biomaterials*, vol. 28, pp. 4113-4123, 2007.

69. Censi, R., T. Vermonden, M. J. van Steenbergen, H. Deschout, K. Braeckmans, S. C. De Smedt, C. F. van Nostrum, P. di Martino and W. E. Hennink, "Photopolymerized Thermosensitive Hydrogels for Tailorable Diffusion-controlled Protein Delivery", *Journal of Controlled Release,* Vol. 140, No. 3, pp. 230–236, 2009.

70. Wolinsky, J., Colson, Y., and M. Grinstaff, "Local Drug Delivery Strategies for Cancer Treatment: Gels, Nanoparticles, Polymeric Films, Rods, and Wafers Public Access", *J. Control. Release,* Vol. 159, No. 1, pp. 14-36.

71. Caliceti, P., S. Salmaso, A. Lante, M. Yoshida, R. Katakai, F. Martellini, L. H. I. Mei, and M. Carenza, "Controlled release of biomolecules from temperature-sensitive hydrogels prepared by radiation polymerization", *Journal of Controlled Release,* Vol. 75, No. 1-2, pp. 173–181, 2001.

72. Koehler, K.C., K.S. Anseth, and C.N. Bowman, "Diels-alder Mediated Controlled Release From A Poly(ethylene Glycol) Based Hydrogel", *Biomacromolecules,* Vol. 14, pp. 538–547, 2013.

73. Park, E. J., T. N. Gevrek, R. Sanyal, and A. Sanyal, "Indispensable Platforms for Bioimmobilization: Maleimide-based Thiol Reactive Hydrogels", *Bioconjugate Chemistry,* Vol. 25, No. 11, pp. 2004-2011, 2014.

74. Thatte, S., "Perspectives On: Polymeric Drugs and Drug Delivery Systems", *Journal of Bioactive and Compatible Polymers,* Vol. 20, No. 6, pp. 585–601, 2005.

75. Lee, C. C., E. R. Gillies, M. E. Fox, S. J. Guillaudeu, J. M. J. Frechet, E. E. Dy, and F. C. Szoka, "A single dose of doxorubicin-functionalized bow-tie dendrimer cures mice bearing C-26 colon carcinomas", *Proc. Natl. Acad. Sci.* Vol. 103, pp. 16649-16654, 2006.

76. Van Den Berghe, H., Coudane, J., and Vert, M. "Isocyanate-terminated Lactic Acid Oligomers as a New Means to Conjugate Functional Drugs or Polymers with Bioresorbable Hydrophobic Segments", *J. Bioact. Compat. Polym.* Vol. 22, No. 637–650, 2007.

77. Gac-Breton, S., J. Coudane, M. Boustta, and M. Vert, "Norfloxacin-poly(L-lysine citramide imide) Conjugates and Structure-dependence of the Drug Release", *Journal of Drug Targeting,* Vol. 12, No. 5, pp. 297–307, 2004.

78. Zovko, M., B. Zorc, P. Novak, P. Tepes, B. Cetina-Cizmek, and M. Horvat, "Macromolecular Prodrugs XI. Synthesis and Characterization of Polymer-estradiol Conjugate", *International Journal of Pharmaceutics*, Vol. 285, No. 1–2, pp. 35–41, 2004.

79. Digilio, G., L. Barbero, C. Bracco, D. Corpillo, P. Esposito, G. Piquet, Traversa, S., and S. Aime, "NMR Structure of Two Novel Polyethylene Glycol Conjugates of the Human Growth Hormone-Releasing Factor, hGRF(1−29)−NH_2", *J. Am. Chem. Soc.* Vol. 125, No. 12, pp. 3458-3470, 2003.

80. Greenwald, R. B., A. Pendri, C. D. Conover, H. Zhao, Y. H. Choe, A. Martinez, K. Shum, and S. Guan, "Drug Delivery Systems Employing 1,4- or 1,6-Elimination: Poly(ethylene glycol) Prodrugs of Amine-Containing Compounds", *J. Med. Chem.* Vol., 42, No. 18, pp. 3657-3667,1999.

81. Hu, X., S. Liu, Y. Huang, X. Chen, and X. Jing, "Biodegradable Block Copolymer-Doxorubicin Conjugates via Different Linkages: Preparation, Characterization, and In Vitro Evaluation", *Biomacromolecules* Vol. 11, No. 8, pp. 2094-2102, 2010.

82. Shamis, M., H. N. Lode, and D. Shabat, "Bioactivation of Self-Immolative Dendritic Prodrugs by Catalytic Antibody 38C2", *J. Am. Chem. Soc.* Vol. 126, No. 6, 1726-1731, 2004.

83. Wang, F., Y. C. Wang, S. Dou, M. H. Xiong, T. M. Sun, and J. Wang, "Doxorubicin-Tethered Responsive Gold Nanoparticles Facilitate Intracellular Drug Delivery for Overcoming Multidrug Resistance in Cancer Cells", *ACS Nano,* Vol. 5, No.5 pp. 3679–3692, 2011.

84. Cengiz, N., H. Kabadayioglu, and R. Sanyal, "Orthogonally Functionalizable Copolymers Based on a Novel Reactive Carbonate Monomer", *Journal of Polymer Science Part A: Polymer Chemistry,* Vol. 48, No. 21, pp. 4737-4746, 2010.

85 Okay, O., "Polymeric cryogels macroporous gels with remarkable properties", *Adv. Polym. Sci*, 2014.

86. Leader, B., Q. J. Baca, and D. E. Golan, "Protein therapeutics: a summary and pharmacological classification", *Nat. Rev. Drug Discov.* Vol. 7, pp. 21-39, 2008.

87. Vermonden, T., R. Censi and W. E. Hennink, "Hydrogels for Protein Delivery", *Chemical Reviews*, Vol. 112, No. 5, pp. 2853–2888, 2012.

88. Holland, T. A., Y. Tabata, and A. G. Mikos, "Dual growth factor delivery from degradable oligo(poly(ethylene glycol) fumarate) hydrogel scaffolds for cartilage tissue engineering", *J. Control. Release,* Vol. 101, pp. 111-25, 2005.

89. Cushing, M. C., and K. S. Anseth, "Hydrogel Cell Cultures", *Science,* Vol. 316, No. 5828, pp. 1133–1134, 2007.

90. Aydin, D., M. Arslan, A. Sanyal, and R. Sanyal, "Hooked on Cryogels: A Carbamate Linker Based Depot for Slow Drug Release", *Bioconjugate Chem.* Vol. 28, No. 5, pp. 1443-1451, 2017.

91. Singh, A., S. Suri, and K. Roy, "In-situ crosslinking hydrogels for combinatorial delivery of chemokines and siRNA–DNA carrying microparticles to dendritic cells", *Biomaterials,* Vol. 30, No. 28, pp. 5187-5200, 2009.

92. Li, J., L. Ma, G. Chen, Z. Zhou, and Q. Li, "A high water-content and high elastic dual-responsive polyurethane hydrogel for drug delivery", *Journal of Materials Chemistry B.* Vol. 3, No. 42, pp. 8401-8409, 2015.

93. Markland, P., Y. Zhang, G. L. Amidon, and V. C. Yang, "A pH- and ionic strength-responsive polypeptide hydrogel: Synthesis, characterization, and preliminary protein release studies", *J. Biomed. Mater. Res.* Vol. 47, No. 4, pp. 595-602, 1999.

94. Qiu, Y., and K. Park, "Environment-sensitive hydrogels for drug delivery", *Adv. Drug Deliv. Rev.* Vol. 64, 49-60, 2012.

95. Zhao, C., X. Zhuang, P. He, C. Xiao, C. He, J. Sun, X. Chen, and X. Jing, "Synthesis of biodegradable thermo- and pH-responsive hydrogels for controlled drug release", *Polymer,* Vol. 50, pp. 4308-4316, 2009.

96. Ahn, S., R. M. Kasi, S. C. Kim, N. Sharma, and Y. Zhou, "Stimuli-responsive polymer gels", *Soft Matter*, Vol. 4, No. 6, pp. 1151, 2008.

97. Quinn, J. F., M. R. Whittaker, and T. P. Davis, "Glutathione responsive polymers and their application in drug delivery systems", *Polymer Chemistry,* Vol. 8, No. 1, pp. 97-126, 2017.

98. Aimetti, A. A., A. J. Machen, and K. S. Anseth, "Poly(ethylene glycol) Hydrogels Formed by Thiol-ene Photopolymerization for Enzyme-responsive Protein Delivery", *Biomaterials*, Vol. 30, No. 30, pp. 6048–6054, 2009.

99. Navath, R. S., A. R. Menjoge, H. Dai, R. Romero, S. Kannan, and R. M. Kannan, "Injectable PAMAM Dendrimer–PEG Hydrogels for the Treatment of Genital Infections: Formulation and in Vitro and in Vivo Evaluation", *Mol. Pharm.* Vol. 8, No. 4, pp. 1209-1223, 2011.

100. Zhang, S., H. Chen, and J. Kong, "Disulfide bonds-containing amphiphilic conetworks with tunable reductive-cleavage", *RSC Adv.* Vol. 6, No. 3, pp. 36568-36575, 2016.

101. Malkoch, M., R. Vestberg, N. Gupta, L. Mespouille, P. Dubois, A. F. Mason, J. L. Hedrick, Q. Liao, C. W. Frank, K. Kingsbury, and C. J. Hawker, "Synthesis of Well-Defined Hydrogel Networks Using Click Chemistry", *Chemical Communications*, No. 26, pp. 2774–2776, 2006.

102. Zhang, J. T., S. X. Cheng, S. W. Huang, and R. X. Zhuo, "Temperature-Sensitive Poly(N-isopropylacrylamide) Hydrogels with Macroporous Structure and Fast Response Rate", *Macromol. Rapid Commun.* Vol. 24, No. 7, pp. 447-451, 2003.

103. Hou, S., L. K. McCauley, and P. X. Ma, "Synthesis and Erosion Properties of PEG-Containing Polyanhydrides", *Macromol. Biosci.* Vol. 7, No. 5, pp. 620-628, 2007.

104. Gok, O., S. Yigit, M. M. Kose, R. Sanyal, and A. Sanyal, "Dendron-polymer conjugates via the diels-alder "click" reaction of novel anthracene-based dendrons", *J. Polym. Sci. Part A Polym. Chem.* Vol. 51, pp. 3191-3201, 2013.

105. Ghosh, S., S. Basu, and S. Thayumanavan, "Simultaneous and reversible functionalization of copolymers for biological applications", *Macromolecules* Vol. 39, No. 17, pp. 5595-5597, 2006.

106. Kharkar, P. M., A. M. Kloxin, and K. L. Kiick, "Dually degradable click hydrogels for controlled degradation and protein release", *J. Mater. Chem. B* Vol. 2, pp. 5511–5521, 2014.

107. Subianto, S., N. K. Dutta, and N. R. Choudhury, "Water-Reprocessable, Reformable, and Ecofriendly Sustainable Material Based on Disulfide-Cross-Linked Polyethyleneimine", *ACS Omega* Vol. 2, No. 6, pp. 3036-3042, 2017.

108. Canadell, J., H. Goossens, and B. Klumperman, "Self-healing materials based on disulfide links", *Macromolecules* Vol. 44, No. 8, pp. 2536-2541, 2011.

109. Billiet, S., X. K. D. Hillewaere, R. F. A. Teixeira, and F. E. Du Prez, "Chemistry of crosslinking processes for self-healing polymers", *Macromol. Rapid Commun.* Vol. 34, No. 8, pp. 290-309, 2013.

110. An, S. Y., D. Arunbabu, S. M. Noh, Y. K. Song, and J. K. Oh, "Recent strategies to develop self-healable crosslinked polymeric networks", *Chem. Commun.* Vol. 51, No. 66, 13058-13070, 2015.

111. Shapiro, Y. E. "Structure and dynamics of hydrogels and organogels: An NMR spectroscopy approach", *Progress in Polymer Science*, Vol. 36, No. 9, pp. 1184-1253, 2011.

112. Jin, R., and P. J. Dijkstra, "Hydrogels for Tissue Engineering Applications", *Biomedical Application of Hydrogels Handbook*, Vol. c, No. 7, pp. 203-225, 2010.

113. Peppas, N. A. "Hydrogels and drug delivery", *Curr. Opin. Colloid Interface Sci.* Vol. 2, pp. 531–537, 1997.

114. Baldwin, A. D., and K. L. Kiick, "Reversible maleimide–thiol adducts yield glutathione-sensitive poly(ethylene glycol)–heparin hydrogels", *Polym. Chem.* Vol. 4, No. 1 pp. 133-143, 2013.

115. Siepmann, J., and N. A. Peppas, "Modeling of drug release from delivery systems based on hydroxypropyl methylcellulose (HPMC)", *Advanced Drug Delivery Reviews,* Vol. 48, No. 2-3, pp. 139-157, 2001.

116. Liu, S. Q., P. L. Rachel Ee, C. Y. Ke, J. L. Hedrick, and Y. Y. Yang, "Biodegradable poly(ethylene glycol)-peptide hydrogels with well-defined structure and properties for cell delivery", *Biomaterials,* Vol. 30, No. 8, pp. 1453-1461, 2009.

117. Fujiki, M., M. Ito, K. Mortensen, S. Yashima, M. Tokita, and M. Annaka, "Friction Coefficient of Well-Defined Hydrogel Networks", *Macromolecules,* Vol. 49, No. 2, pp. 634-642, 2016.

118. Malkoch, M., R. Vestberg, N. Gupta, L. Mespouille, P. Dubois, A. F. Mason, J. L. Hedrick, Q. Liao, C. W. Frank, K. Kingsbury, and C. J. Hawker, "Synthesis of well-defined hydrogel networks using Click chemistry", *Chem. Commun.* No. 26, pp. 2774-2776, 2006.

119. Sawicki, L. A., and A. M. Kloxin, "Design of thiol–ene photoclick hydrogels using facile techniques for cell culture applications", *Biomaterials Science,* Vol. 2, No. 11, pp. 1612-1626, 2014.

120. Yang, T., H. Long, M. Malkoch, E. G. Kristofer, L. Berglund, and A. Hult, "Characterization of well-defined poly(ethylene glycol) hydrogels prepared by thiol-ene chemistry", *Journal of Polymer Science Part A: Polymer Chemistry*, Vol. 49, No. 18, pp. 4044-4054, 2011.

121. Nair, D. P., M. Podgorski, S. Chatani, T. Gong, W. Xi, C. R. Fenoli, and C. N. Bowman, "The Thiol-Michael addition click reaction: A powerful and widely used tool in materials chemistry", *Chemistry of Materials*, Vol. 26, No. 1, pp. 724-744, 2014.

122. Quaglia, F., G. Varricchio, A. Miro, M. I. L. Rotonda, D. Larobina, and G. Mensitieri, "Modulation of drug release from hydrogels by using cyclodextrins: The case of nicardipine/β-cyclodextrin system in crosslinked polyethylenglycol", *Journal of Controlled Release*, Vol. 71, No. 3, pp. 329-337, 2001.

123. Hirayama, F., and K. Uekama, "Cyclodextrin-based controlled drug release system",*Adv. Drug Deliv. Rev.* Vol. 36, No. 1, pp. 125-141, 1999.

124. Harada, A., M. Furue, and S. I. Nozakura, "Cyclodextrin-Containing Polymers. 1. Preparation of Polymers", *Macromolecules*, Vol. 9, No. 5, pp. 701-704, 1976.

125. Arslan, M., D. Aydin, A. Degirmenci, A. Sanyal, and R. Sanyal, "Embedding Well-Defined Responsive Hydrogels with Nanocontainers: Tunable Materials from Telechelic Polymers and Cyclodextrins", *ACS Omega*, Vol. 2, No. 10, pp. 6658-6667, 2017.

126. Connors, K. A. "The Stability of Cyclodextrin Complexes in Solution", *Chemical Reviews*, Vol. 97, No. 5, pp. 1325-1358, 1997.

127. Sobocinski, J., W. Laure, M. Taha, E. Courcot, F. Chai, N. Simon, A. Addad, B. Martel, S. Haulon, P. Woisel, N. Blanchemain, and J. Lyskawa, "Mussel inspired coating of a biocompatible cyclodextrin based polymer onto CoCr vascular stents", *ACS Applied Materials and Interfaces*, Vol. 6, No. 5, pp. 3575-3586, 2014.

128. Shih, H., and C. C. Lin, "Photoclick hydrogels prepared from functionalized cyclodextrin and poly(ethylene glycol) for drug delivery and in situ cell encapsulation", *Biomacromolecules*, Vol. 16, No. 7, pp. 1915-1923, 2015.

129. Rojas, M. T., R. Koeniger, J. F. Stoddart, and A. E. Kaifer, "Supported Monolayers Containing Preformed Binding Sites. Synthesis and Interfacial Binding Properties of a Thiolated Beta-Cyclodextrin Derivative", *Journal of American Chemical Society,* Vol. 117, No. 1, pp. 336–343, 1995.

130. Ellman, G. L., "Tissue Sulfhydryl Groups", *Archives of Biochemistry and Biophysics*, Vol. 82, No. 1, pp. 70–77, 1959.

131. Riddles, P. W., R. L. Blakeley, and B. Zerner, "Reassessment of Ellman's Reagent", *Methods Enzymology*, Vol. 91, pp. 49–60, 1983.

132. Vashist, A., A. Vashist, Y. K. Gupta, and S. Ahmad, "Recent advances in hydrogel based drug delivery systems for the human body", *J. Mater. Chem. B,* Vol. 2, No. 2, pp. 147-166, 2014.

133. Tan, H., and K. G. Marra, "Injectable, biodegradable hydrogels for tissue engineering applications", *Materials*, Vol. *3*, No. 3, pp. 1746-1767, 2010.

134. Kaga, S., M. Arslan, R. Sanyal, and A. Sanyal, "Dendrimers and Dendrons as Versatile Building Blocks for the Fabrication of Functional Hydrogels", *Molecules*, Vol. 21, No. 4, 2016.

135. Slaughter, B. V., S. S. Khurshid, O. Z. Fisher, A. Khademhosseini, and N. A. Peppas, "Hydrogels in Regenerative Medicine", *Adv. Mater.*, Vol. 21, No. 32-33, pp. 3307-3329, 2009.

136. Van Vlierberghe, S., P. Dubruel, and E. Schacht, "Biopolymer-based hydrogels as scaffolds for tissue engineering applications: A review", *Biomacromolecules,* Vol. 12, No. 5, pp. 1387-1408, 2011.

137. Okay, O., "Hydrogel Sensors and Actuators", *Springer Series on Chemical Sensors and Biosensors*, Vol. 6, pp. 1-15, 2010.

138. Ullah, F., M. B. H. Othman, F. Javed, Z. Ahmad, and H. M. Akil, "Classification, processing and application of hydrogels: A review", *Mater. Sci. Eng. C,* Vol. 57, pp. 414-433, 2015.

139. Willner, I., "Stimuli-Controlled Hydrogels and Their Applications", *Accounts of Chemical Research*, Vol. *50*, No. 4, pp. 657-658, 2017.

140. Peppas, N. A., K. B. Keys, M. Torres-Lugo, and A. M. Lowman, "Poly(ethylene glycol)-containing Hydrogels in Drug Delivery", *Journal of Controlled Release*, Vol. 62, No. 1–2, pp. 81–87, 1999.

141. Rosiak, J. M., and Yoshii, F. "Hydrogels and their medical applications", *Nuclear Instruments Methods in Physics Research B Beam Interaction with Materials Atoms*, Vol. 151, No.1, pp. 56-64, 1999.

142. Kosif, I., E. J. Park, R. Sanyal and A. Sanyal, "Fabrication of Maleimide Containing Thiol Reactive Hydrogels via Diels−Alder/Retro-Diels−Alder Strategy", *Macromolecules*, Vol. 43, No. 9, pp. 4140–4148, 2010.

143. Amat-Guerri, F., M. Liras, M.L. Carrascoso, and R. Sastre, "Methacrylate-tethered Analogs Of The Laser Dye PM567--synthesis, Copolymerization With Methyl Methacrylate And Photostability Of The Copolymers.", *Photochemistry and photobiology*, Vol. 77, pp. 577–584, 2003.

144. Lutolf, M. P. and J. A. Hubbell, "Synthesis and Physicochemical Characterization of End-linked Poly(ethylene glycol)-co-peptide Hydrogels Formed by Michael-type Addition", *Biomacromolecules*, Vol. 4, No. 3, pp. 713–722, 2003.

145. Hofmann-Amtenbrink, M., B. Von Rechenberg, and H. Hofmann, "Superparamagnetic nanoparticles for biomedical applications", *Adv. Drug Deliv. Rev.*, Vol. 65, No. 5, *pp. 119-149*, 2009.

146. Du, K., Y. Zhu, H. Xu, and X. Yang, Multifunctional magnetic nanoparticles: Synthesis modification and biomedical applications. *Progress in Chemistry,* Vol. 23, No. 11, pp. 2287-2298, 2011.

147. Lee, N. and T. Hyeon, "Designed Synthesis of Uniformly Sized Iron Oxide Nanoparticles for Efficient Magnetic Resonance Imaging Contrast Agents", *Chemical Society Reviews*, Vol. 41, No. 7, pp. 2575–2589, 2012.

148. Gupta, A. K., and M. Gupta, "Synthesis and surface engineering of iron oxide nanoparticles for biomedical applications", *Biomaterials,* Vol. 26, No. 18, pp. 3995-4021, 2005.

149. Zhang, L., W. F. Dong, and H. B. Sun, "Multifunctional superparamagnetic iron oxide nanoparticles: design, synthesis and biomedical photonic applications", *Nanoscale,* Vol. 5, No. 17, pp. 7664, 2013.

150. Boyer, C., M. R. Whittaker, V. Bulmus, J. Liu, and T. P. Davis, "The design and utility of polymer-stabilized iron-oxide nanoparticles for nanomedicine applications", *Journal of Materials Chemistry*, Vol. 2, No. 1, pp. 23-30, 2010.

151. Chen, W. Y., and Y. C. Chen, "Affinity-based mass spectrometry using magnetic iron oxide particles as the matrix and concentrating probes for SALDI MS analysis of peptides and proteins", *Analytical and Bioanalitical Chemistry,* Vol. 386, No. 3, pp. 699-704, 2006.

152. Wu, W., Z. Wu, T. Yu, C. Jiang, and W. S. Kim, Recent progress on magnetic iron oxide nanoparticles: Synthesis, surface functional strategies and biomedical applications. *Science and Technoogy of Advanced Materials*, Vol. 16, No. 2, pp. 23501, 2015.

153. Marco, M. Di, S. Shamsuddin, K. A. Razak, A. A. Aziz, C. Devaux, E. Borghi, L. Levy, and C. Sadun, "Overview of the main methods used to combine proteins with nanosystems: Absorption, bioconjugation, and encapsulation", *International Journal of Nanomedicine*, Vol. 5, pp. 37-49, 2010.

154. Patil, U. S., H. Qu, D. Caruntu, C. J. O'Connor, A. Sharma, Y. Cai, and M. A. Tarr, "Labeling primary amine groups in peptides and proteins with N-hydroxysuccinimidyl ester modified Fe_3O_4@SiO_2 nanoparticles containing cleavable disulfide-bond linkers", *Bioconjugate Chemistry*, Vol. 24, No. 9, pp. 1562–1569, 2013.

155. Zhen, G., B. W. Muir, B. A. Moffat, P. Harbour, K. S. Murray, B. Moubaraki, K. Suzuki, I. Madsen, N. Agron-Olshina, L. Waddington, P. Mulvaney, and P. G. Hartley, "Comparative study of the magnetic behavior of spherical and cubic superparamagnetic iron oxide nanoparticles", *J. Phys. Chem.* C, Vol. 115, pp. 327-334, 2011.

156. Oyeneye, O. O., W. Z. Xu, and P. A. Charpentier, "Adhesive RAFT agents for controlled polymerization of acrylamide: effect of catechol-end R groups", *RSC Adv.* Vol. 5, No. 94, pp. 76919-76926, 2015.

157. Carlsson, J., H. Drevin, and R. Axen, "Protein thiolation and reversible protein-protein conjugation. N-Succinimidyl 3-(2-pyridyldithio)propionate, a new heterobifunctional reagent", *Biochem. J.* Vol. 173, No. 3, pp. 723-737, 1978.

158. Xu, C., K. Xu, H. Gu, R. Zheng, H. Liu, X. Zhang, Z. Guo, and B. Xu, "Dopamine as a robust anchor to immobilize functional molecules on the iron oxide shell of magnetic nanoparticles", *J. Am. Chem. Soc*., Vol. 126, pp. 9938-9939, 2004.

APPENDIX A: ADDITIONAL DATA

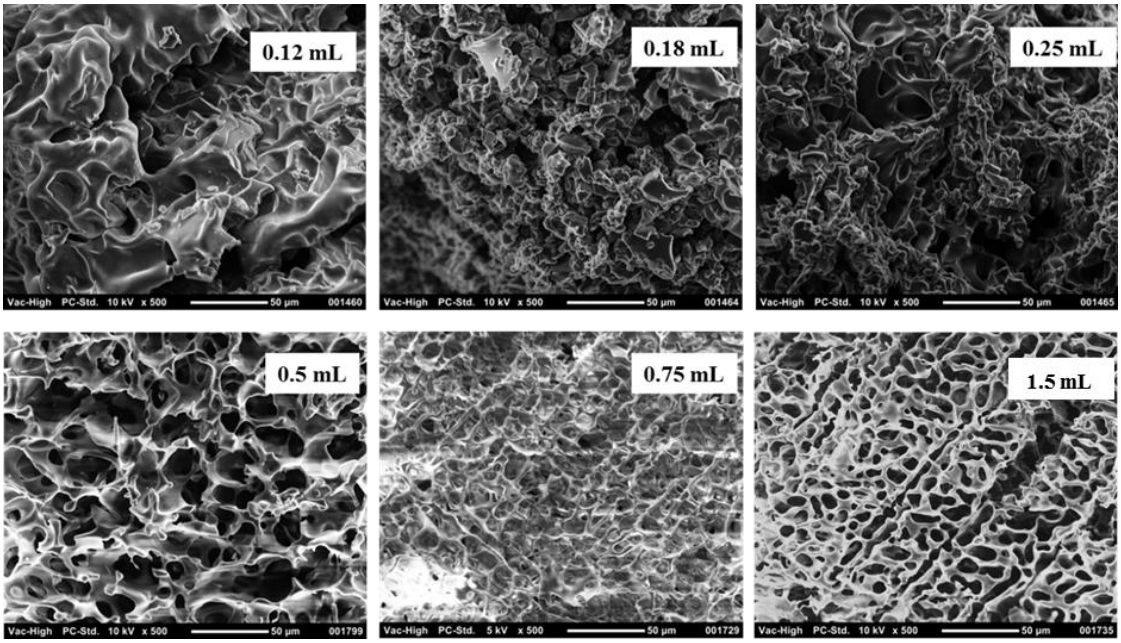

Figure A.1. SEM images of CH1 with different amounts of solvent.

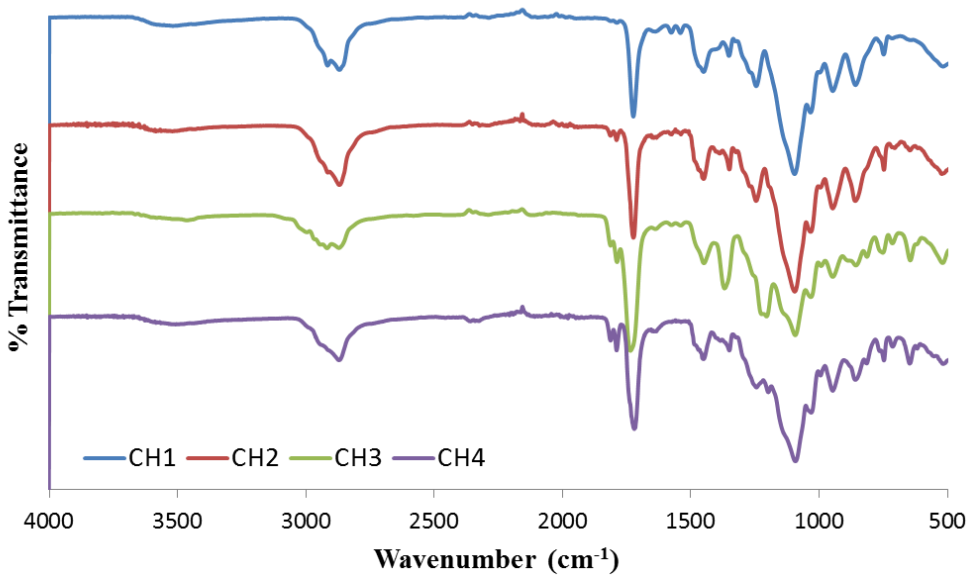

Figure A.2. FTIR spectra of cryogels.

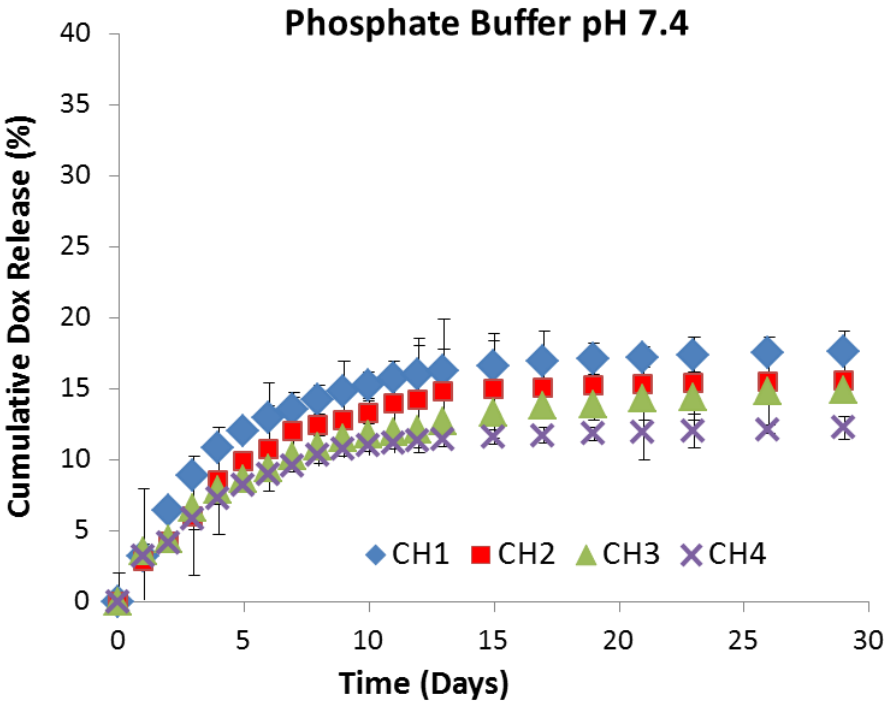

Figure A.3. Release profiles of DOX from cryogel in PBS pH = 7.4.

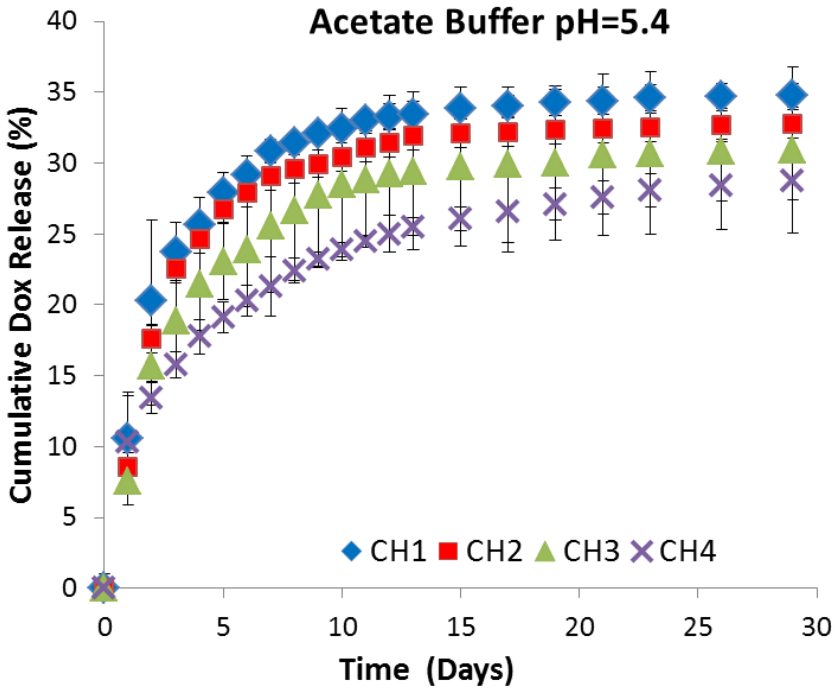

Figure A.4. Release profiles of DOX from cryogel in acetate buffer pH = 5.4.

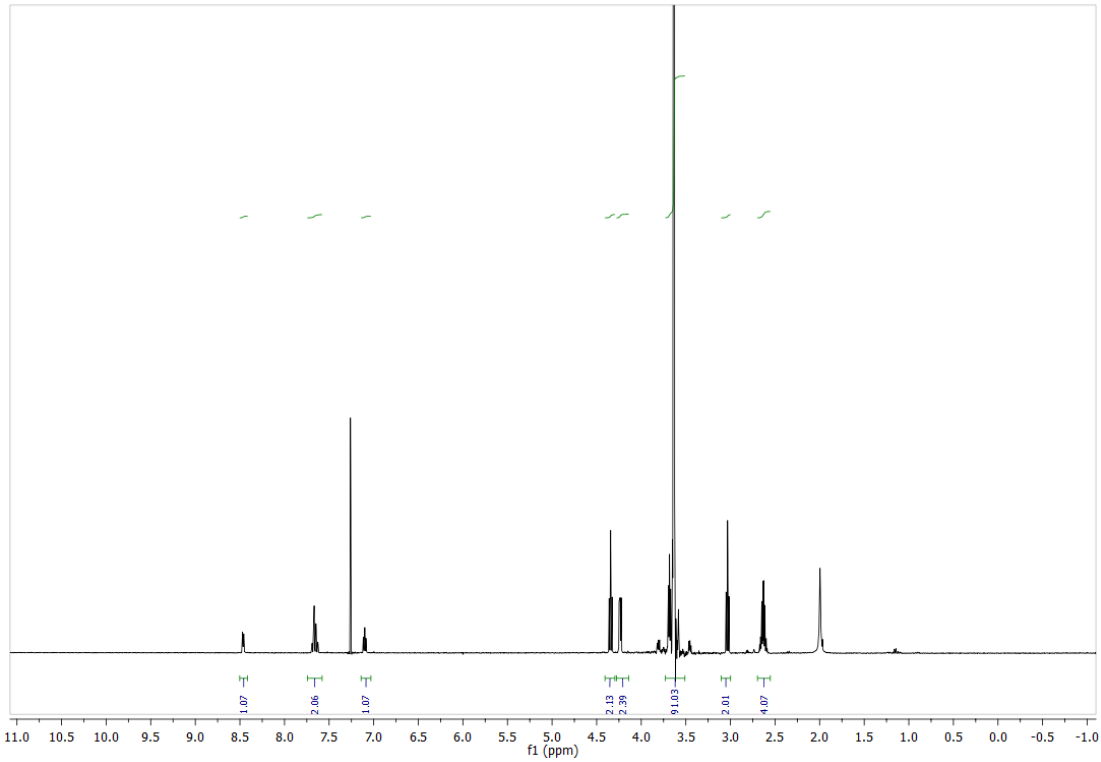

Figure A.5. ^{1}H NMR spectra of bispyridyldisulfide PEG (2 kDa)

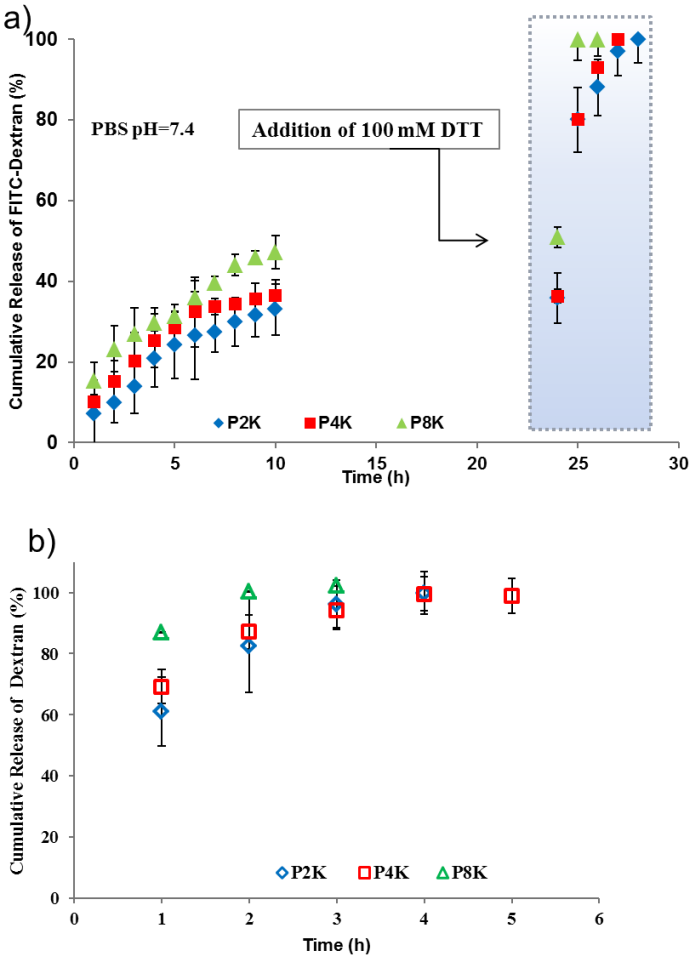

Figure A.6. FITC labeled Dextran release (20 kDa) from hydrogels in the presence of a) PBS and b) DTT.

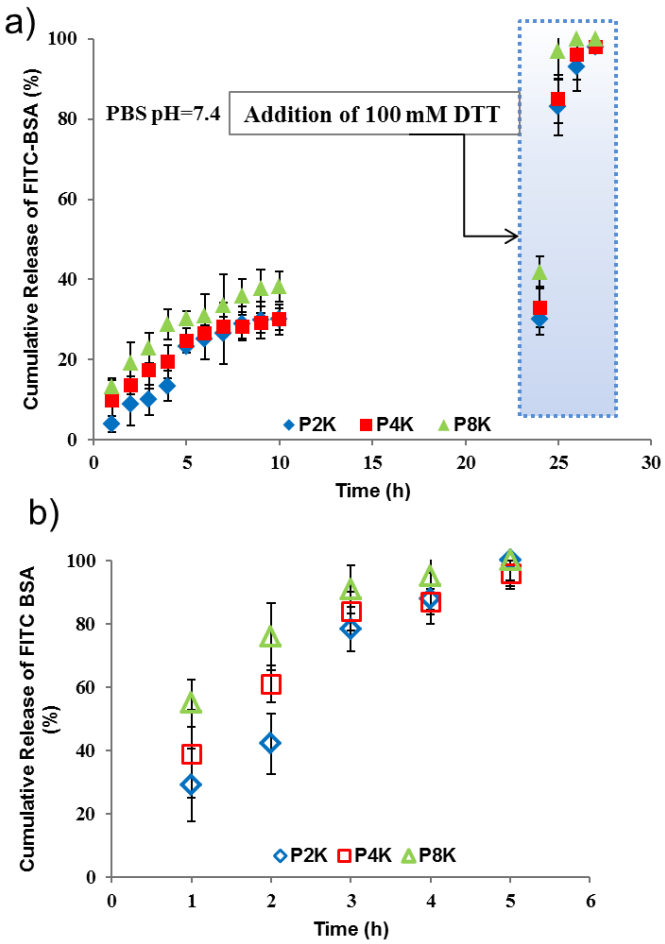

Figure A.7. FITC labeled BSA release from hydrogels in the presence of a) PBS and b) DTT.

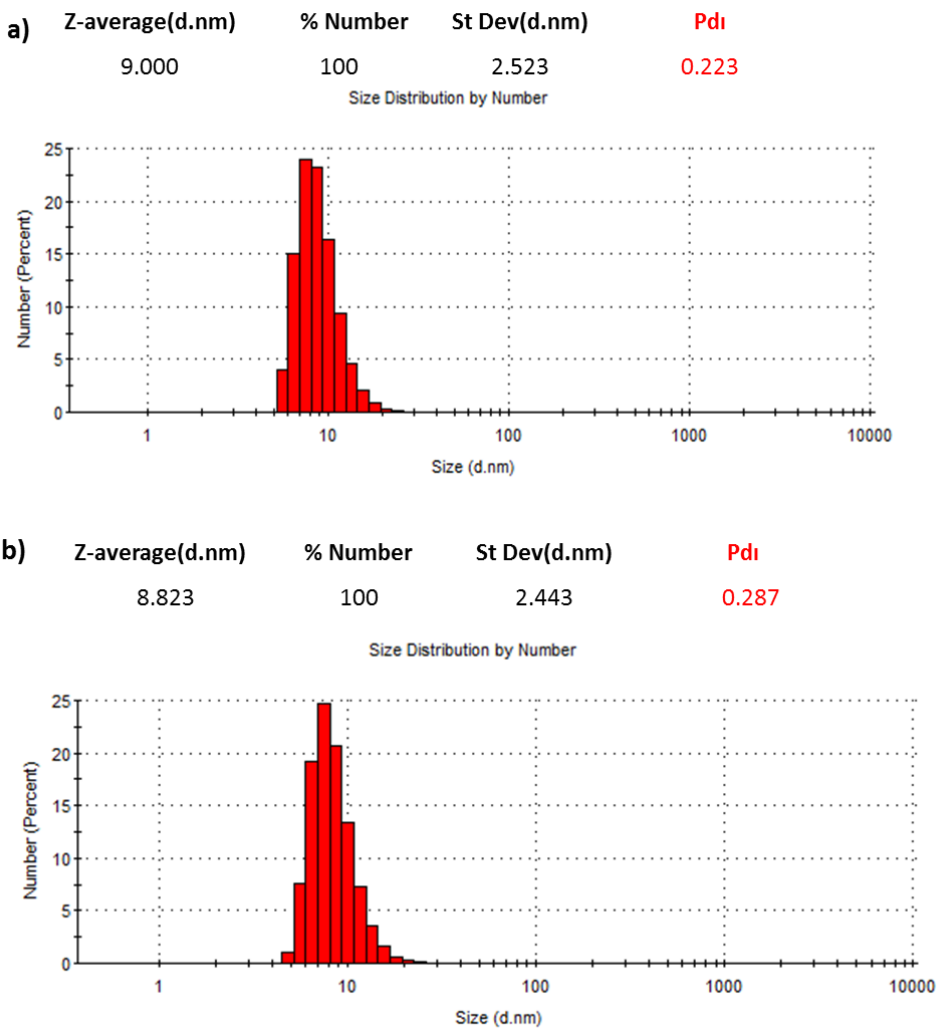

Figure A.8. DLS size and histograms of (a) 20 % and (b) 40 % PDSMA containing polymer coated MNPs.

APPENDIX B: PERMISSIONS FOR FIGURES

Title:	Self-Cross-Linked Polymer Nanogels: A Versatile Nanoscopic Drug Delivery Platform
Author:	Ja-Hyoung Ryu, Reuben T. Chacko, Siriporn Jiwpanich, et al
Publication:	Journal of the American Chemical Society
Publisher:	American Chemical Society
Date:	Dec 1, 2010

PERMISSION/LICENSE IS GRANTED FOR YOUR ORDER AT NO CHARGE

This type of permission/license, instead of the standard Terms & Conditions, is sent to you because no fee is being charged for your order. Please note the following:

- Permission is granted for your request in both print and electronic formats, and translations.
- If figures and/or tables were requested, they may be adapted or used in part.
- Please print this page for your records and send a copy of it to your publisher/graduate school.
- Appropriate credit for the requested material should be given as follows: "Reprinted (adapted) with permission from (COMPLETE REFERENCE CITATION). Copyright (YEAR) American Chemical Society." Insert appropriate information in place of the capitalized words.
- One-time permission is granted only for the use specified in your request. No additional uses are granted (such as derivative works or other editions). For any other uses, please submit a new request.

If credit is given to another source for the material you requested, permission must be obtained from that source

Figure B.1. Permission for Figure 1.3.

Title:	Facile Synthesis and Characterization of Disulfide-Cross-Linked Hyaluronic Acid Hydrogels for Protein Delivery and Cell Encapsulation
Author:	Sun-Young Choh, Daisy Cross, Chun Wang
Publication:	Biomacromolecules
Publisher:	American Chemical Society
Date:	Apr 1, 2011

Figure B.2. Permission for Figure 1.4.

Title: High Viability of Cells Encapsulated in Degradable Poly(carboxybetaine) Hydrogels

Author: Hsiu-Wen Chien, Xuewei Xu, Jean-Rene Ella-Menye, et al

Publication: Langmuir

Publisher: American Chemical Society

Date: Dec 1, 2012

PERMISSION/LICENSE IS GRANTED FOR YOUR ORDER AT NO CHARGE

This type of permission/license, instead of the standard Terms & Conditions, is sent to you because no fee is being charged for your order. Please note the following:

- Permission is granted for your request in both print and electronic formats, and translations.
- If figures and/or tables were requested, they may be adapted or used in part.
- Please print this page for your records and send a copy of it to your publisher/graduate school.
- Appropriate credit for the requested material should be given as follows: "Reprinted (adapted) with permission from (COMPLETE REFERENCE CITATION). Copyright (YEAR) American Chemical Society." Insert appropriate information in place of the capitalized words.
- One-time permission is granted only for the use specified in your request. No additional uses are granted (such as derivative works or other editions). For any other uses, please submit a new request.

If credit is given to another source for the material you requested, permission must be obtained from that source.

Figure B.3. Permission for Figure 1.5.

Title: Cryogels-versatile tools in bioseparation
Author: Gizem Ertürk,Bo Mattiasson
Publication: Journal of Chromatography A
Publisher: Elsevier
Date: 29 August 2014

Licensed Content Publisher	Elsevier
Licensed Content Publication	Journal of Chromatography A
Licensed Content Title	Cryogels-versatile tools in bioseparation
Licensed Content Author	Gizem Ertürk,Bo Mattiasson
Licensed Content Date	29 August 2014
Licensed Content Volume	1357
Licensed Content Issue	n/a
Licensed Content Pages	12
Type of Use	reuse in a thesis/dissertation
Portion	figures/tables/illustrations
Number of figures/tables/illustrations	1
Format	both print and electronic
Are you the author of this Elsevier article?	No
Will you be translating?	No
Original figure numbers	Figure 1
Title of your thesis/dissertation	NOVEL FUNCTIONAL HYDROGELS AND POLYMER COATED MAGNETIC NANOPARTICLES WITH DEGRADABLE LINKERS FOR BIOMEDICAL APPLICATIONS
Expected completion date	Jan 2018
Estimated size (number of pages)	190
Requestor Location	Duygu AYDIN Bogazici University Chemistry Department istanbul, 34342 Turkey Attn: Duygu AYDIN
Total	0.00 USD

Figure B.4. Permission for Figure 1.6.

Title:	Synthesis and Structure–Property Relationships of Cryogels
Author:	Oguz Okay, Vladimir I. Lozinsky
Publication:	Springer eBook
Publisher:	Springer Nature
Date:	Jan 1, 2014

Licensed Content Publisher	Springer Nature
Licensed Content Publication	Springer eBook
Licensed Content Title	Synthesis and Structure–Property Relationships of Cryogels
Licensed Content Author	Oguz Okay, Vladimir I. Lozinsky
Licensed Content Date	Jan 1, 2014
Type of Use	Thesis/Dissertation
Requestor type	academic/university or research institute
Format	print and electronic
Portion	figures/tables/illustrations
Number of figures/tables/illustrations	1
Will you be translating?	no
Circulation/distribution	<501
Author of this Springer Nature content	no
Title	NOVEL FUNCTIONAL HYDROGELS AND POLYMER COATED MAGNETIC NANOPARTICLES WITH DEGRADABLE LINKERS FOR BIOMEDICAL APPLICATIONS
Instructor name	Amitav sanyal
Institution name	Institute of Graduate Studies in Science and Engineering
Expected presentation date	Jan 2018
Portions	figure 5
Requestor Location	Duygu AYDIN Bogazici University Chemistry Department istanbul, 34342 Turkey Attn: Duygu AYDIN
Total	0.0 USD

Figure B.5. Permission for Figure 1.7.

ROYAL SOCIETY OF CHEMISTRY LICENSE TERMS AND CONDITIONS

Jan 03, 2018

Review Order

Please review the order details and the associated terms and conditions.

No royalties will be charged for this reuse request although you are required to obtain a license and comply with the license terms and conditions. To obtain the license, click the Accept button below.

Licensed Content Publisher	Royal Society of Chemistry
Licensed Content Publication	Biomaterials Science
Licensed Content Title	'Clickable' hydrogels for all: facile fabrication and functionalization
Licensed Content Author	Luca Beria,Tugce Nihal Gevrek,Asli Erdog,Rana Sanyal,Dario Pasini, Amitav Sanyal
Licensed Content Date	Aug 22, 2013
Licensed Content Volume	2
Licensed Content Issue	1
Type of Use	Thesis/Dissertation
Requestor type	non-commercial (non-profit)
Portion	figures/tables/images
Number of figures/tables/images	1
Distribution quantity	1
Format	print and electronic
Will you be translating?	no
Order reference number	
Title of the thesis/dissertation	NOVEL FUNCTIONAL HYDROGELS AND POLYMER COATED MAGNETIC NANOPARTICLES WITH DEGRADABLE LINKERS FOR BIOMEDICAL APPLICATIONS
Expected completion date	Jan 2018
Estimated size	190
Requestor Location	Duygu AYDIN Bogazici University Chemistry Department istanbul, 34342 Turkey Attn: Duygu AYDIN
Total	0.00 USD

Figure B.6. Permission for Figure 1.9.

Title:	Fabrication of Maleimide Containing Thiol Reactive Hydrogels via Diels–Alder/Retro-Diels–Alder Strategy
Author:	Irem Kosif, □un-Ju Park, Rana Sanyal, et al
Publication:	Macro□olecules
Publisher:	American Chemical Soci□ty
Date:	May 1, 2010

PERMISSION/LICENSE IS GRANTED FOR YOUR ORDER AT NO CHARGE

This type of permission/license, instead of the standard Terms & Conditions, is sent to you because no fee is being charged for your order. Please note the following:

- Permission is granted for your request in both print and electronic formats, and translations.
- If figures and/or tables were requested, they may be adapted or used in part.
- Please print this page for your records and send a copy of it to your publisher/graduate school.
- Appropriate credit for the requested material should be given as follows: "Reprinted (adapted) with permission from (COMPLETE REFERENCE CITATION). Copyright (YEAR) American Chemical Society." Insert appropriate information in place of the capitalized words.
- One-time permission is granted only for the use specified in your request. No additional uses are granted (such as derivative works or other editions). For any other uses, please submit a new request.

If credit is given to another source for the material you requested, permission must be obtained from that source.

Figure B.7. Permission for Figure 1.10.

Figure B.8. Permission for Figure 1.11.

Title:	Biodegradable Hydrogels for Time-Controlled Release of Tethered Peptides or Proteins
Author:	Ferdinand Brandl, Nadine Hammer, Torsten Blunk, et al
Publication:	Biomacromolecules
Publisher:	American Chemical Society
Date:	Feb 1, 2010

PERMISSION/LICENSE IS GRANTED FOR YOUR ORDER AT NO CHARGE

This type of permission/license, instead of the standard Terms & Conditions, is sent to you because no fee is being charged for your order. Please note the following:

- Permission is granted for your request in both print and electronic formats, and translations.
- If figures and/or tables were requested, they may be adapted or used in part.
- Please print this page for your records and send a copy of it to your publisher/graduate school.
- Appropriate credit for the requested material should be given as follows: "Reprinted (adapted) with permission from (COMPLETE REFERENCE CITATION). Copyright (YEAR) American Chemical Society." Insert appropriate information in place of the capitalized words.
- One-time permission is granted only for the use specified in your request. No additional uses are granted (such as derivative works or other editions). For any other uses, please submit a new request.

If credit is given to another source for the material you requested, permission must be obtained from that source.

Figure B.9. Permission for Figure 1.12.

ROYAL SOCIETY OF CHEMISTRY LICENSE TERMS AND CONDITIONS

Jan 02, 2018

Publisher	Royal Society of Chemistry
Licensed Content Publication	RSC Advances
Licensed Content Title	Best of both worlds: Diels–Alder chemistry towards fabrication of redox-responsive degradable hydrogels for protein release
Licensed Content Author	Ismail Altinbasak,Rana Sanyal,Amitav Sanyal
Licensed Content Date	Aug 3, 2016
Licensed Content Volume	6
Licensed Content Issue	78
Type of Use	Thesis/Dissertation
Requestor type	non-commercial (non-profit)
Portion	figures/tables/images
Number of figures/tables/images	1
Distribution quantity	1
Format	electronic
Will you be translating?	no
Order reference number	
Title of the thesis/dissertation	NOVEL FUNCTIONAL HYDROGELS AND POLYMER COATED MAGNETIC NANOPARTICLES WITH DEGRADABLE LINKERS FOR BIOMEDICAL APPLICATIONS
Expected completion date	Jan 2018
Estimated size	190
Customer Tax ID	TR2123597204
Customer VAT ID	TR2123597204
Total	0.00 USD

Figure B.10. Permission for Figure 1.13.

ROYAL SOCIETY OF CHEMISTRY LICENSE TERMS AND CONDITIONs

Licensed Content Publish r	Royal Society of Chemistry
Licensed Content Publication	Soft Matter
Licensed Content Title	Supramolecular hydrogels based on cyclodextrin–polymer polypseudorotaxanes: materials design and hydrogel properties
Licensed Content Author	Kerh Li Liu,Zhongxing Zhang,Jun Li
Licensed Content Date	Oct 5, 2011
Licensed Content Volume	7
Licensed Content Issue	24
Type of Use	Thesis/Dissertation
Requestor type	non-commercial (non-profit)
Portion	figures/tables/images
Number of figures/tables/images	1
Distribution quantity	1
Format	print and electronic
Will you be translating?	no
Order reference number	
Title of the thesis/dissertation	NOVEL FUNCTIONAL HYDROGELS AND POLYMER COATED MAGNETIC NANOPARTICLES WITH DEGRADABLE LINKERS FOR BIOMEDICAL APPLICATIONS
Expected completion date	Jan 2018
Estimated size	190
Total	0.00 USD

Figure B.11. Permission for Figure 1.14.

Title: Fabrication of poly(ethylene glycol)-based cyclodextrin containing hydrogels via thiol-ene click reaction
Author: Mehmet Arslan,Tugce Nihal Gevrek,Rana Sanyal,Amitav Sanyal
Publication: European Polymer Journal
Publisher: Elsevier
Date: January 2015

Licensed Content Publisher	Elsevier
Licensed Content Publication	European Polymer Journal
Licensed Content Title	Fabrication of poly(ethylene glycol)-based cyclodextrin containing hydrogels via thiol-ene click reaction
Licensed Content Author	Mehmet Arslan,Tugce Nihal Gevrek,Rana Sanyal,Amitav Sanyal
Licensed Content Date	January 2015
Licensed Content Volume	62
Licensed Content Issue	n/a
Licensed Content Pages	9
Type of Use	reuse in a thesis/dissertation
Portion	figures/tables/illustrations
Number of figures/tables/illustrations	1
Format	both print and electronic
Are you the author of this Elsevier article?	No
Will you be translating?	No
Original figure numbers	figure 4 and scheme 1
Title of your thesis/dissertation	NOVEL FUNCTIONAL HYDROGELS AND POLYMER COATED MAGNETIC NANOPARTICLES WITH DEGRADABLE LINKERS FOR BIOMEDICAL APPLICATIONS
Expected completion date	Jan 2018
Estimated size (number of pages)	190
Requestor Location	Duygu AYDIN Bogazici University Chemistry Department istanbul, 34342 Turkey Attn: Duygu AYDIN
Total	0.00 USD

Figure B.12. Permission for Figure 1.15.

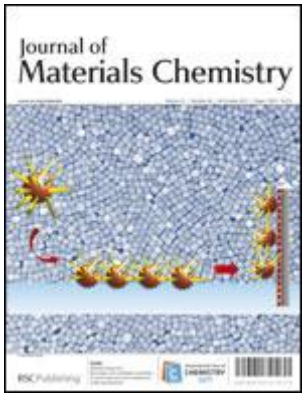

Title: The stabilization and bio-functionalization of iron oxide nanoparticles using heterotelechelic polymers
Author: Cyrille Boyer,Volga Bulmus,Priyanto Priyanto,Wey Yang Teoh,Rose Amal,Thomas P. Davis
Publication: Journal of Materials Chemistry
Publisher: Royal Society of Chemistry
Date: Nov 11, 2008

Licensed Content Publisher	Royal Society of Chemistry
Licensed Content Publication	Journal of Materials Chemistry
Licensed Content Title	The stabilization and bio-functionalization of iron oxide nanoparticles using heterotelechelic polymers
Licensed Content Author	Cyrille Boyer,Volga Bulmus,Priyanto Priyanto,Wey Yang Teoh,Rose Amal,Thomas P. Davis
Licensed Content Date	Nov 11, 2008
Licensed Content Volume	19
Licensed Content Issue	1
Type of Use	Thesis/Dissertation
Requestor type	non-commercial (non-profit)
Portion	figures/tables/images
Number of figures/tables/images	1
Distribution quantity	1
Format	electronic
Will you be translating?	no
Title of the thesis/dissertation	NOVEL FUNCTIONAL HYDROGELS AND POLYMER COATED MAGNETIC NANOPARTICLES WITH DEGRADABLE LINKERS FOR BIOMEDICAL APPLICATIONS
Expected completion date	Jan 2018
Estimated size	190
Requestor Location	Duygu AYDIN Bogazici University Chemistry Department istanbul, 34342 Turkey Attn: Duygu AYDIN
Total	0.00 USD

Figure B.13. Permission for Figure 1.16.

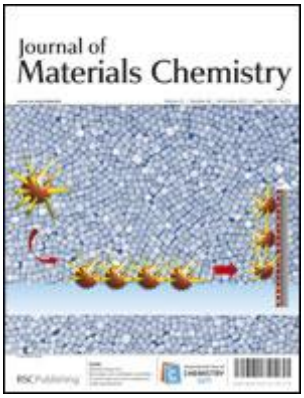

Title: Fluorescent-magnetic poly(poly(ethyleneglycol)monomethacrylate)-grafted Fe3O4 nanoparticles from post-atom-transfer-radical-polymerization modification: synthesis, characterization, cellular uptake and imaging

Author: Xiaomei Lu,Rongcui Jiang,Quli Fan,Lei Zhang,Hongmin Zhang,Minhua Yang,Yanwen Ma,Lianhui Wang,Wei Huang

Publication: Journal of Materials Chemistry

Publisher: Royal Society of Chemistry

Date: Feb 29, 2012

Licensed Content Publisher	Royal Society of Chemistry
Licensed Content Publication	Journal of Materials Chemistry
Licensed Content Title	Fluorescent-magnetic poly(poly(ethyleneglycol)monomethacrylate)-grafted Fe3O4 nanoparticles from post-atom-transfer-radical-polymerization modification: synthesis, characterization, cellular uptake and imaging
Licensed Content Author	Xiaomei Lu,Rongcui Jiang,Quli Fan,Lei Zhang,Hongmin Zhang,Minhua Yang,Yanwen Ma,Lianhui Wang,Wei Huang
Licensed Content Date	Feb 29, 2012
Licensed Content Volume	22
Licensed Content Issue	14
Type of Use	Thesis/Dissertation
Requestor type	non-commercial (non-profit)
Portion	figures/tables/images
Number of figures/tables/images	1
Distribution quantity	1
Format	print and electronic
Will you be translating?	no
Order reference number	
Title of the thesis/dissertation	NOVEL FUNCTIONAL HYDROGELS AND POLYMER COATED MAGNETIC NANOPARTICLES WITH DEGRADABLE LINKERS FOR BIOMEDICAL APPLICATIONS
Expected completion date	Jan 2018
Estimated size	190
Total	0.00 USD

Figure B.14. Permission for Figure 1.18.

Title:	Modular Fabrication of Polymer Brush Coated Magnetic Nanoparticles: Engineering the Interface for Targeted Cellular Imaging
Author:	Yavuz Oz, Mehmet Arslan, Tugce N. Gevrek, et al
Publication:	Applied Materials
Publisher:	American Chemical Society
Date:	Aug 1, 2016

Figure B.15. Permission for Figure 1.20.